Contents

Riassunto

Introduzione La Fibrillazione Atriale, nota anche con le abbreviazioni AF e Afib, é una patologia cardiaca di tipo aritmico che riguarda gli atrii, molto diffusa su scala mondiale, soprattutto in Europa e negli Stati Uniti, dove rispettivamente 4.5 e 2.2 milioni di persone sono affette da tale patologia. I sintomi che permettono solitamente di individuarla sono un battito cardiaco accelerato, palpitazioni, nei casi piú gravi angina pectoris e svenimenti. Ma essa puó anche essere asintomatica, dunque la sua inviduazione si basa sull'analisi di una traccia ECG, dove la sua presenza si manifesta con la sostituzione dell'onda P, rappresentativa della depolarizzazione degli atrii, con una serie di onde a bassa ampiezza con frequenza tra i 3 e 12 Hz, dette onde f, in inglese fibrillatory waves; inoltre, siccome la fibrillazione atriale spesso genera un' aritmia di tipo ventricolare, un ulteriore sua evidenza é data dagli intervalli RR, che sono caratterizzati da valori piú bassi e una variabilitá maggiore rispetto al normale ritmo sinusale.
I meccanismi responsabili per la fibrillazione atriale non sono ancora totalmente noti, ma si é focalizzato come possibile inizio un battito ectopico, generato dal tessuto atriale; in particolare, nella maggioranza dei casi studiati, la provenienza

di questi battiti é assegnata a quella porzione di atrio sinistro dove convergono le 4 vene polmonari. Questi extra battiti si possono ripetere per un tempo prolungato, ore o giorni, e causano affaticamento del cuore, che si contrae piú spesso del normale e quando non é completamente riempito.
Per il suo trattamento ci sono varie opzioni: se si sceglie di curare la tachicardia ventricolare che la fibrillazione spesso genera, si prescrivono dei farmaci anti-artimici per il controllo del battito cardiaco, mentre se si vuole andare alla radice del meccanismo generativo, il metodo ad oggi piú utilizzato é l'ablazione, con un catetere, di quelle zone considerate come foci della fibrillazione atriale. L'ablazione consiste nel rilascio di energia (RF, laser,ultrasuoni) e quindi di calore in tali zone fino alla loro bruciatura e disattivazione.
Come giá anticipato, la fibrillazione atriale é in grande diffusione, in America ogni anno vengono diagnosticati circa mezzo milioni di nuovi casi. La fibrillazione puó provocare ictus dunque ne deriva l'importanza di fare detezione, sia tramite lo studio dei sintomi, sia tramite l'analisi di segnali come tracce ECG che caratterizzano un paziente. L'elaborazione di segnali gioca un ruolo chiave, infatti permette non solo la detezione della fibrillazione atriale, ma anche la sua classificazione in parossistica, persistente o permanente, tramite l'analisi di registrazioni Holter.
Ci sono due principali vie d'azione per fare detezione:

- l'analisi dell'attivitá ventricolare, che consisite nello studio degli intervalli RR;

- l'analisi dell'attivitá atriale, che consiste nel tracking del contenuto in frequenza delle onde f.

Sebbene l'attivitá ventricolare sia piú semplice da estrarre e la computazione degli intervalli RR é ormai una procedura standard, in questo lavoro di tesi si é scelto il frequency tracking dell'attivitá atriale in presenza di fibrillazione atriale, in quanto tale patologia puó provocare una tachicardia ventricolare, ma

questo non é il sintomo che ne permette la diagnosi, essendoci dei pazienti con fibrillazione atriale totalmente asintomatici. Inoltre lo studio della distribuzione degli intervalli RR non é in grado di individuare episodi dell'ordine di secondi, mentre il frequency tracking da questo punto di vista ha ancora una chance.

Metodi

Il frequency tracking e gli algoritmi utilizzati Due algoritmi sono stati considerati, entrambi in grado di stimare la frequenza di una sinusoide sepolta in un background rumoroso:

1. un filtro notch adattativo, Adaptive Notch Filter (ANF)
2. uno stimatore diretto di frequenza, Direct Frequency Estimator (DFE)

Il primo algoritmo consiste nel processare la sinusoide rumorosa con un filtro notch, la cui frequenza centrale ω é adattativa e dipende da un coefficiente α secondo la seguente relazione:

$$\alpha = \cos\omega \tag{1}$$

Il coefficiente α viene aggiornato ad ogni iterazione, tramite la minimizzazione di una funzione di costo J che tiene conto della differenza tra l'uscita del filtro a spillo $x(n)$ e l'uscita dell'oscillatore discreto, il quale a sua volta prende in ingresso $x(n)$ e dá in uscita una sua elaborazione secondo l'equazione oscillatoria, che una sinusoide deve rispettare:

$$x(n) = 2\alpha x(n-1) - x(n-2) \tag{2}$$

Tale modello oscillatorio é la vera innovazione di questo algoritmo. Il processo di minimizzazione della funzione di costo porta ad un coefficiente α ottimale, a cui corrisponde la stima della frequenza della sinusoide in ingresso.
Sono stati fatti dei test per valutare la capacitá di tracking, la stabilitá in presenza di cambiamenti bruschi del contenuto in frequenza, il ritardo introdotto ed infine

la robustezza in condizione di rumore. I segnali utilizzati consistono in funzioni a gradino dove ogni gradino é una sinusoide con una certa frequenza. L'algoritmo é in grado di seguire cambiamenti repentini in modo stabile, anche in presenza di rumore; la stima fornita presenta overshoots e ritardo, due caratteristiche legate tra loro dal fattore d'oblio presente nell'equazione di aggiornamento per il coefficiente α: piú questo é basso, piú saranno pronunciati gli overshoots e minimo il ritardo, diversamente la stima sará piú smussata ma raggiungerá la condizione di regime con un ritardo maggiore.

Il secondo algoritmo ha la stessa funzione del primo, ovvero estrarre la frequenza ω di una sinusoide $s(n)$ sepolta nel rumore, applicando l'algoritmo LMS per minimizzare una funzione di costo predittiva lineare. La stima di $s(n)$ é funzione del segnale misurato $x(n)$ ed é data dalla seguente espressione:

$$\hat{s}(n) = 2\cos(\hat{\omega})x(n-1) - x(n-2) \tag{3}$$

dove $\hat{\omega}$ é la stima della frequenza ω. La funzione di costo da minimizzare é il valore atteso dell'errore quadratico di predizione, calcolato come la differenza tra il segnale misurato e quello predetto all'istante n:

$$E\{e^2(n)\} = E\{(x(n) - \hat{s}(n))^2\} \tag{4}$$

L'applicazione dell'LMS porta alla seguente equazione di aggiornamento:

$$\hat{\omega}(n+1) = \hat{\omega}(n) - \mu e(n)[(x(n) + x(n-2))\cos\hat{\omega}(n) + x(n-1)] \tag{5}$$

dove μ é lo step size del processo adattativo. In base alla teoria LMS esso puó assumere valori che devono appartenere all'intervallo [0, $1/2\sigma_s^2$], con σ_s^2 potenza della sinusoide. Tale appartenenza garantisce la stabilitá e la convergenza dell'algoritmo di minimizzazione. Il valore di μ deve essere scelto trovando un compromesso tra varianza della stima e velocitá di convergenza, infatti piú μ é alto, piú la convergenza é veloce, ma la stima della frequenza risulta caratterizzata da una varianza alta, mentre con un μ minore la stima risulta piú smussata, ma la convergenza richiede un tempo maggiore.

Il DFE é stato testato per le medesime caratteristiche usando gli stessi segnali dell'ANF. Tali test hanno dato i seguenti risultati: la stima risulta essere stabile quando il parametro μ ha valori nell'intervallo [0, $1/2\sigma_s^2$], ma é stata osservata la perdita della capacitá di tracking e di stabilitá nel momento in cui ci sono ampie variazioni del contenuto in frequenza. Introduce un certo ritardo, che puó essere ridotto scegliendo opportuni valori di μ e accettando una stima piú spiky. L'errore quadratico medio tende a ridursi con l'aumentare del SNR e in corrispondenza dell'intervallo di stabilitá di μ.
Questi due algoritmi sono stati messi a confronto con il fine di scegliere quello che meglio si prestava ad applicazioni su segnali ECG. Il confronto é stato fatto considerando una relazione di equivalenza tra il parametro μ del DFE e il coefficiente d'oblio δ dell'ANF:

$$\mu = 1 - \delta \tag{6}$$

Utilizzando funzioni di frequenza a gradino e mettendo a confronto le performance, sono state tratte le seguenti conclusioni:

- *(ritardo)* il DFE presenta un ritardo indipendente dal SNR, quasi costante, dipendente solo da μ, mentre l'ANF presenta un ritardo maggiore e dipendente dal SNR;

- *(stabilitá)* il DFE é totalmente instabile in caso di gradini molto alti, perde il tracking della frequenza, mentre l'ANF risulta essere in grado di seguire anche queste ampie e repentine variazioni del contenuto in frequenza;

- *(qualitá della stima)* la stima del DFE risulta caratterizzata da una varianza maggiore rispetto all'ANF;

- *(errore quadratico medio)* i valori dell'errore quadratico medio, registrati con SNR crescenti, per il DFE sono maggiori rispetto a quelli dell'ANF.

Tenendo presente che l'utilizzo finale dell'algoritmo di tracking é l'applicazione a segnali ECG, che, essendo segnali biologici, sono caratterizzati da rumore,

cambiamenti continui del contenuto in frequenza, si ritiene che l'ANF sia il piú adatto a tale applicazione, per la stabilitá che garantisce, anche in condizione di SNR sfavorevole e variazioni repentine della frequenza.

La detezione Come giá menzionato in precedenza, la detezione della fibrillazione atriale tramite il processing dei tracciati ECG gioca un ruolo molto importante per la diagnosi, ma non solo. Considerando il tracking della frequenza di un tracciato Holter, lungo 24 ore, la selezione automatica dei segmenti con fibrillazione atriale sarebbe auspicabile, in modo tale da potersi focalizzare soltanto sugli episodi di fibrillazione atriale. La maggior parte dei metodi presenti in letteratura usa la varianza degli intervalli RR che, durante episodi di fibrillazione atriale, é maggiore che nel caso di normale ritmo sinusale. In questo lavoro di tesi, é stato implementato un nuovo metodo, basato sulla pura attivitá atriale. Tale metodo, rispetto a quelli che elaborano l'attivitá ventricolare é piú pesante dal punto di vista computazionale, ma ha anche un grande vantaggio: é in grado di individuare episodi dell'ordine di qualche secondo, mentre altri metodi, tra quelli sopracitati, possono individuare episodi dell'ordine di minuti, dato che guardano la distribuzione degli intervalli RR su un numero elevato di battiti.

La detezione si basa sulla diversa stima in frequenza che l'ANF dá se viene accoppiato con un pre-filtro passa banda. Tale pre-filtraggio ha lo scopo di ridurre il range di frequenza da stimare ed é il fattore chiave per la detezione: infatti é stato notato che la stima della frequenza per un episodio di fibrillazione atriale non cambia con o senza pre-filtro, perché la frequenza del segnale di ingresso é dominante e l'algoritmo la identifica anche senza pre-filtro; diversamente dal ritmo sinusale, per il quale c'é una sovrastima di 4 Hz senza l'accoppiamento del pre-filtro, da attribuirsi al contenuto spettrale piú variegato, dove non c'é una frequenza dominante, ma diversi picchi, anche dovuti alla cancellazione del QRS e dell'estrazione dell'attivitá atriale.

Data questa differenza tra le performance, il metodo proposto effettua la de-

tezione degli episodi di fibrillazione atriale eseguendo una sottrazione tra i due segnali di frequenza stimata (con e senza prefiltro) e confrontando il risultato con una soglia. Siano f_1 e f_2 le stime in frequenza con e senza pre-filtraggio, rispettivamente, e sia sub il segnale dato dalla sottrazione dei due. sub ha valori vicini allo zero per i campioni con fibrillazione atriale, dato che le due stime sono uguali, mentre ha valori maggiori di zero in presenza di ritmo sinusale, per la sovrastima che dá l'ANF senza pre-filtraggio. La discriminazione di AF dal ritmo sinusale viene determinata dalla seguente espressione:

$$\begin{cases} \text{if } sub < th & AF \\ \text{if } sub > th & SR \end{cases}$$

É da puntualizzare che prima di eseguire la sottrazione sia f_1 che f_2 sono stati sottoposti a decimazione e ad un filtraggio mediano, al fine di ridurre gli overshoots delle stime e rendere il segnale adatto per il confronto con la soglia.

Risultati

PAF simulati La capacitá di fare detezione é stata testata costruendo dei segnali che "mimassero" la PAF, Paroxysmal Atrial Fibrillation, ovvero quel tipo di fibrillazione atriale che termina spontaneamente. Si é usato il termine costruire perché i segnali utilizzati, a cui ci si riferisce con il nome di *segnali simulati*, sono un collage di segmenti di sola fibrillazione atriale e segmenti di solo ritmo sinusale, provenienti da brevi registrazioni ECG o Holter, a cui é stato rimosso il QRS; in particolare i segmenti di fibrillazione atriale provengono sia da tracce Holter che da ECG, mentre il ritmo sinusale solo da tracce ECG. I segnali sono costruiti alternando segmenti di fibrillazione atriale con segmenti di ritmo sinusale, e variandone la lunghezza ad ogni simulazione.

La precisione e l'efficacia della detezione sono state valutate facendo uso di due segnali binari, il primo associato al segnale simulato e ottenuto assegnando zero ai segmenti con ritmo sinusale e uno ai segmenti con fibrillazione atriale; il secondo associato al segnale sub: dopo il confronto con la soglia, viene assegnato

ai campioni sopra la soglia (SR) il valore zero, ai campioni sotto soglia (AF) il valore uno.
Si sono considerati due tipi di errori:

1. *errore in campioni*, il quale viene calcolato a partire dal confronto campione per campione dei due segnali binari, con la seguente formula:

$$errore = \frac{campioni\ mal\ classificati}{totale\ lunghezza\ del\ segnale} * 100 \tag{7}$$

La minimizzazione di questo errore é stato il criterio utilizzato per settare sia i parametri del filtro ANF, quali coefficiente d'oblio δ e banda del filtro a spillo β, sia i parametri caratteristici del metodo, quali la banda passante del pre-filtro Δf e l'ordine del filtro mediano N. Essi sono:

- δ = 0.96
- β = 0.94
- Δf = 7 Hz
- N = 80

Per quel che riguarda la soglia, é necessario menzionare che essa ha un valore ottimale che dipende dalla lunghezza minima dell'episodio di fibrillazione atriale considerato, infatti piú questo é corto, piú la soglia va innalzata, altrimenti campioni di fibrillazione atriale vengono considerati come ritmo sinusale. Questo é fondamentalmente dovuto ai campioni necessari all'ANF per convergere verso il valore di regime, se tali campioni diminuiscono il valore raggiunto alla fine sará diverso da quello di regime ed é per questo che la soglia deve aumentare.

2. *errore episodico*, il quale viene definito con la seguente espressione:

$$\epsilon_{episodico} = \frac{falsi\ negativi\ +\ falsi\ positivi}{numero\ totale\ degli\ episodi\ di\ AF} * 100 \tag{8}$$

Per falsi negativi si intendono gli episodi che erroneamente non sono stati individuati, o perché troppo corti oppure perché due episodi molto vicini

tra loro sono stati individuati come un unico episodio; mentre i falsi positivi sono episodi rivelati, ma non veri, la cui rivelazione é da imputarsi ad una stima in frequenza con un'alta varianza che ha eluso il confronto con la soglia. I falsi positivi sono stati ridotti per la maggior parte, grazie al fatto che in letteratura sono stati ritrovati dei riferimenti per i quali un episodio di fibrillazione atriale, per dirsi tale, non puó durare meno di 6 secondi, circa. Con questa informazione, una volta fatta la detezione degli episodi, la durata temporale di ognuno é stata calcolata, e gli episodi con durata inferiore a 6 secondi sono stati riconosciuti come falsi positivi, ed eliminati, migliorando le percentuali di successo del metodo.

L'errore episodico é stato utilizzato per ottimizzare due parametri importanti, quali risoluzione temporale, ovvero la minima distanza a cui due episodi possono essere per venire riconosciuti come distinti, e la durata minima che un episodio deve avere per essere individuato. Ognuno di questi parametri é stato relazionato alla soglia, ovvero sono state valutate diverse combinazioni (soglia-risoluzione temporale, soglia- durata minima), per ognuna delle quali sono state eseguite 10 simulazioni e l'errore é stato riportato in opportune tabelle, dalle quali si evince che il metodo é in grado di individuare episodi lunghi $8 - 10$ secondi, distanti tra loro almeno 20 secondi, con soglia settata a 2, con un errore episodico del 5%.

Inoltre é stato valutato il ritardo, sia nella detezione del campione d'inizio che di fine episodio. Sono state eseguite 40 simulazioni, 20 con segmenti di fibrillazione atriale provenienti da tracce Holter e 20 con segmenti provenienti da tracce ECG, mentre i segmenti di ritmo sinusale avevano tutti la stessa provenienza, ovvero tracce ECG. I risultati ottenuti, per entrambi i gruppi, sono stati utilizzati per calcolare media e deviazione standard del ritardo di detezione di fine ed inizio episodio. Guardando tali valori, si nota come essi siano inferiori per il gruppo con fibrillazione atriale proveniente dall'ECG, sia perché la tracce ECG sono meno affette da rumore rispetto alle Holter, sia per una questione di

continuitá con il ritmo sinusale, anch'esso proveniente da ECG.

PAF reali Dopo aver testato il metodo su simulazioni, lo si é applicato ad un dataset di 10 ECG di pazienti affetti da PAF, in particolare uno proveniente dall'Ospedale di Valenzia, i 9 rimanenti provenienti dal Database Physionet. Ognuno di questi segnali conteneva uno o piú episodi per un totale di 15 episodi, di durate variabili da un minimo di 16 secondi ad un massimo di 244 minuti. Tutti questi episodi sono stati correttamente identificati, anche se con 7 falsi positivi, e con ritardo di detezione di inizio e fine episodio, valutato, come con i segnali simulati, in media e deviazione standard.

Discussione e Conclusioni La maggior parte dei metodi presenti in letteratura si basa sull' irregolaritá dell'attivitá ventricolare, descritta dalla distribuzione degli intervalli RR. Questi metodi sono robusti e in grado di fare un accurata detezione, peró hanno un limite: non sono in grado di individuare episodi molto brevi, dell'ordine di secondi. Lo scopo di questo lavoro di tesi é stato duplice:

1. implementare un algortimo in grado di estrarre dal segnale atriale la frequenza;

2. sviluppare un metodo che, basandosi su quest'informazione in frequenza, proveniente direttamente dagli atri e non dai ventricoli, fosse in grado di individuare episodi di fibrillazione atriale sotto il minuto.

Per quel che riguarda il frequency tracking, due algoritmi, ANF e DFE, sono stati implementati, testati e confrontati. L'ANF é risultato vincente tra i due, in quanto ha mostrato stabilitá, anche in diverse condizioni di rumore, e la capacitá di estrarre la frequenza anche in presenza di brusche variazioni della stessa, dunque piú adatto per applicazioni a segnali ECG. Per quel che riguarda il detettore, si puó concludere che é stato in grado di inviduare tutti gli episodi senza mancarne

nessuno ed ha assolto al compito di individuare anche gli episodi sotto il minuto, ma presenta una serie di svantaggi quali:

- alta sensibilitá alla generazione di falsi positivi, dovuti soprattutto a segnali di ingresso troppo rumorosi, tali per cui il track in frequenza caratterizzato da spikes che quindi portano a superamento della soglia anche campioni di fibrillazione atriale.

- l'introduzione di un ritardo nella detezione sia dell'inizio che della fine dell'episodio, che deve essere compensato per rendere il metodo piú affidabile ed accurato.

- il costo computazionale piú alto rispetto ad altri metodi di detezione, in quanto é necessaria la rimozione del QRS prima di processare il segnale con l'ANF, che di per sé deve essere applicato due volte.

Concludendo, il frequency tracking con l'ANF é meritevole di ulteriori e piú approfonditi studi sulle sue possibili implicazioni, mentre il detettore é in grado di individuare episodi molto brevi, peró necessita di un numero maggiore di pazienti su cui essere applicato e di forme di compensazione sia del ritardo che dei falsi positivi, in modo tale da poter competere con gli altri metodi di detezione presentati fin ora in letteratura.

Abstract

Introduction The atrial fibrillation, also known as AF of Afib, is a haert disease that consists in an irregular contraction of the atria such that multiple impulses travel through the atria at the same time and reach the atrial-ventricular node, resulting in an irregular and rapid heartrate. This patology is worldwidespread, above all in Europe and USA, where there are 4.5 and 2.2 milions of cases, respectively. The symptoms are palpitation, faster heart rate, angina pectoris and sometimes faints. But it can be also asymptomatic, so its detection has to be based on processing ECG trace. In presence of atrial fibrillation, P-waves, representatives of the atria depolarization, are replaced by the so called f-waves, or fibrillatory waves, that consist in a series of low amplitude waves with frequency in the range 3 to 12 Hz. Furthermore, sometimes, in presence of atrial fibrillation, the heart rate is more irregular and RR intervals are characterized by lower values and larger variability than sinus rhythm.

The mechanisms involved in the initiation of atrial fibrillation are still not clear, but it seems that, even if paroxysmal, atrial fibrillation can be initiated in correspondence of ectopic beats generated by the atrial tissue, and mainly by the

region where the four pulmonary veins converge. The repetition of those extra beats over a long time, such hours or days, can induce the heart to contract more often than normal and when the ventricles are not totally filled, with the result of fatigue for the heart.

For the threatment there are many options: if the aim is to cure the ventricular tachycardia, then anti-arrythmics drugs are used for the heart rate control; but nowdays the most common way to resolve problem at its initiation is the ablation, with a catheter, of regions believed to be foci of atrial fibrillation. The ablation procedure used RF, laser or ultrasound, for burning and hence disactiving those areas.

As it was said before, there is a big spread of this patology; in America, every year half milion new cases are diagnosticated. Atrial fibrillation can bring stroke, therefore the detection is really important, either with the study of sympthoms, either with processing the ECG traces of patients. Signal processing plays a key role, in fact it allows detection, but also classification of atrial fibrillation into the three categories, paroxysmal, persistent or permanent, by the analysis of Holter recordings. There are two main branches for stuyding and detecting atrial fibrillation:

- considering the ventricular activity and analysing the RR intervals;
- considering the atrial activity and analysing of the frequency content of the f-waves.

Although the ventricular activity is easily to exctract from an ECG and the computation of RR intervals is a standard procedure, in this project it has been chosen the frequency tracking of the atrial activity when atrial fibrillation occurs, since it can generate ventricular tachycardia, but this is not the symptom that allows diagnosis, since there are patients with atrial fibrillation that are totally asymptomatics. Besides using RR intervals episodes of order on segments can't be detected, while the frequency tracking of the f-waves from this point of view has still a chance.

Methods

Algorithms for frequency tracking Two algorithms have been considered, both able to estimate the frequency of a sinusoid embedded in a noisy background:

1. an adaptive notch filter (ANF)
2. a direct frequency estimator (DFE)

The first algorithm consists in processing a noisy sinusoid with a notch filter, with central frequency ω adaptive and dependent on a coefficient α with the following relationship:

$$\alpha = \cos \omega \tag{9}$$

The α coefficient is updated at every iteration, through the minimization of a cost function J, that takes in account the difference between the output of the notch filter $x(n)$ and the output of the discrete oscillator, that takes as input $x(n)$ returning its computation, according the oscillatory equation, that every sinusoid has to respect:

$$x(n) = 2\alpha x(n-1) - x(n-2) \tag{10}$$

The oscillatory model is the real innovation of this algorithm. The minimizing process of the cost function results in an ottimal α coefficient, that individuates the estimate of the frequency of the input sinusoid.
Test have been done to evaluate the tracking capability, stability in presence of sharp variations of the frequency content, the introduced delay and finally the robustness in case of noise. The signals used for these test are stepwise functions where every step is a sinusoid with a certain frequency. The algorithm is able to track sharp variations, keeping the stability even in presence of noise; the provided estimate presents overshoots and delay, two characteristics related each other by the forgetting factor, considered in the updating equation for the α

coefficient: the lower forgetting factor, the higher overshoots and shorter delay and viceversa.

The second algorithm solves the same problem of the first one, the extraction of frequency ω of a sinusoid $s(n)$ embedded by noise, applying the algorithm LMS in order to minimize a linear predictive cost function. The estimate of $s(n)$ is dependent on the measured signal $x(n)$, and the dependency is given by the following expression:

$$\hat{s}(n) = 2\cos(\hat{\omega})x(n-1) - x(n-2) \tag{11}$$

where $\hat{\omega}$ is the estimate of the frequency ω. The cost function to minimize is the expected value of the prediction squared error, computed as the difference between the measured signal and the one predicted at time n:

$$E\{e^2(n)\} = E\{(x(n) - \hat{s}(n))^2\} \tag{12}$$

By applying the LMS algorithm, the updating equation becomes:

$$\hat{\omega}(n+1) = \hat{\omega}(n) - \mu e(n)[(x(n) + x(n-2))\cos\hat{\omega}(n) + x(n-1)] \tag{13}$$

with μ stepsize of the adaptive process. According to the LMS theory, μ can assume values that must belong in the range [0, 1/($2\sigma_s^2$)], with σ_s^2 sinusoid power, because in this way stability and convergence of the algorithm are guarateed. The stepsize is tipically chosen as trade-off between variance of the estimate and speed of convergence, that means that as the stepsize increases, the convergence is faster, but this is paid with an estimate of the frequency that is characterized by a larger variance; viceversa if μ decreases.

The DFE has been tested for the same features and using the same signals of ANF. The test have given the following results: the estimate is stable when μ belongs to the interval [0, 1/$2\sigma_s^2$], but it has noticed the loss of tracking capability and stability in correspondence of wide variation of the frequency content. There is the introduction of delay, that can be reduced by choosing high values of μ and accepting a spiky estimate. The mean squared error tends to decrease

with an increasing SNR and for the stability interval of the stepsize.
These algorithms have been compared in order to identify the better one for ECG applications. The comparison has been done considering a relation of equivalence between the μ parameter of the DFE and the forgetting factor δ of the ANF:

$$\mu = 1 - \delta \tag{14}$$

Applying both algorithms to the same stepwise functions, the conclusions are:

- (*delay*) the DFE presents a delay that is indipendent by the SNR, almost constant, influenced only by μ, while the ANF presents a larger delay, dependent on SNR;

- (*stability*) the DFE is totally unstable in case of wide steps, looses the tracking of the frequency, while the ANF does not;

- (*quality of the estimate*) the estimate of the DFE is characterized by a larger variance than the ANF;

- (*mean squared error*) the error values, for increasing SNR, are larger for the DFE than for the ANF.

Given that the algorithm has to track the frequency of an ECG trace and given that biological signals are charaterized by noise, frequent variation of the frequency content, the ANF algorithm is the more indicate for ECG application for the stability that is guaranteed even in condition of unfavourable SNR and sharp variations of the frequency.

The detection As aforementioned, the detection of atrial fibrillation through the processing of the ECG recordings plays an important role for diagnosis, but there is more. Considering the tracking of the frequency of a Holter recording, 24 hours long, the automatic selection of the segments with atrial fibrillation would be helpful, in order to focus only on the segments containing atrial fibrillation

episodes. The main part of the methods in literature makes use of the variance of the RR intervals, that is larger than normal when atrial fibrillation occurs. In this project, it has been implemented a new method, based on the pure atrial activity. This method is less efficient, from a computational point of view, respect to the ones that elaborate ventricular activity, but it has also a significant advantage: it is able to detect episodes of order on some seconds, while RR based methods can detect episodes of order on minutes, since they analyse the distribution of the RR intervals, computed by considering a large amount of beats.

The detection is based on the different estimate that the ANF returns if it is coupled with a pass band pre-filter. This pre-filtering aims to reduce the range of frequency to estimate and it is the key factor for detection: in fact it has been noticed that the estimate of the frequency for an episode of atrial fibrillation doesn't change with or without pre filtering, because the frequency of the input signal is dominant and the algorithm can identify it even without pre-filtering; instead for sinus rhythm there is an overestimate of 4 Hz without the coupling with the prefiltering, due to the spectral content that is more various, where there is not a dominant frequency, but many peaks, that may be attributed to the QRS cancellation and atrial activity extraction. Given this difference between the perfomances, the proposed method detects atrial fibrillation episodes by computing the subtraction between the two signals of estimated frequency (with and without prefiltering) and comparing the result with a threshold. Let f_1 and f_2 be the estimates in frequency with and without prefiltering, and sub be the result of the subtraction of f_1 and f_2. sub presents values close to zero for the samples with atrial fibrillation, since both the estimates are equals, while it has values larger than zero in presence of sinus rhythm, since there is the overestimate of the ANF without pre-filtering. The discrimination of atrial fibrillation from sinus rhytm is determined by the followin expression:

$$\begin{cases} \text{if } sub < th & AF \\ \text{if } sub > th & SR \end{cases}$$

It has to be pointed out that before computing the subtraction, both f_1 and f_2 have been decimated and filtered with a median filter, in order to reduce the estimate's overshoots and rendering the signal adapt to be compared with the threshold.

Simulations and Results

Simulated PAF The detection capability has been tested building signals that could mimic PAF, paroxysmal atrial fibrillation, that is that kind of atrial fibrillation that ends spontaneusly. The term build is adoperated because the used signals, that will be called simulated signals, are a collage of segments of only atrial fibrillation and segments of only sinus rhythm, coming from short registrations ECG or Holter, depurated from the QRS complex; in particular atrial fibrillation segments come from both Holter and ECG traces, while the sinus rhythm only from ECG recordings. The signals are built alternating segments of atrial fibrillation and segments of sinus rhythm, and varying the length of each segments at every simulation.

The precision and the effectiveness of detection have been evalutuated with the help of two binary signals, the former associated at the simulated signal and generated by assigning zero to the segments with sinus rhythm and one to the segments with atrial fibrillation; the latter associated to the signal sub: after thresholding, zero is attributed to the samples that exceed the threshold (SR), one to the ones that don't (AF).

Two kind of errors are considered:

1. *samples error*, that is computed starting by the comparison sample by sample of the two binary signals, according the following formula:

$$error = \frac{wrong\ samples}{total\ length\ of\ signals} * 100 \tag{15}$$

   The minimization of this error has been the critery used for the setting of the parameters of both the ANF, forgetting factor δ and the bandwidth

of the notch filter β, and the method, bandwidth of the pre-filter Δf and median filter order N. The found values are:

- δ = 0.96
- β = 0.94
- Δf = 7 Hz
- N = 80

For what that concerns the threshold it is necessary clearify that it has an ottimal value that depends on the minimun length of the considered atrial fibrillation episodes, in fact the shorter episode needs a higher threshold to be detected, otherwise atrial fibrillation samples are labelled as sinus rhythm. This is basically due to the number of samples that ANF requires to converge to the steady state value; if those samples are reduced, the achieved value in the end will be lower that the steady state and this why the threshold has to be raised up.

2. *episodes error*, that is defined with the following expression:

$$\epsilon_{episodes} = \frac{false\ negatives\ +\ false\ positives}{total\ number\ of\ episodes\ of\ AF} * 100 \tag{16}$$

The false negatives are the episodes that are erroneously not identified, because too short or because two episodes too close to each other are detected as an unique episode; while the false positives are episodes erroneously detected, because of the high variance of the frequency estimate that has eluded the threshold. The false positives has been reduced for the main part thanks to evidence found in literature, according to an atrial fibrillation episode, to be considered such, cannot be shorter than 6 seconds. With this information, after the detection of the episodes, the duration of all the detected episodes is calculated end the episodes shorter than 6 segments are recognized as false positive and eliminated, improving in this way the success percentage of the method.

The episodes error has been used to optimize of two important parameters, temporal resolution, that is the minimum distance between two episodes such that they are recognized as distints, and the minimum duration that an episode has to have for being detected. Each of this parameters has been related to the threshold, and many combinations have been valuated (threshold- temporal resolution, threshold- minimum duration), for each of them 10 simulations have been run and the error has been reported in tables, from which it gathers that the method is able to individuate $8-10$ seconds episodes, distant each other at least 20 seconds, considering threshold set to 2 and error of 5%.

Besides it has been evaluated the delay, both in detection of the onset sample and ending sample. Have been run 40 simulations, 20 with segments of atrial fibrillation coming form Holter traces and 20 coming from the ECG traces, while the sinus rhythm segmentss have all the same origin, ECG traces. The obtained results, for both the groups are used for computing mean and standard deviation of the delay in detecting onset and ending sample of an episode. Looking at those values, it is noticeble that they are smaller for the group with atrial fibrillation segments from ECG traces, because they are less affected by noise than Holter traces, but also because of a sort of continuity with the sinus rhythm, coming from the ECG traces as well.

Real PAF After testing the method on simulated signals, a dataset of 10 patients affected by PAF has been considered, one coming from the Valencia's Hospital and the remaining nine from the Physionet Database. Each of those signals contained one or more atrial fibrillation episodes, so that in total they were 15, of variable duration from 16 seconds to 244 minutes. All those episodes were correctely detected, even if with 7 false positives and delay in detection of both onset and end of the episode; this delay has been investigated in terms of mean and standard deviation.

Discussions and Conclusions The main part of the methods, presented in literature, is based on the irregularity of the ventricular activity, described by the distribution of the RR intervals. Those methods are robust and able to accurate detection, but they have a limit: the uncapability to detect episodes of order of seconds. The purpose of this thesis has been double:

1. providing an algorithm for frequency tracking of the atrial signal;
2. developping a method that, based on the obtained frequency track, could be able to detect atrial fibrillation, above all short episodes.

For what concerns the frequency tracking, two algorithms, ANF and DFE, have been implemented with MATLAB, tested and compared. The ANF results to be the most suitable for ECG applications, for stability to different noise conditions and tracking capability of frequency changes. For what concerns the detector, it has been able to detect all episodes, even the ones shorter than one minutes, but it shows the following negative aspects:

- the generation of spurious peak (false positive episodes) that are not excluded, above all when the input signal is too noisy;
- the introduction of a delay, that has to be compensated, in order to make the method more reliable and accurate in the detection;
- the computational cost is higher than most of the detection methods, present in literature, because a QRS removal has to be done prior to the application of the method, that provides it self the running of the ANF algorithm twice.

Finally the frequency tracking with ANF deserves deeper studies and researches of its possible implications, while the detector can detect short atrial fibrillation episodes, overcoming the limit of the RR based methods, but needs of a larger number of patients to be applied to and compensation of delay and false positives, in order to compete with the other detection methods that heve been presented in literature so far.

Chapter 1

Introduction

Atrial Fibrillation, commonly known as Afib or AF, is a heart disease that consists in an irregular contraction of the atria such that multiple impulses travel through the atria at the same time and reach the atrial-ventricular node, resulting in an irregular and rapid heart rate. According to its duration, the atrial fibrillation can be classified as:

- paroxismal, where the atrial fibrillation episode can be few seconds or days long, and the heart comes back spontaneously to the normale sinus rhythm;
- persistent, where the atrial fibrillation is still present in episodes, but drugs or medical treatments are necessary to force the heart to come back to the normal sinus rhythm;
- permanent, where the heart is always in atrial fibrillation.

This disease can occur as a result of some other heart's pathological conditions, like

- left ventricular hypertrophy, an enlargement of the ventricular walls, due to extra load to the left ventricle;
- valve diseases, that can be congenital or caused by infections, calcification or degeneration with age;

- malfunction of the SA node, that produces irregularly elettrical pulses;
- hypertension, the raise up of the blood pressure.

Possible symptoms are pulpitations, chest pain and sometimes faints, but it has been found that this arrhythmia can be both symptomatic and asymptomatic and, since it is labelled like a possible risk factor for stroke and death, a lot of work is focused in its detection from a ECG signal.
The ECG feature that characterizes atrial fibrillation is the lack of the P-wave, that normally represents the atrial depolarization, and its replacement with the so called f-waves, or fibrillatory waves, that consist in a series of low amplitude waves with frequency in the range 3 to 12 Hz. Furthermore, sometimes, in presence of atrial fibrillation, the heart rate is more irregular and hence the RR-intervals have a distribution with a variance larger than normally.
From this point of view signal processing plays an important role, because even if the patient that is affected by atrial fibrillation doesn't have any symptoms, it is possible to detect the disease by analyzing and processing ECG. This is also relevant for screening operations that are recomandable, since this pathology is always more frequent in the world's popolation, above all in USA and Europe. Its incidence is related to factors like addiction, for exemple alcool and cigarettes, diabetes, and age; the latter factor is most alarming, because the popolation is getting older and this means that the number of atrial fibrillation cases is destined to grow up; hence proper and reliable tools for detection and screening are required.
There are two main pathways that can be taken in processing atrial fibrillation:

- RR-intervals precessing, considering only the ventricular activity;
- frequency tracking of the pure atrial activity

Processing the ventricular activity is one of the most common way for the detection of atrial fibrillation, because extraction procedure for the ventricular activity is simpler and returns a more reliable and accurate result than the atrial

one, since the QRS complex in the ECG is the predominant part and even in a noisy record it's detectable. Many methods based on ventricular activity have been implemented, in order to detect, classify and extrapolate information of atrial fibrillation. The most important are the followings:

- RR intervals histograms: from a 24-hour Holter recording, the histogram of the RR-intervals is computed and the shape of the histogram gives information about the peacemaker cells activity of the atrial ventricular node and their refractory period; tipically a bi-modal shape of the histogram establishes the presence of atrial fibrillation, due to a two different timing in the ventricle's contraction.

- Poincaré plot: the current RR interval is plotted versus the previous one and the plot that results has a certain pattern for regular sinus rhythm, where the points are on the main diagonal, while, in presence of atrial fibrillation, the pattern of the points is totally different, in fact it is wider and cone-shape.

These methods have the advantage to be based on RR intervals, that are computed in a robust and easy way, but they have one main limit: they are able to detect episodes that are some minutes long, because they have to take in account a certain number of RR-intervals values in order to analyze the distribution, hence they can't detect shorter episodes, for exemple some seconds long, that often characterize paroxysmal atrial fibrillation.
To overcome this limit, methods that consider the atrial activity may help.
The goal of this thesis is double: on one hand there is the implementation of an algorithm of frequency tracking to apply to ECG or Holter records, depurated from ventricular activity; on the other hand there is the development of a method that, based on the frequency signal estimated by this algorithm, is able to detect atrial fibrillation episodes on order of seconds.
Given this double goal, the thesis can be seen as divided in two parts:

1. *the first part*, made by the Chapter 3, concerns the implementation of two different algorithms for frequency tracking, ANF or adaptive notch filter and DFE or direct frequency estimator. The first one consists in processing a signal embedded in a noisy background with a notch filter whose central frequency is adaptive and the adaptation process is based on a comparison between the estimate signal and the one given by a discrete oscillatory model. The second one consists in comparing the signal (the same used with ANF) with a predicted one, where the prediction process is based on LMS algorithm, in order to reduce the mean squared error and find the prediction's coefficients that give the best estimate of the noisy signal frequency. In this chapter the results of simulations for both the frequency tracking algorithms are included in order to evaluate their performances, make a comparison between them and choose the one that works better in real noisy conditions. The signals built for tests are basically stepwise functions where each step is a sinusoid with a certain frequency, that the algorithms have to track. Tracking capability in presence of frequency variation, even very sharp, is evaluated with different noise conditions; stability and delay of the estimate are also studied. Each algorithm is tested separately, then the comparison is done. In order to make this comparison unbiased, an equivalence between the principal parameters of those filters is considered. The choice between them is made according to the best behaviour in presence of noisy conditions and quick frequency variations, that are features that characterize a real ECG signal.

2. *the second part*, made by Chapter 4 and 5, presents the developed detector that takes the frequency estimation, given by ANF, the algorithm chosen in the first part, and, by processing it, it is able to detect atrial fibrillation episodes. The feature that permits a differential detection is the different estimate that the ANF returns if its working is coupled or not with a band-pass prefilter: in fact in presence of atrial fibrillation episode the estimate

is the same, with or without prefiltering, but in case of sinus rhythm the estimate changes. So making a subtraction between the ANF estimates with or without prefiltering, a signal that has different values for atrial fibrillation and sinus rhythm is obtained and then thresholded, in order to detect atrial fibrillation episodes. Before the subctraction, some processing, such as decimation and the application of a median filter, is done, resulting in a less spiky frequency estimate. Then this detector has been tested using simulated signals, that are basically made by segments of atrial fibrillation alternated to segments of sinus rhythm, coming from different registrations, in order to reproduce the same trend of a paroxysmal atrial fibrillation signal. In this way it was known when atrial fibrillation started and ended and the performance of the detector was checked and sized, in terms of error percentage, delay, temporal resolution and minimun length of a detectable episode. The latter is particularly important because it is the advantage that this method has compared with the standard RR intervals methods, so a lot of effort has been put in reducing the length of the detectable episode. The detector has been tested in 10 patients with PAF, so it processed real signals, where the localization of onset and ending time was done manually by specialists.

This is the core of the thesis, that is enriched by Chapter 2, where the atrial fibrillation has been presented by different points of view, such as pathology, incidence, epidemiology, treatments and the contribute of signal processing in this field. At the end there is Chapter 6, where discussion and conclusions are exposed.

Chapter 2

Atrial Fibrillation

2.1 Atrial Fibrillation: a clinical overview

Atrial fibrillation (AF), is a cardiac arrhythmia that involves only the atria, the two upper chambers of the heart. It can often be identified by the pulse and observing that the heartbeats do not occur at regular intervals; symptoms are related to a rapid heart rate, palpitations, exercise intolerance and angina, but also fainting and chest pain, even if sometimes AF can be asymptomatic. The possible lack of symptoms leads to an underestimation of the AF incidence [1]. A study based on Holter monitoring over 24 hours concluded that the ratio of symptomatic and asymptomatic AF episodes was $1 : 12$ [2].
An important evidence of the presence of AF is given by the ECG signal, that is modified with respect to the normal one. An ECG signal is characterized by 3 main parts, as shown in Figure 2.1:

1. P wave, that represents the atrial depolarization, that consists in the propagation of the depolarizing stimulus generated by the pacemaker cells, in the sinoatrial node;

2. QRS complex, the most powerful part of the signal that corresponds to ventricular depolarization;

3. T wave, that is the repolarization of the ventricles.

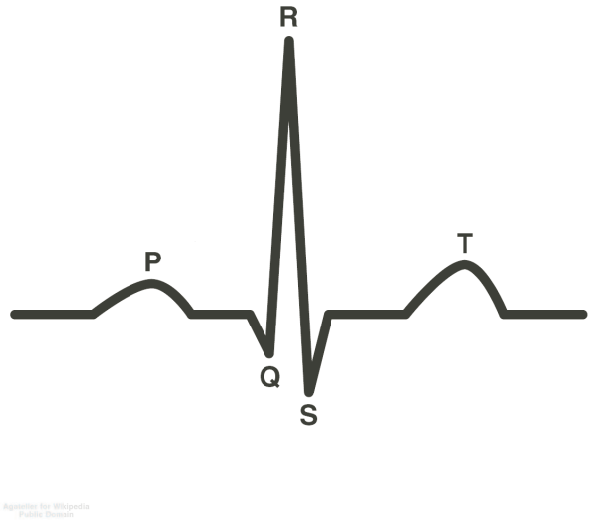

Figure 2.1: The characteristic waves of an ECG signal.

A normal ECG recording with sinus activity is presented in Figure 2.2.

Figure 2.2: ECG during sinus rhythm.

A characteristic of the AF ECG signal is the absence of the P-waves, as shown in Figure 2.3.

Figure 2.3: ECGin presence of AF.

P waves are replaced by an oscillating baseline that consists of a series of low amplitude waves, fibrillatory or f waves. Two features of the f waves are important:

- amplitude, usually classified into fine or coarse, if the amplitude is respectively smaller and larger than 50 μV [3];
- repetition rate, that is constrained to the range from 3 to 12 Hz [1].

These features do not vary randomly for an individual patient, but there are large inter-patient differences. In fact f-waves can be regular with high amplitude or irregular with low amplitude, as they can be present in both ways at the same time.
The replacement of P waves with f-waves is often accompanied by irregular ventricular tachycardia. During AF, the RR intervals are shorter than in sinus rhythm, and they have larger variability.

There are many classifications in the literature. One of the most common is the following; AF can be defined as [17]:

- *paroxysmal*, AF with duration less than 7 days, with spontaneous termination (usually after 24-48 hours);
- *persistent*, AF duration longer than 7 days, with no spontaneous termination (only with a pharmacological or electrical intervention);
- *permanent*, AF with duration longer than 7 days, with no restoration of sinus rhythm.

2.1.1 Incidence and Epidemiology

AF is the most common arrhythmia in clinical practice, accounting for approximately one-third of hospitalizations for cardiac rhythm disturbances. Most data regarding epidemiology, prognosis, and quality of life in AF have been obtained in the United States and western Europe. It has been estimated that 2.2 million

people in America and 4.5 million in the European Union have AF.

During the past 20 years, there has been a 66% increase in hospital admissions for AF due to a combination of factors including the aging of the population, a rising prevalence of chronic heart disease, and more frequent diagnosis through use of ambulatory monitoring devices. AF is an extremely costly public health problem, with hospitalizations as the primary cost driver (52%), followed by drugs (23%), consultations (9%), further investigations (8%), loss of work (6%), and paramedical procedures (2%) [4]. The number of new cases increases by 160.000 each year in the US and there is the same scenario in Europe. This trend seems to continue also in the future, because of the rise of middle age of the population. It has been estimated that in the US the number of people affected by AF will become between 12.1 and 15.9 milions in 2050, a rise of about 10 million in less than 50 years [5]: a kind of epidemic [6]. Furthermore, AF can be considered as an independent risk factor for stroke and death, more influential on elder people than young subjects affected by AF.

There are different parameters that affect the incidence of AF:

1. *age*, from the Framingham experience [7]. It is known that the prevalence of AF is dependent of age and it becomes twice after the 50^{th} year. In a trial of subjects older than 55, in The Netherlands, the prevalence of AF, estimated as 5.5%, increases by 0.7% in the age between 55 and 59 [8];

2. *gender*, AF occurs more frequently in men than in women, this is also demonstrated by a study on patients over 65, where the prevalence of AF is 9.1% in men and 4.8% in women, almost half of the male percentage. The reason for this is still unknown, but given that women's prospective of life is longer than that of the men and the AF increases the risk if stroke and death, this trend is quite reasonable [9];

3. *diabetes* [10];

4. *presence of heart diseases*, such as ventricular hypertrophy, arterial hyper-

tension, valvular heart disease or a previous stroke [11];

5. *cigarette smoking*, above all in women [12].

2.1.2 Initiation and maintenance of AF

The heart can be categorized as a muscular pump that has four chambers connected by valves. Blood flows into the right atrium into the right ventricle of the heart. The right ventricle then pumps oxygen-depleted blood through the pulmonary valve to the lungs. After the blood flows through the lungs, it returns to the left side of the heart, oxygenated, through the pulmonary veins or PV, that are two for each lung; so there are four PVs, right inferior and superior, left inferior and superior, that carry the oxigenated blood to the left atrium. Both frontal and posterior view, in Figure 2.4 and 2.5 respectively, show the disposition of the four PVs.

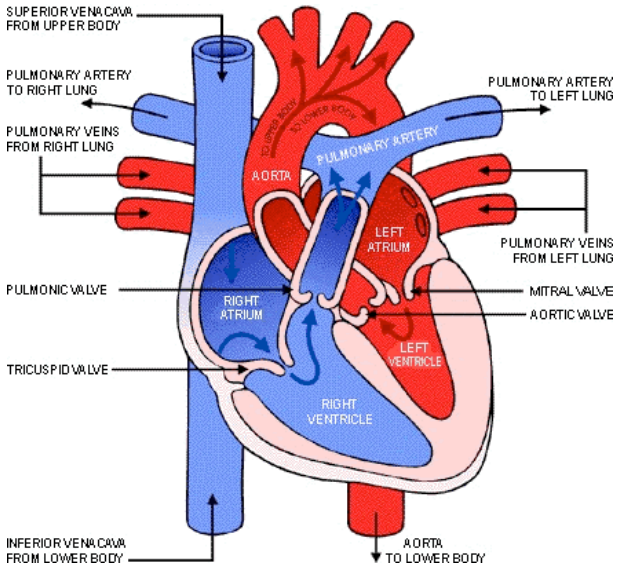

Figure 2.4: Frontal view of opened heart, where on the left and right side there the couple of PVs coming from the left and the right lung respectively.

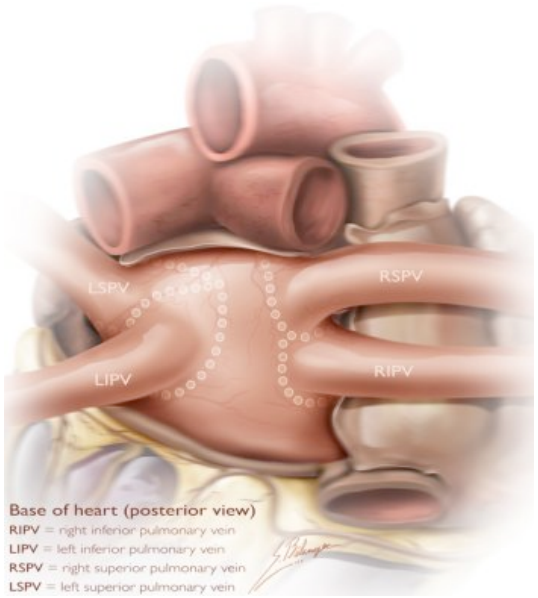

Figure 2.5: Posterior view of the left atrium, where the main particular is the insertion of the four PVs in the left atrium's wall.

The mechanisms involved in the initiation of AF are still not clear, but it seems that, even if paroxysmal, AF can be initiated in correspondence of ectopic beats generated both in the atrial tissue or in the pulmonary veins. These ectopic beats have been detected in different foci as the crista terminalis (a vertical crest on the interior wall of the right atrium that lies to the right of the sinus of the vena cava), ostium of the coronary sinus (the collection of veins joined together to form a large vessel that collects blood from the myocardium), interatrial septum (the wall of tissue that separates the right and left atria), atrial free wall and, in most of the cases, the pulmonary veins [18]. Myocardial sleeves, which are defined as extensions of left atrial myocardium over the PVs [20], play an important role in this onset. Most of the foci that initiate AF are from the superior pulmonary veins, since the myocardial sleeves in inferior PVs are less developed. Even though there are cases of patients with spontaneous AF initiated by ectopic beats originating in the superior vena cava [21].

After that the ectopic impulse is generated by one of those possible foci, the conduction system of the heart is responsible for the conduction of this impulse to

the ventricles.

The conduction system is a part of myocardium, called specific myocardium, that links functionally the atria and ventricles muscolature. It is made by different components, that are showed in Figure 2.6; they are, in activation order:

- Sinus-Atrial node, or SA node, where peacemaker cells pruduce the impulses that give to the heart the normal sinus rhythm;
- internodal tracts, where the electrical activity travels from the SA node to the AV (atrium-ventricle) node.
- Atrium-ventricle node, or AV node, which is the main responsible for introducting delay in the contraction of the ventricles respect to the contraction of the atria; without it the ventricles's contraction would happen when the ventricle is not full;
- His bundle, that brings the depolarization to muscle walls of the left and right ventricle;
- Purkinje bundle, the final part, that brings the depolarization in the muscle cells that stay deeper than the walls.

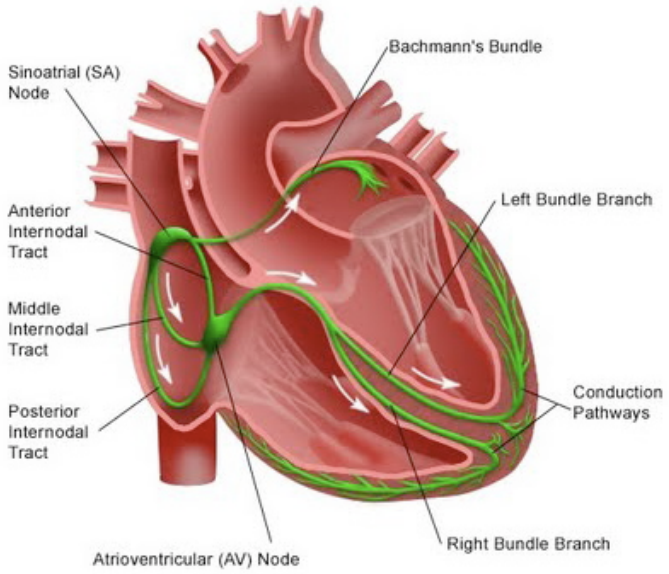

Figure 2.6: The conduction system in all its components.

This conduction system carries both elettric pulses generated by SA node, that consist in the normal sinus rhythm, and the ectopic pulses generated by one of the possible foci, abovementioned. The result is an uncoordinated contraction of the atria, unefficient for the blood driving, and an irregular heartbeat.

The research has been focused on figuring out a possible way to slow down and stop these wavelets; there are drugs to control the ventricular arrythmia. On the other hand, some institutes have published papers evaluating the location of the foci of premature atrial beats originating spontaneous onset of AF and the possibility of stopping the initiation of the fibrillation by a focal ablation [19]. Nakashima relates the initiation of AF with the appearance of rapid focal activations (RFA), which he describes as ”rapid disorganized activation with a cycle length shorter than 200 msec originating from a local site”. RFA starting on one or several of the pulmonary veins, but visible in all four PVs (as in the coronary sinus) seem to be the trigger of the fibrillation although its contribution in the maintenance of AF has not been proved.

2.1.3 Treatment

The treatment of AF has two main goals: to prevent temporary circulatory instability by using drugs for rate or rhythm control, and to prevent stroke by anticoagulation. Possible solutions are [1]:

- for stroke and thromboembolic complication, anticoagulation therapy that can persist during the whole life of the patient, above all if AF is persistent, is recommended in order to make the blood more fluent and take down the risk of formation of embolus or thrombus.
- for rate control, drugs that act on the atrio-ventricular node are often used, in order to control the ventricular activity, that performs irregularly in the presence of AF, above all in young subjects;
- for sinus rhythm restoration, there are the following options:
  - pharmacological cardioversion, using antiarrythmic drugs that sometimes are unefficient and have collateral effects that are worse than the fibrillation itself ;
  - electrical cardioversion, when AF is sustained for more than 48 hours;
  - ablation

Nowadays catheter ablation is a quite successful technique to cure paroxysmal AF. If the AF is associated to another cardiac disease, for which an invasive surgery is required, the ablation is done during the surgery. If AF is isolated, the catheter ablation is a non invasive corrective solution consiting in the insertion in a vein of the inguinal region of a catheter that reaches usually the left atrium and burns, with radiofrequency or ultrasounds or microwaves or laser, the region of PVs, the points of initiation of AF. This ablation produces a circular scar that blocks any impulses firing from within the pulmonary vein, thereby ”disconnecting” the pathway of the abnormal rhythm and preventing AF. The scars can be

many, because each of them create an electrical isolation that avoids the formation of alternative circuits for the AF pulses, that are send in blind holes, where they terminate.

The ablation with RF is the most common and there are two different types: unipolar and bipolar. In the unipolar ablation the electric circuit is closed between the catheter, placed in contact with the cardiac region to threat, and one of the electrodes that is placed on the skin of the patient, generally on posterior part of his chest wall; in this way the tissue in the middle is warmed up resistively. In the bipolar ablation instead there are two electrodes that are both in contact with the cardiac region to threat, one on each side, and, since the current flows from one side to the other one, there is a larger penetration of the tissue in the middle. Furthermore, with this procedure it is possible to clamp the blood vessel to ablate, and in this way avoiding the heat dispersion due to the blood flow in the vessel and improving the heat trasmission throught the clamped cardiac muscle.

There are many ways to lesionate the left atrium, all well reported by literature, such as the one proposed by Pappone at al. in [22]. In this study patients with paroxysmal recurrent AF were threated with radiofrequency catheter ablation by creating long linear lesions in the atria, as the Figure 2.7 shows. To achieve line continuity, a 3D electroanatomic nonfluoroscopic mapping system was used. Another method, still proposed by Pappone at al. in [23], consists in isolating each PV from the left atrium by circumferential radiofrequency lesions, put in evidence in Figure 2.8, around their ostia. Also for this method a 3D electroanatomic nonfluoroscopic mapping system was adoperated.

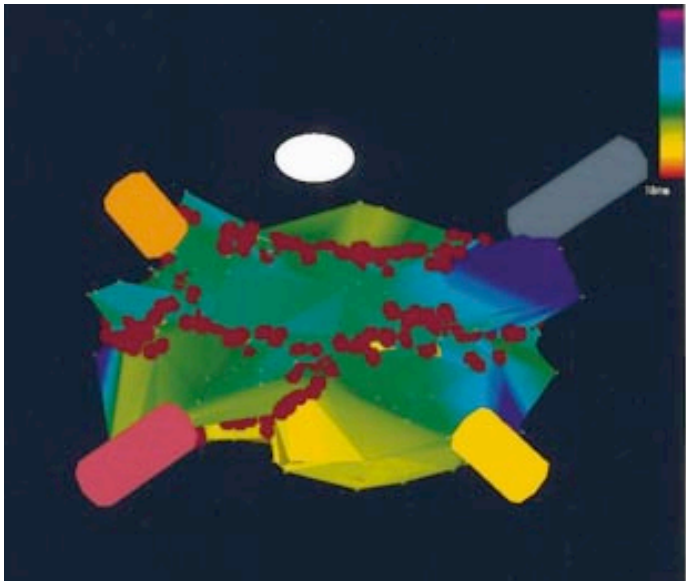

Figure 2.7: A 3D left atrium map is shown where the red dots represent the ablation points, set in a reticular patter, made by lines that have anatomic continuity. Reprinted from [22].

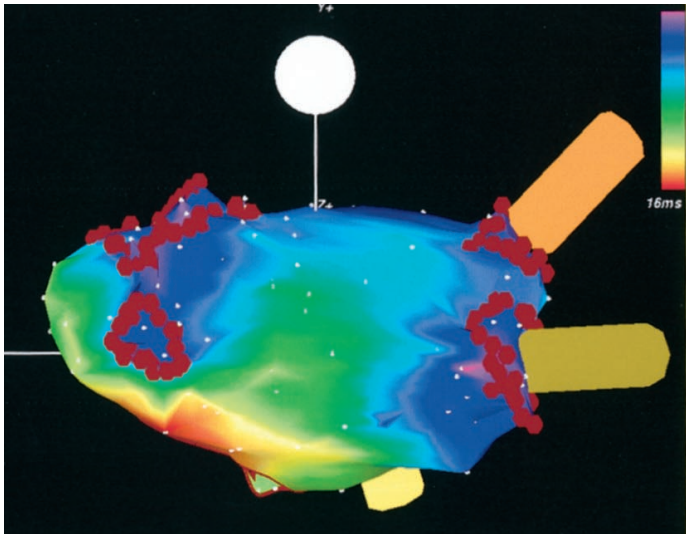

Figure 2.8: A 3D left atrium map is shown where the red dots represent the ablation points, all located roundly around the ostium of each PV. Reprinted from [23].

.

Haissaguerre et al. in [24] evaluated instead the extention of ostial ablation necessary to electrically disconnect the pulmonary vein from the left atrium, starting by the distrubution of the activation points of the PV muscles; they found

that there are specific breakthroughs from the left atrium that allow ostial PV disconnection by use of partial perimetric ablation, instead of running through the whole perimeter. In another study, [25], the end point for the catheter ablation was investigated in patients with drug resistent AF. The RF ablation was applied to all the PV points that generated arrythmia, considering the end point the total elimination of ectopy and of the muscle conduction; with this rationale, the follow up for the threated patiens was succesful.
To determine if ablation is an appropriate treatment, a thorough evaluation will be performed, which may include:

- A review of the subject's medical history,
- Complete physical examination,
- Electrocardiogram (ECG),
- Echocardiogram,
- Holter monitor test.

The success of the ablation procedure also depends on a good knowledge of the heart's anatomy, since PVs characteristics (number, location and size) differ from patient to patient [13]. Thereby it is indispensable to perform imaging of the left atrium and the pulmonary veins in order to avoid procedure-related complications during and after the invasive process; even if the safety of catheter ablation of PVs and left atrium has been demostrated, some other complications as cerebral emboli or PV stenosis may occur. Advanced techniques such as computer tomography (CT) and magnetic resonance angiopraghy (MRA) provide useful information not only for chosing the best location for the ablation, but to analyze the results of the procedure afterwards as well. Some other imaging methods may be used, such as:

- *Fluoroscopy*,

- *Intracardiac echocardiography (ICE)*,
- *Nonfluoroscopic 3-dimensional catheter navigation*,
- *Image integration*.

Basically, most of the attention on AF is focused on the two main goals:

- identification of AF initializing triggers and their ablation;
- identification of patterns that affect ECG when AF occurs, in order to target the area that are responsible for the maintenance of reentry circuits of AF.

The first point has been discussed in this first section, the second one will be developed in the next section.

2.2 Signal processing: detection and monitoring of AF

As mentioned at the beginning of this chapter, surface ECG carries useful information for detecting the presence of AF as well as some other heart diseases such as atrial flutter or sinus tachycardia. Recording systems such as the Holter monitor entail minimum risk for the patient and tape the heart activity for 24 or 48 hours so that AF can be classified in terms of duration. Nevertheless it is not totally reliable since it does not have any control over the recording conditions. For instance, it is not easy to measure the influence of body movements or exercise activities on the ECG. It is recommended, in this case, either or ask the patient to keep a recording of daily activities in order to avoid wrong interpretations of the signal obtained or develop more complex systems [26]. It is also possible to transmit the heart rhythm and have real time monitoring. These devices are called transtelephonic monitors and even though they could record abnormal rhythm whenever the patient feels that it has started, are mostly used by pacemaker patients for home routine scheduled checkups.

Signal processing techniques can be applied to the recorded ECG in order to analyze the ventricular and atrial activity and thereby, describe the behaviour of the heart not only during the AF but also before and after; a good tracking of the fibrillatory wave frequency provides, for instance, the specialists with a basis for predicting the initiation of AF and allows them to observe the patient's response to different treatments such as drugs or ablation procedures [1].
Both atrial and ventricular activity can be useful for the characterization of AF, because permit the extraction of different information corcerning this patology.

2.2.1 Ventricular Activity Processing

In matter of AF, the ventricular activity is used to both make detection of episodes (some methods will be cited and described in Chapter 4) and to extract information about initiation and maintenance of AF. This Paragraph deals with methods developped in order to investigate the correlation between the ventricular arrhythmia, caused by AF, and the conduction system of the heart.
In the main part of the patients with AF, it is present the alteration of the ventricular activity. This is basically caused by the conduction of the atrial impulses to the ventricles. The responsible for this conduction is the AV node. The state of art is now focused on the possible correlation between the AV conduction pathways and the variation of the ventricular activity, when AF occurs. In fact the ventricular activity seems to be chaotic and uncorrelated but there are in literature studies suggesting tools capable to underline hidden coerence anc correlations. Those tools are the following [1]:

- the RR-intervals histogram
- the Poincaré plot
- the Poincaré Surface Profile

The RR-intervals histogram This tool plays an important role in the analysis of the conduction rate of the AV node, because from the pattern of the histogram, uni or multi modal, considerations have been done about the possible pathways of the conduction, like the bi-modal pattern that is a ”sympton” of a dual working of the AV.

The tecnique used to construct the histogram is the so called Heart Rate Stratified Histogram [1]; segments of ECG made by a constant number of beats are exctracted, then the mean of the RR-intervals of the beats belonging to the each segment is computed, so that each segment is classified into an heart rate level. The segments can be overlapped and there are recluting rules for the beats, such as noise absence and the normality, that means that if a beat is considered as abnormal, its interval is not taken in account for the histogram and with it also the previous and the next one. With this method there is a reduction of the possible clusters of intervals to only two families, so that the patterns are or uni or bimodal. Finally, smoothing is performed in order to uniform the peaks belonging to one of the two families and the location of the principal peak of a family is yielded by a second order polynomial, passing by the highest bin and four adjacent ones.

At the end, with this procedure two peaks are distinguishable and the highest is named as dominant peak, while the second as non dominant and, according to the length of the RR-interval, they represent the slow and the fast peak values. The dominance of the peaks depends on the heart rate, in fact at lower heart rate, the dominant peak will be placed at RR-intervals values, larger than the ones occupied by the dominant peak in case of higher heart rate. During the raising of the heart rate, it can be noticed the traslation of the dominant peak from larger to shorter values of the RR-intervals.

A bimodal histogram is observed in many patients affected by AF and, as abovementioned, it may suggests the presence of two different pathways for AV to conduct the fibrillatory pulses of the atrium to the ventricles, with the result of

ventricles arrhythmia. This duality may be caused by two refractory periods that divide the AV node in a distal and proxymal region, with a different conduction rate each. So one of the possible application of this histogram pattern is to be an outcome predictor for the ablation procedure with radiofrequency of the AV node.

An exemple is the study of Rokas et al. [35]. In this study 32 patients with chronic AF were considered, to whom an ablation procedure had to be performed. For each patient the day before the ablation, the HRSH was computed on a 24h ECG recordings; the histograms had uni, bi, multimodal pattern. Then the ablation procedure came and for the ones with a successful result, no symptoms or minimal symptoms were registred. For the 25 patients that had a bimodal histogram, the ablation was successfull and it provided the elimination of the RR population with short RR-intervals, such Figure 2.9 shows:

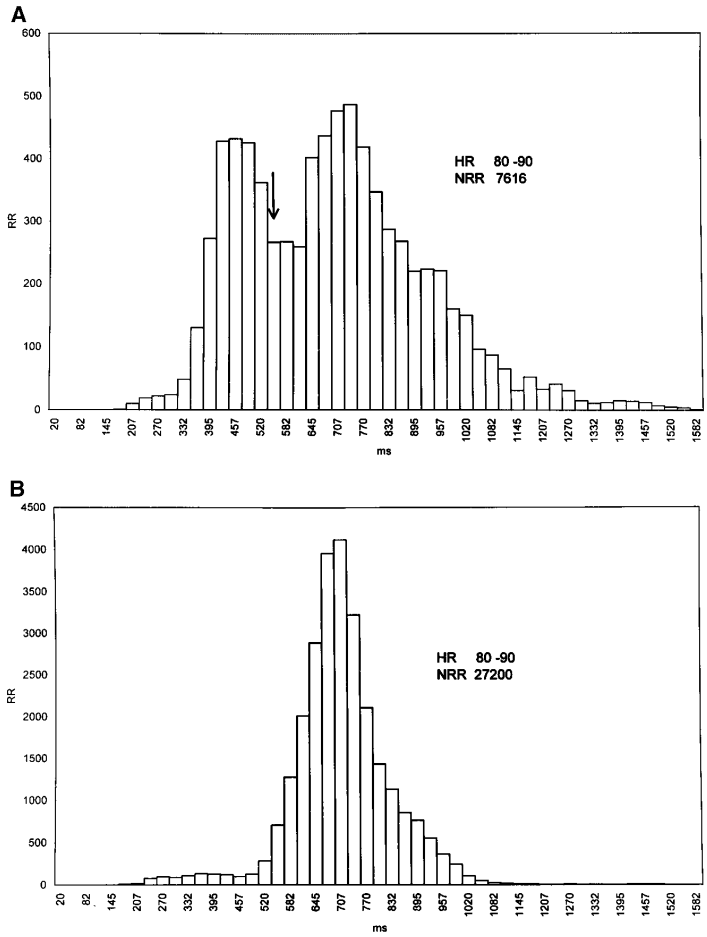

Figure 2.9: A: Bimodal pre-ablation pattern of RR interval histogram. B: After successfull ablation the bimodal patter shifted to the unimodal distribution, with an increase of number of RR intervals at the same heart rate. Reprinted from [35].

The rate of success in patiens with bimodal distribution was 94%, while for half patients with unimodal pattern the procedure failed or provided AV block. Furthermore a small number of ablative attempts, and fluoroscopy evaluations, was used for the bimodal pattern patients, while in the unimodal ones, almost twice attempts and fluoroscopy time were necessary. The conclusion of this study was the the morphology of the RR-interval histograms reflects the electrophysiological properties of the AV node, despite it is reasonable correlating a bimodal distribution of the RR intervals with atrial fibrillation and finally by checking the elimination of the population with short RR interval from the his-

togram, a ventricular rate control is achieved.

The Poincaré plot It is still a representation based on the RR-intervals distribution, but with an additional information about the sequence of the intervals, in fact each interval is plotted versus the preciding one, generating plots that permit to distinguish sinus rhythm, flutter and AF [1]. The lower envelope of the plot is retained to be an estimate of the cicle length dependence from the firing rate peak of the AV node. This can be calculated with a linear regression, fitting a certain number of points, where each represent the minumum of all the point belonging to the same bin. Anyway this tecnique is not robust enough in presence of outliers, so better ways are used, such as the Hough transform, that aims to find the slope and the intercept of the line that should be the lower envelope of the Poincaré plot. Those parameters have been used to describe the dependence of the firing rate peak from the conduction of AV node.
In the Poincaré plot of patients with AF with a bi-modal histogram , a double sector shape is individuated, where the vertex are indicative of the firing rate peak of each population of the bi-modal histogram, as Figure 2.10 shows.

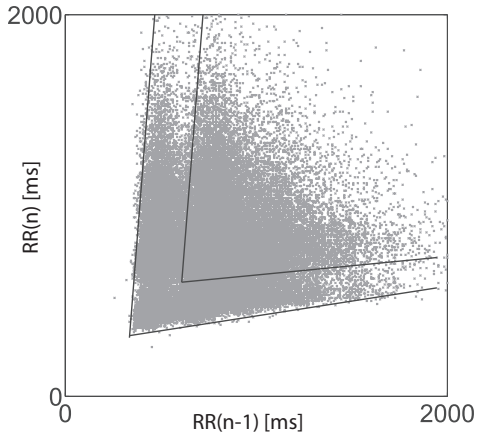

Figure 2.10: The vertices of the sectors are evidenced handly: the leftmost one is representative of the slower pathway of the AV conduction, while the rightmost one of the faster pathway. Reprinted from [1].

The Poincaré Surface Profile This method, known also like Bidimensional Histogram Surface, has been suggested by [36] and it is focused on the so called preferential RR intervals that can be found in histograms of AF patients. Here the histogram is not computed like HRSH, because all the population of RR intervals are required, since the goal is trying to correlate the preferential intervals with the refractary period of the AV node. In fact the main limitation of the HRSH is the low sensibility, due to the fact that patients with uni modal histogram can still have a double conduction pathway of the AV node and a bimodal distribution can be present even in patients that have been threated [37]. The ventricular responce variability tells more than it seems, so analysis of larger points of view are necessary.

This plot can be constructed by adding the number of occurences of RR-intervals pairs to the regular Poincaré plot, and then filtering with a two dimensional Gaussian low-pass filter, so that the peaks are evidenced and the noise around the peaks is reduced. The identification of the local maxima is performed with a three steps procedure that tests:

1. the slope, that has to change from positive to negative;
2. the amplitude, that has to exceed a threshold;
3. the distance between two identified peaks, that has to be large enough.

The local maxima are the preferential RR intervals and they have been compared with the dominant atrial cycle length, discovering that the position of preferential RR intervals is correlated with multiples of atrial rate during AF. This shows that ventricular activity in presence of AF can't be threated like chaotic and irregular , but it contains correlations that are important for monitoring effects of rate control pharmacological threatments, nowdays preferred to the approach of restoring and maintaing of the sinus rhythm.

2.2.2 Atrial activity extraction

The atrial activity needs to be extraced from the ECG trace. The SNR of the residual ECG will depend on the quality of this extracting methods and the amount of signal remaining from the ventricular activity and other noisy artifacts. The main difficulty in this process is the low amplitude of the desired signal which has values from 0.02 to 0.12 mV. This can be first tackled by choosing the signal obtained in the leads II or V1, represented in Figure 2.11, where the f-wave to QRS-T signal ratio is larger [27]. In the case of V1, the mean amplitudes of R and S waves, in a normal heart, are 0.14 and 0.58 mV respectively [28].

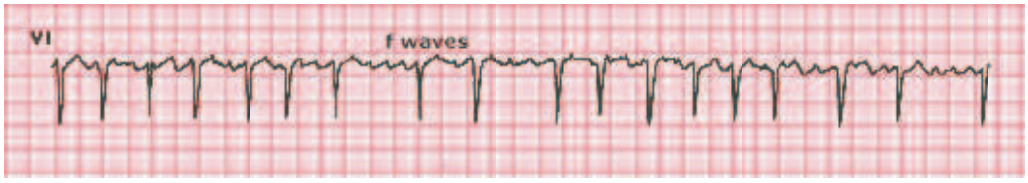

Figure 2.11: Capture of the lead V1 in an AF episode.

There are two paths that lead to this atrial signal;

- investigate ECG segments where ventricular activity is not present (basically avoiding QRS complexes);
- consider the resulting ECG after the cancellation of the ventricular activity.

The former approach has to analyze the entire ECG signal, while the latter approach takes in account only the TQ intervals. So usually, in order to be more accurate, several methods have been implemented with the goal of atrial activity extraction and those are not simply linear filtering procedure, since the spectral profile of atrial and vetricular activity are overlapped. Here are presented the most cited methods in literature.

average beat subtraction (ABS) The central idea is to compute an average beat, that has to represent the ventricular activity, and subtract it to a single lead

ECG recording, such that the result is the atrial activity with the f-waves. The base assumption is that during AF the atrial activiy is uncoupled with the ventricular activity, so the subtraction does not cut off any samples of atrial activity. The average beat is computed as average of sinus beats, or rather the median that is a more robust estimate, and the result of the subtraction is more satisfactory if the taken in account sinus beats are numerous, while the result gets worse if there are in the processed record ectopic beats, beacuse they have a different morphology, so, prior to the subtraction, an average beat has to be computed for each of them. Finally, the necessary condition for the success of this method is the temporal alignment of the QRST complex, because in this way the subtraction's result will not have any QRST samples. This method is used very often, but it has the main limit to be based on single lead records, that are sensitive to variations of QRST morphology, due to respiration and muscle activity that make the electrical axes of the heart change position. The next method tries to overcome this limit.

spatiotemporal QRST cancellation The rationale is the same of ABS, but the average beat for each lead is a combination of itself and the average beats coming from adjacent leads. So instead of having X, the recorded matrix, as a column vector with M samples from a single lead, now the matrix is rectangular, MxL, where L is the number of considered leads. Given the same assumption of the ABS, the matrix can be seen as the sum of atrial and ventricular activity, plus a noise matrix [1].

$$X = X_a + X_v + W \tag{2.1}$$

The goal is the estimate of the ventricular activity and its subctration from X. The computation of the matrix X_v takes the following steps:

- express the ventricular activiy in this way:

$$X_v = J_\tau X S \tag{2.2}$$

where J_τ is the shift matrxix that permits the temporal alignment, and S is the spatial alignment matrix

- express the shift matrix in this way:

$$S = DQ \tag{2.3}$$

where D is a diagonal scaling matrix that takes into account the variation of the heart position and tissue conductivity and scales the leads amplitude, while Q is a rotation matrix.

- estimate D, Q and τ, hence the X_v.

- cancellate the estimated QRST complex.

The improvement given by the multi-lead approach of QRST cancellation is visible in Figure 2.12, where the two methods have been applied and the QRST one returns an atrial activiy with a minor presence of ventricular samples.

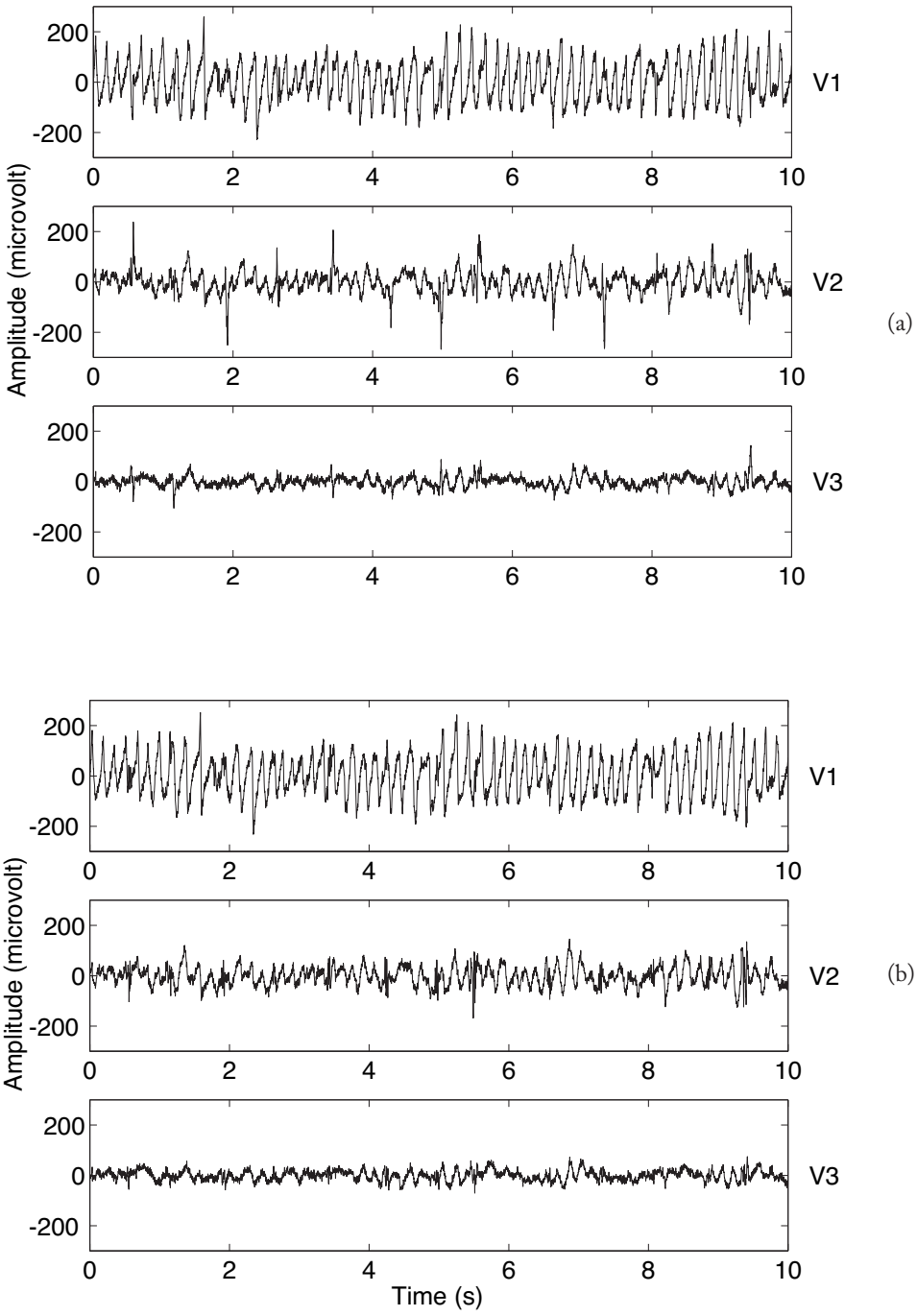

Figure 2.12: Atrial activity extraction of a three leads recording, with (a) ABS, (b) QRST cancellation. Reprinted from [1].

single beat cancellation The approach considers one heatbeat at time and provided the extraction of atrial activity from ECG records means two steps:

1. estimating the T wave, representative of the depolarization of the ventricles, and subtracting it from the ECG. T wave has almost the same morphology in different leads, this is why it is also called dominant, and it is evaluated with the Singular Value Decomposition of the X matrix, a MxL matrix, where M is the number of the JQ intervals and L is the number of the considered leads.

2. estimating the atrial activity that is contained in the QRS complex throught sinusoidal interpolation of atrial activity of the two JQ intervals, surrounding the QRS.

Finally, for each heartbeat, the collage between the untuched P wave and the estimate of the atrial activity during the QRS is done, being carefully to jumps at the interval boundaries.

principal component analysis (PCA) The key concept of this method, and also of the next one, is that the atrial and ventricular activity come from different elettrical sources, and what is recorded from the body surface by the ECG electrodes, supposed to be linear, is a mix of those sources. So the X matrix is now called mixing matrix and the assumptions that are made about the sources's properties and their relations give the structure to this matrix. In the PCA analysis, sources are uncorrelated with each other and the mixing matrix is orthogonal. The analysis can be sigle lead or multi-lead, but in both cases the PCA is able to estimate ventricular activity by projecting each beat in the ventricular subspace, that is created by the combination of the ventricular eigenvectors, since usually the eigenvectors corrisponding to the larger eigenvalues are representatives for QRST complex. So the goal is the computation of a template for the QRST complex to subtract to the ECG trace, like the ABS, but with a better result.

independent component analysis (ICA) Here different assumptions are made about the sources $s(n)$: they are statistically mutually indipendent at each instant

time, with a non Gaussian probability density function. The mixing matrix, here called A, is unknown, so the separation of the sources in ventricular, atrial and other ones, is "blind". The sources and the mixing matrix are so related:

$$x(n) = As(n) \tag{2.4}$$

The goal is to estimate $s(n)$, but, given its high order statistics, a transformation is required.

$$y(n) = Bx(n) \tag{2.5}$$

where $y(n)$ has indipendent components and B is the transformation matrix, that is evaluated by the maximization of a function that is measure of statistical indipendence, such as the kurtosis.

2.2.3 Atrial Activity Processing

In signal processing there are two main approaches that deal with atrial activity frequency:

- Frequency analysis, a static approach that is focused on the determination of the location of the dominant spectral peak in ECG signal during AF;
- Time frequency analysis, a dynamic approach that aims to evaluate the variation in time of the spectral peaks.

Frequency analysis After the extraction of the atrial activity through one of the aforementioned methods, the power spectrum of the residual signal is computed and the main peak corresponds to the principal fibrillatory rate. This power spectrum analysis can be parametric or nonparametric. Most studies make use of nonparametric, Fourier-based spectral analysis in which the ECG signal is divided into shorter, overlapping segments, each segment subjected to windowing. The desired power spectrum is obtained by averaging the power spectra of the respective segments (e.g. Welchs method).

The length of the segment is an important parameter to set. It has to attend to:

- accuracy. If the segments are quite long, the estimate is less spiky, the computation is faster, but the accuracy is not satisfying. On the other hand, if the length of the segment is chosen to be smaller, then an higher accuracy is achieved, paying it with a longer computation.

- spectral resolution; it determines how close two peaks can be located to be detected as different. From this point of view, longer segments provide a good spectral resolution.

It is considered more important to identify the main frequency peak in the fibrillation signal accurately so this feature is preferred to spectral resolution. In parametric spectral analysis an important operation is sampling rate decimation, in order to avoid the presence of spurious spectral peaks [30]. From a clinical point of view, the evaluation of the main fibrillatory rate is relevant for many applications, such as the prediction of AF termination or the identification of candidates for pharmacological cardioversion [1].

As it has been said above, this kind of analysis can be defined as static, because it does not catch the time variability of the AF frequency that can be helpful information for example to explain some multimodal peaks that sometimes characterize the power spectrum; this may be due to temporal variation of AF frequency [31]. In this context, the time frequency analysis has found its way, so it moves from the main limitation of the Fourier Analysis, the inability to track temporal variation of fibrillatory rate, and characterizes variation on the location of the spectral peak.

Time Frequency Analysis Time frequency analysis goal is to evaluate the temporal distribution of the AF frequency. The dynamic of the frequency is clinically important to determine how the electrical activation wavefront behaves during AF in the atria and how time dependent properties of fibrillatory waves

are related with the atrial activation. With time-frequency analysis, it is possible to track variation in AF frequency, that may be due to an intervention or it can be physiological, like the influence of the parasympathetic and sympathetic stimulation, that makes the AF frequency decrese during the night and increase in the morning [32].

So far different appraoches have been elaborated, such as:

- *STFT*, short term Fourier transform, a linear time frequency distribution, rather, that depends linearly on the signal $x(t)$. Basically the signal to be transformed is multiplied by a window function which is nonzero for only a short period of time. The Fourier transform (a one-dimensional function) of the resulting signal is taken as the window is sliding along the time axis, resulting in a two-dimensional representation of the signal. X(τ,ω) is essentially the Fourier Transform of $x(t)w(t-\tau)$, a complex function representing the phase and magnitude of the signal over time and frequency. The magnitude squared of the STFT yields the spectrogram of the function.

$$X(\tau,\omega) = \int_{-\infty}^{\infty} x(t)w(t-\tau)e^{-j\omega t}dt \tag{2.6}$$

$$spectrogram\{x(t)\} = \mid X(\tau,\omega) \mid^2 \tag{2.7}$$

  An important feature in this scenario is the resolution. The width of the windowing function relates to how the signal is represented: it determines whether there is good frequency resolution (frequency components close together can be separated) or good time resolution (the time at which frequencies change). A wide window gives better frequency resolution but poor time resolution. A narrower window (said to be compactly supported) gives good time resolution but poor frequency resolution. These are called narrowband and wideband transforms, respectively.

- *Wiener Ville distribution and Cross Wiener Ville distribution* where the dependency on the signal $x(t)$ becomes quadratic, instead of linear. This

leads to an improvement of resolution both in time and in frequency, even if there is the introduction of cross terms. In the Cross Wiener Ville distribution, the innovation consists of adding to the normal Wiener Ville distribution an iterative procedure to better estimate the wanted frequency [1]

- *Spectral Profile Method* that tries to overcome the limitations of the WVD, putting more attention to the harmonic component of the power spectrum, since it has been shown that the harmonic components can be a feature that characterizes AF episodes. Furthermore, those harmonic components can give an idea of what the degree of organization of the AF is; this is the reason why, in this context, the organization index is introduced, defined as the ratio between the area under the considered harmonic and the total area under the power spectrum. With this method the peaks become more distinct, because of operations such as fequency shifting, amplitude scaling and spectral averaging; hence the detection of harmonics component in the atrial signal is facilitated [1] .

Chapter 3

Description of the applied algorithms

3.1 Introduction

The goal of this chapter is to illustrating the two algorithms that have been analyzed and tested in order to be applied later on to ECG signals. They are:

1. Adaptive Notch Filter (ANF) based on a discrete oscillator model
2. Direct Frequency Estimator (DFE) applying the LMS algorithm

Both of these algorithms estimate the frequency of a sinusoidal signal in noise, but they operate in different ways. The first one resorts to a bandpass filter whose central frequency moves depending on the minimization of the error that considers the application of the oscillator model. The bandwidth is quite narrow and this is the reason why the filter is labeled as Notch Filter. The second one implements a predictor, that gives an estimate of the wanted sinusoid as a combination of previous input samples and of a cosine factor, whose frequency is the estimate of the real one and it is adaptively updated by the application of the LMS algorithm. Those two algorithm belong to the algorithms family that makes an estimate of the main frequency to nonstationary signals, where the main frequency

can suddenly change. Therefore a good tracking of the frequency is a required property of those ones, above all because of their future application to biological signals. This is the reason why more classical techniques are not considered, such as the Maximum Likelihood or Pisarenko's harmonic retrieval method, that provide a more accurate main frequency estimate, but only in case of stationary signals. In time-frequency analysis the input signal, that corresponds to noisy f-waves, is divided in shorter time segments that can de overlapped. Some spectral analysis i.e. short-term Fourier transform, is applied to these segments, keeping in mind that the time-frequency resolution obtained will depend on the length of the segments. The spectral profile method [1], which is based in the same principles as the other time-frequency analysis, can be applied to atrial signals as well. In this case, not only the fundamental frequency but also the harmonics of the f-waves are considered.

3.2 Algorithms

3.2.1 Adaptive Notch Filter

This algorithm has been proposed for the first time by Ho–En Liao in [33], and its goal is to identify the main frequency of a sinusoid component embedded in a noisy background, using an adaptive notch filter.

The input signal is considered like the sum of a sinusoid component $d(n)$ and a zero mean noise $w(n)$:

$$u(n) = d(n) + w(n) \tag{3.1}$$

The innovation is the introduction of a oscillator discrete model for the updating of the filter coefficients, according to the sinusoid component should satisfy the oscillator equation:

$$d(n) = 2\alpha d(n-1) - d(n-2) \tag{3.2}$$

where α is a parameter that is related to the desired frequency by the relation:

$$\alpha = \cos\omega \tag{3.3}$$

The notch filter is implemented with a second order band pass filter (BPF), whose bandwidth is controlled by a parameter, β, through the following relationship:

$$\Delta\omega = \arccos\frac{2\beta}{1+\beta^2} \tag{3.4}$$

The filter is a second order filter with zero phase shift, unit gain at the central frequency and the transfer function given by:

$$H(z;n) = \frac{1-\beta}{2}\frac{1-z^{-2}}{1-\alpha(n)[1+\beta]z^{-1}+\beta z^{-2}} \tag{3.5}$$

In order to derive α in mean square sense, the minimization criteria is applied to the following cost function

$$J = E\{[x(n) - 2\alpha(n+1)x(n-1) + x(n-2)]^2\} \tag{3.6}$$

Putting the gradient of this cost function w.r. to $\alpha(n+1)$ equal to zero, the expression for the filter coefficients is

$$\alpha(n+1) = \frac{E\{x(n-1)[x(n)+x(n-2)]\}}{E\{2x^2(n-1)\}} \tag{3.7}$$

This solution to the optimization problem is found mathematically, but it is not real time computable, so both numerator and denominator are replaced by their exponentially weighted time average estimation, named $P(n)$ and $Q(n)$

$$Q(n) = \delta Q(n-1) + (1-\delta)x(n-1)[x(n)+x(n-2)] \tag{3.8}$$

$$P(n) = \delta P(n-1) + (1-\delta)x^2(n-1) \tag{3.9}$$

where δ is the parameter that controls the updating rate.

Then the coefficient updating algorithm becomes:

$$\alpha(n+1) = \frac{Q(n)}{2P(n)} \tag{3.10}$$

The estimated coefficient is one step ahead, in fact at time index n, the updated coefficient is at time index $n + 1$. When the adaptation process ends, the steady α represents the estimate of the frequency of the sinusoid component embedded in the noisy background, that has to be identified. Therefore the input signal $u(n)$ is filtered with the BPF, whose transfer function is (1.5) and the extracted component has only one frequency and behaves like a sinusoid.

This implementation takes up the adaptive line enhancer (ALE), with the difference that the reference signal is not just a delayed version of the input, but satisfies the discrete oscillator model, the real innovation of the algorithm.

The application of the MSE minimization criterion guarantees three features:

- the achieved estimate is unbiased;
- the learning curve of α does not need smoothing;
- the convergence rate is faster than some other methods, i.e. Constrained Minimization Updating algorithm, also discussed in [33].

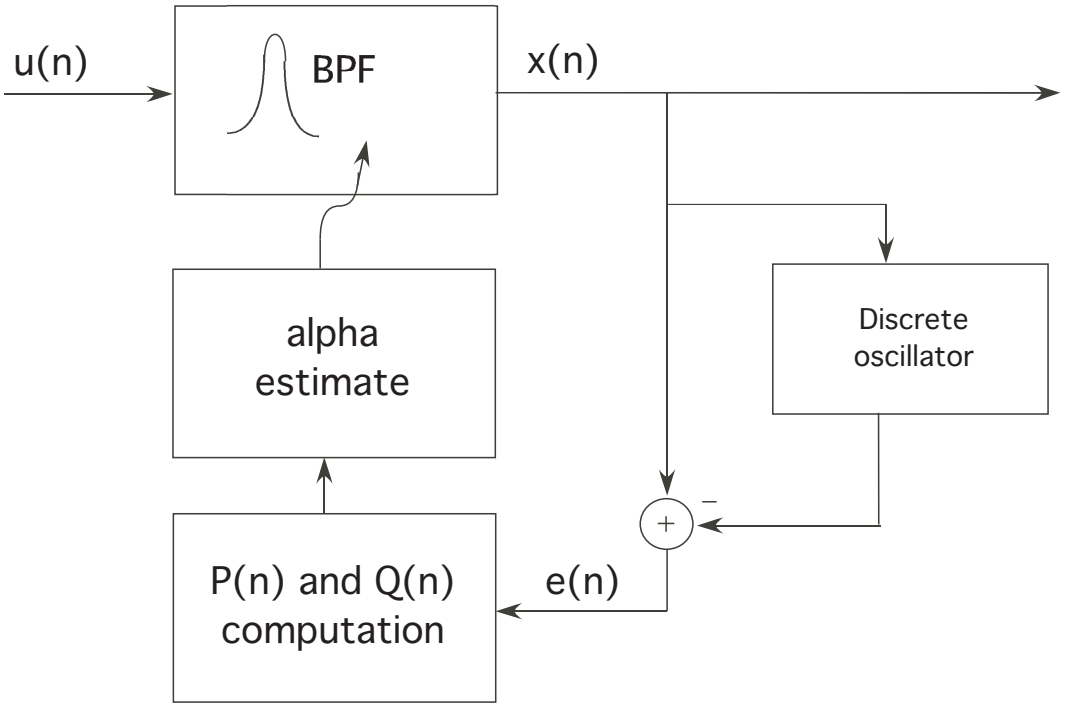

Figure 3.1: Block scheme of the ANF.

In the Figure 3.1, it is represented the block scheme of this Adaptive Notch filter based on the discrete oscillator model. As will be shown, when processig real signals a pre-filter will be placed before the Band Pass Filter since the frequency expected for the f-waves is constrained to the range between 3 and 12Hz. As a consequence, the SNR of the signal at the input will be increased.

3.2.2 Direct Frequency Estimator

This algorithm has been proposed in [34] and it applies the LMS algorithm in order to minimize a linear predictor cost function. The noisy sinusoid is represented as

$$x(n) = s(n) + q(n) \tag{3.11}$$

where $s(n)$ is the sinusoidal component; its amplitude, frequency and phase are unknown.

$$s(n) = \alpha cos(\omega n + \phi) \tag{3.12}$$

$q(n)$ is the noise component, defined as a zero mean white random process, with unknown variance σ_q^2 . Since all the information about $s(n)$ are unknown, an estimate is computed as expression of the measured signal $x(n)$

$$\hat{s}(n) = 2\cos(\hat{\omega})x(n-1) - x(n-2) \tag{3.13}$$

This is a linear predicted version of $s(n)$ based on the frequency $\hat{\omega}$, the estimate of ω. Defining the linear error as the difference between the measured signal and the predicted one, at time index n

$$e(n) = x(n) - \hat{s}(n) \tag{3.14}$$

the cost function to minimize is given by the expected value of the mean square error $e(n)$.

$$E\{e^2(n)\} = 4[\cos(\hat{\omega}) - \cos(\omega)]^2\sigma_s^2 + 2[2 + \cos(2\hat{\omega})]\sigma_q^2 \tag{3.15}$$

where σ_s^2 is the sinusoid power and defined as $\alpha^2/2$. Assuming that the noise power is unknown, a scaled version of the cost function is considered instead.

$$E\{\zeta^2(n)\} = \frac{E\{e^2(n)\}}{2[2 + \cos(2\hat{\omega})]} + \sigma_q^2 \tag{3.16}$$

The minimization of this scaled cost function is equivalent to the minimization of the previous cost function, because of the introduction of the following constraint: $2[2 + \cos(2\hat{\omega})]$ has to be constant. This kind of approach can be seen as a specific application of the unbiased impulse response estimation algorithm, derived from minimizing the mean square value of the equation error under a constant norm constraint. The LMS application requires the gradient of the cost function in order to update the frequency coefficient, so the partial derivative w.r. to $\hat{\omega}(n)$ is computed

$$\frac{\partial\zeta^2(n)}{\partial\hat{\omega}(n)} = \frac{\sin\hat{\omega}(n)}{[2 + \cos(2\hat{\omega}(n))]}e(n)[(x(n) + x(n-2))\cos\hat{\omega}(n) + x(n-1)] \tag{3.17}$$

The quotient $\frac{\sin\hat{\omega}(n)}{[2+\cos(2\hat{\omega}(n))]}$ does not change sign for $\hat{\omega}(n)$ between 0 and π, it does not affect the gradient sign either, so it can be neglected such that the updating equation of the LMS is simplified:

$$\hat{\omega}(n+1) = \hat{\omega}(n) - \mu e(n)[(x(n) + x(n-2))\cos\hat{\omega}(n) + x(n-1)] \quad (3.18)$$

μ is the step size of the adaptive algorithm and it is chosen as a trade off between speed of convergence and variance, but always belonging to the range that guarantees stability and convergence; this range for LMS filters is [0, $1/2\sigma_s^2$]. At each iteration, the predicted version is improved and when the error goes to zero, the adaptation process stops, the frequency coefficient after convergence is the optimal and represents the main frequency of the sinusoid component of the signal that has to be identified.
There are some observations that can be made:

1. The stability of the DFE is checked by the evaluation of the expected value of the gradient in $\hat{\omega} = \omega$, and it gives

   $$E\{e(n)[(x(n) + x(n-2))\cos\hat{\omega}(n) + x(n-1)]\} = 2\sigma_s^2 \sin\omega(2\cos^2\omega + 1) \quad (3.19)$$

   that is an always positive quantity for ω in the range(0, π).

2. Considering the local convergence of $\hat{\omega}(n)$ that approaches to ω, it can be shown that the convergence rate does not depend on the noise level.

3. The LMS responds to the requirements of good tracking, accurate estimation and computational complexity.

4. The RLS algorithm is also another option, that returns a smaller variance of the frequency estimate, but it requires a larger amount of calculation than the LMS.

Figure 3.2 shows the block scheme of the DFE algorithm.

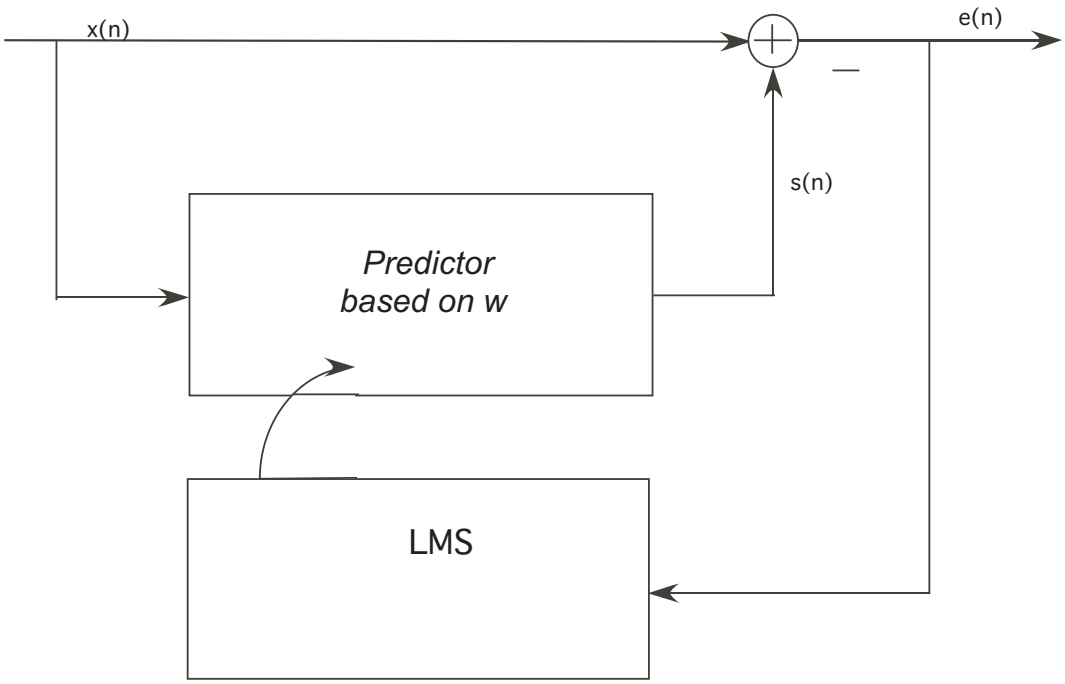

Figure 3.2: Block scheme of the DFE

3.3 Tests on the algorithms

3.3.1 The ANF algorithm Performance

There are many features that need to be tested on a simulated signal, in order to check the correct functioning of the algorithm, before its application to the real ECG signal. Those features are:

1. adaptation of the central frequency of the BPF to the input frequency;
2. tracking of the frequency changes in the input signal;
3. influence of additive noise;
4. influence of the filter parameters (β,δ).

To test the first property, a simulated signal is generated as a sinusoid of 2000 samples with frequency equal to 9Hz, then the frequency responce of the band

pass filter (BPF) is computed and normalized to the maximum value. At each iteration the main peak of this spectrum changes its position until it is in correspondence with the input frequency; then the adaptation process ends.

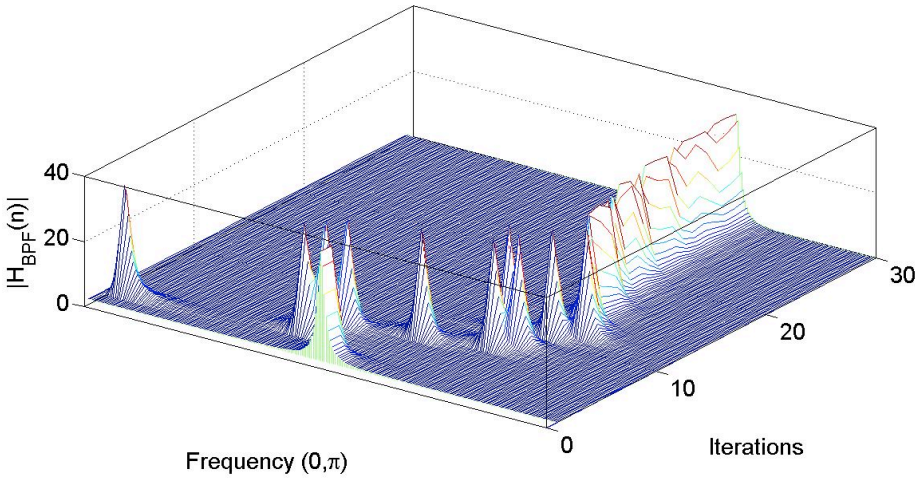

Figure 3.3: Adaptation of the BPF-central frequency to the input frequency

In the Figure 3.3 the power spectrum of the BPF is plotted at seven different iterations; the peak moves forward and then backward in order to reach the 9Hz input frequency. This backwards movement demonstrates that there is some overshoot on the estimate.

The second property is tested by designing a stepwise function that represents the varying trend of α, that has to be tracked by the algorithm. The central frequency is time varying and at each time instant the adaptive process described above is computed.

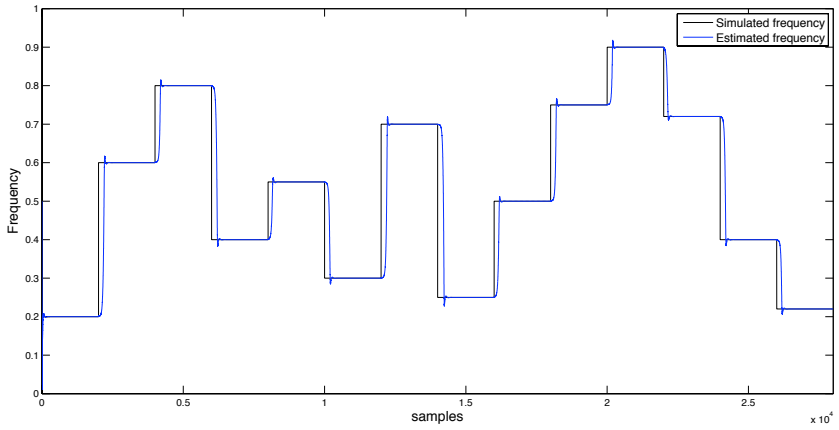

Figure 3.4: Tracking of a stepwise signal

The Figure 3.4 shows that the tracking is quite satisfying, even if it presents ringing, short delay and small overshoot at the beginning of the new step value. The ringing is probably due to the variance of the method, as the overshoot; while the presence of a delay is attributed to the adaptive process, that usually acts introducing a delay. In this case, our simulated signal is composed by segments 1000 samples longs and a SNR of 10 dB; the delay observed is about 100 samples. Later in the chapter, the delay and how it affects the estimate will be treated in depth.

The influence of additive gaussian noise is evaluated considering the bias of the estimate, where bias is computed as the difference between the real value and the estimated value, at each moment of the adaptive process. In order to test that, a sinusoid of 500samples and with frequency equal to 9Hz is taken; then 50 simulations have been run, where the addive noise of 5dB was random, gaussian and changing at every simulation. The mean and the standard deviation of this Bias are computed over all the simulations and plotted rispectively in Figure 3.5 and 3.6. Looking at the Figures, it is clear that the mean of the bias is close to zero and the estimate can be considered unbiased, aboveall when the estimate reaches the staedy state.

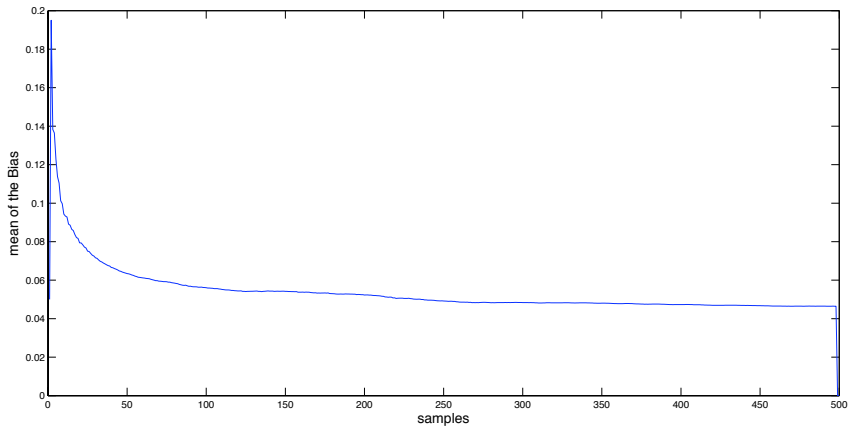

Figure 3.5: The mean of the bias for 50 simulations is plotted, and its trend decrease as the estimate achieves the steady state

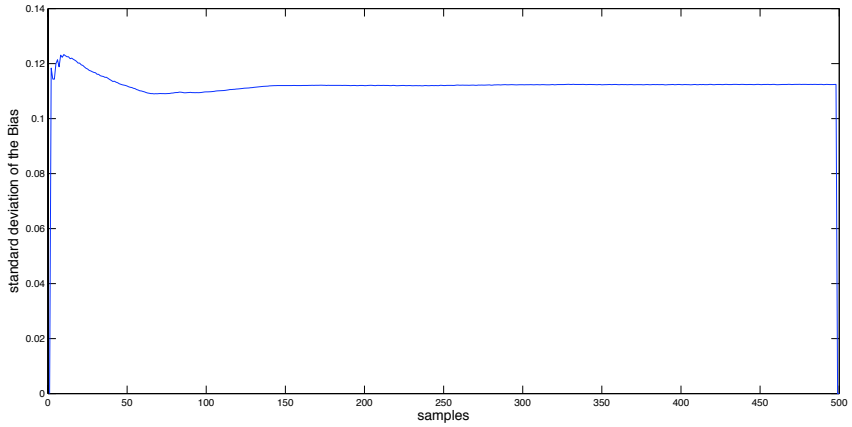

Figure 3.6: The standard deviation of the bias for 50 simulation is plotted; after the adaptation process, that regards mostly the first samples, it is quite constant.

Finally, the influence of the three filter parameters is checked. β is responsible for the width of the bandpass filter, as much it is close to 1, then the band is narrow and, as consequence, the selection of the main frequency is accurate. Therefore the larger β, the smaller mean square error, like the Figure 3.7 confirms.

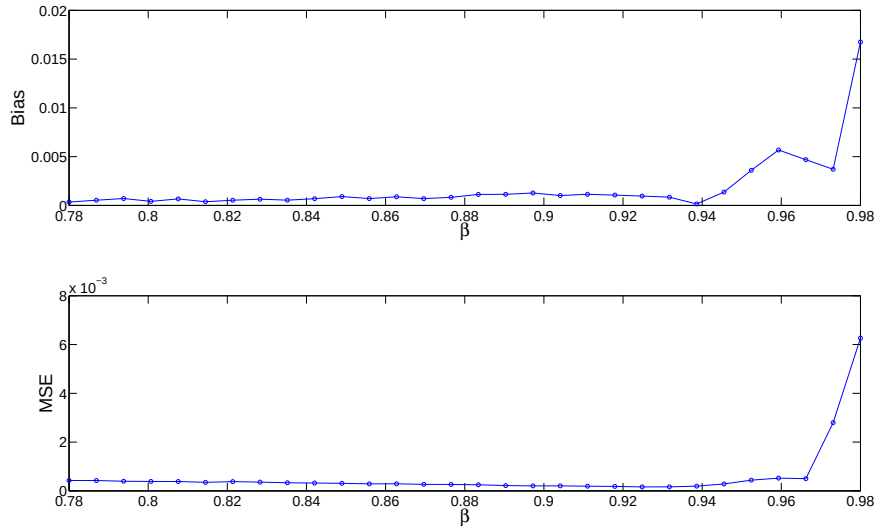

Figure 3.7: The bias and mean square error of the estimate, for different β.

The other parameter (δ) represents the forgetting factor of the numerator and denominator of the α updating equation. Even though it is treated as two different variables in [33] (δ and γ), during this study they will be given the same values. This forgetting factor (δ) is the measure of the trust in the present samples, in fact as the forgetting factor is close to one, as the estimate is based on the present samples, that gives a good tracking of frequency changes and a faster convergence, paying the price of a larger variance of the estimate, cfr. Figure 3.8. In order to understand it better, it could be stated that the adaptive algorithm is tracking the noise component instead of the sinusoid.

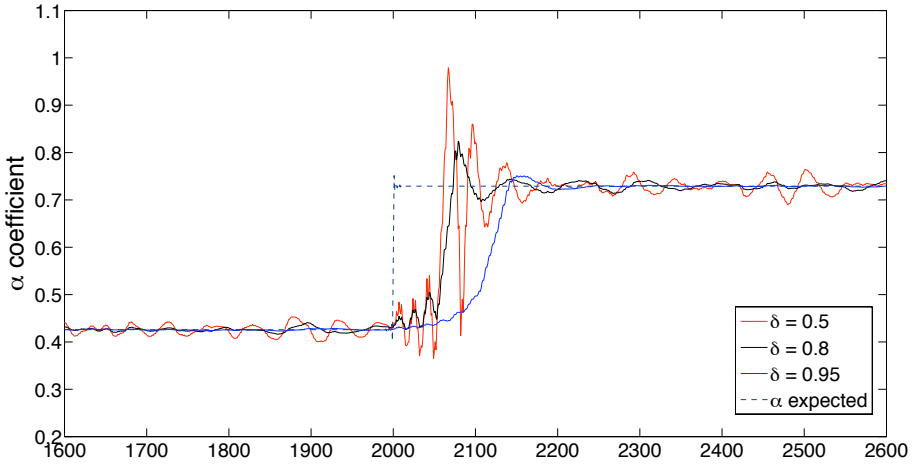

Figure 3.8: The α convergence considering different forgetting factors.

To not lose generality, the trend of bias and mean square error with different values of δ is plotted in the Figure 3.9. The mean square error goes to zero ad δ increases, even if there are some outliers. The bias has same trend of the mean square error, except for δ close to 1. For those values the bias races up slightly.

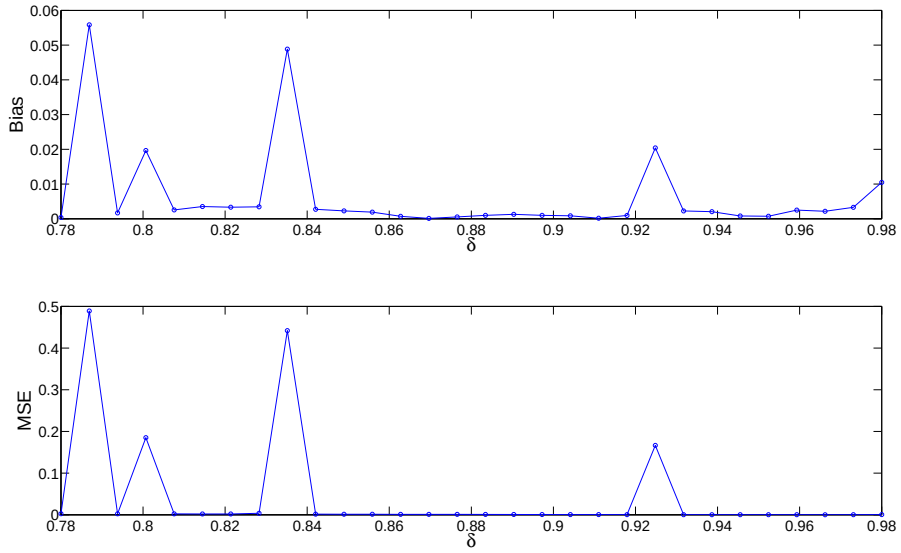

Figure 3.9: The bias and mean square error of the estimate, for different δ.

We conclude with the plot of some spectrograms of the extracted component, that are obtained by filtering the input signal with optimal α coefficient, found by application of the adaptive algorithm at each instant time. In Figure 3.10, the input is a simulated signal, consisting of shorter sinusoids that follow each other, with the same amplitude, but with different frequency. The spectrogram is defined as Short Time Fourier Transform and gives the plot of the frequency content of the extracted signal varying with the time, dividing the signal in time segments and applying to each of them the Fourier Transform. In order to improve the frequency resolution, the segments are taken quite large.

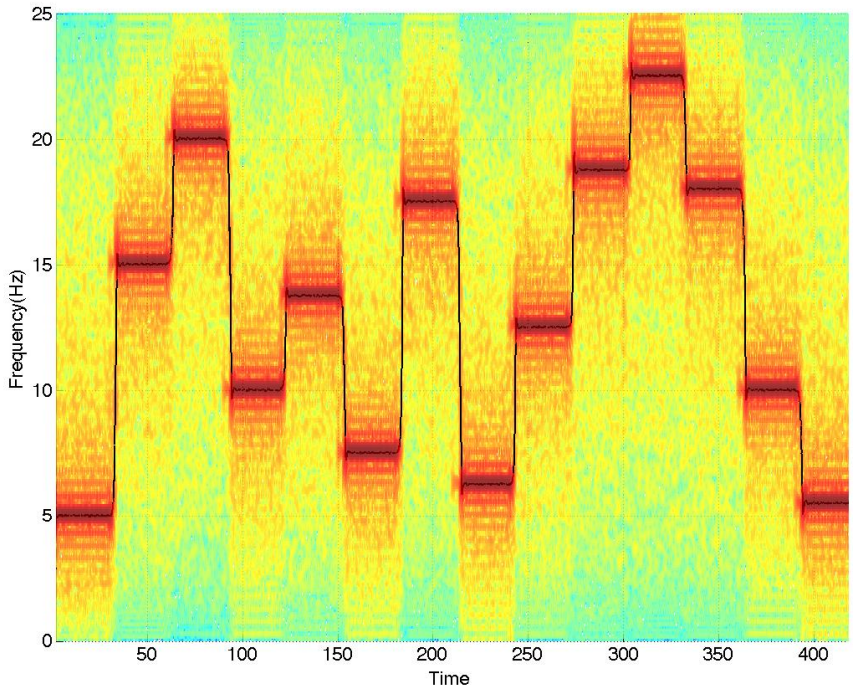

Figure 3.10: Spectrogram of the extracted component with the frequency estimation superimposed

Finally, in Figure 3.11 the frequency tracking is studied by creating 3 stepwise functions in the same way as before, but setting different values for the SNR at the input: 0, 5 and 10 dB. A slightly greater ringing or ripple in the frequency estimated from those signals is noted when the SNR decreases.

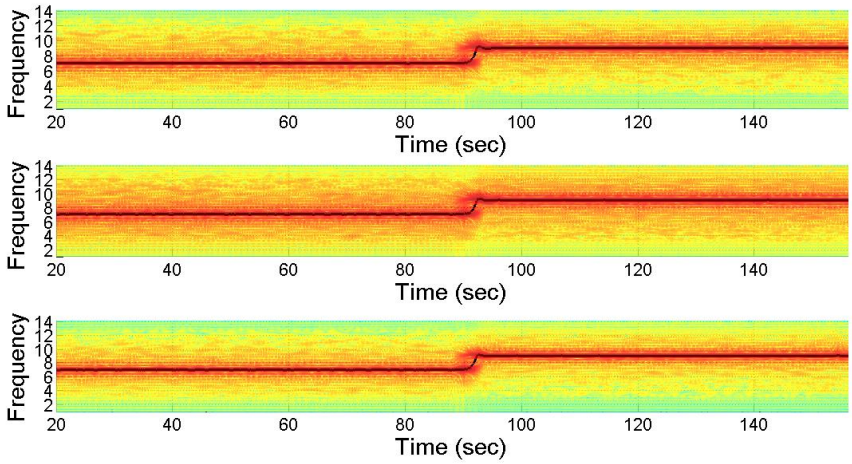

Figure 3.11: Spectrogram and frequency estimation for SNR = (0, 5, 10 dB).

3.3.2 The DFE algorithm Performance

This algorithm is tested on simulated signals in order to evaluate the goodness of the estimate and to make a comparison with the ANF algorithm. The result, in term of estimated frequency, is given as a normalized fraction of ω. The influence of many parameters is investigated:

1. tracking of the frequency changes in the input signal;
2. adding noise at different SNR;
3. varying of the step-size;
4. differences of the performance according to ω;

The simulated signal is supposed to have α equal to $\sqrt{2}$, such that the resulting signal has unity power, and zero phase, since it is not that relevant as the frequency.

$$s(n) = \sqrt{2}cos(\omega n) \tag{3.20}$$

Then, as done for the ANF test, the simulated signal consists basically in a series of cosines with different frequency.

The first property is studied, considering a simulated signal as described above, with additive noise at SNR =10dB, where each cosine segment is 1.500 samples long and the stepsize, μ , is 0.005. The length of the cosine segment depends on the step size, in fact, since it is quite small, the algorithm needs more samples to converge.

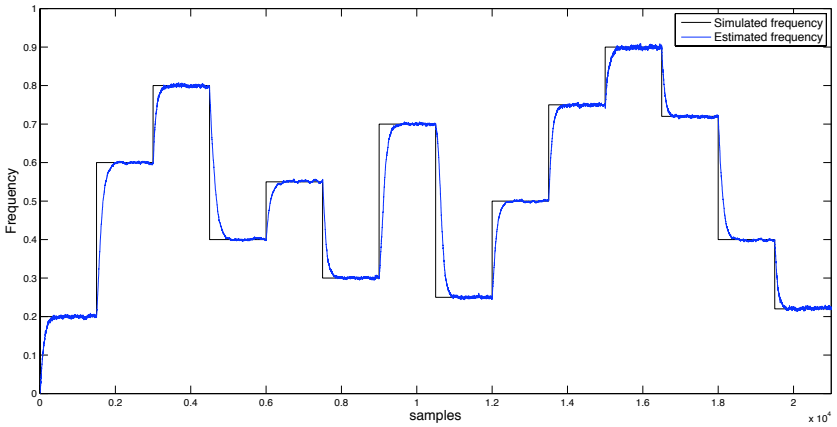

Figure 3.12: Tracking of a stepwise function of ω (SNR=10dB, μ=0.005).

As Figure 3.12 shows, the tracking is quite satisfying and confirms an already known property of the LMS. There is the introduction of a small delay, that can be reduced increasing the step size, as will show later. The tracking ability is tested also for different SNRs.

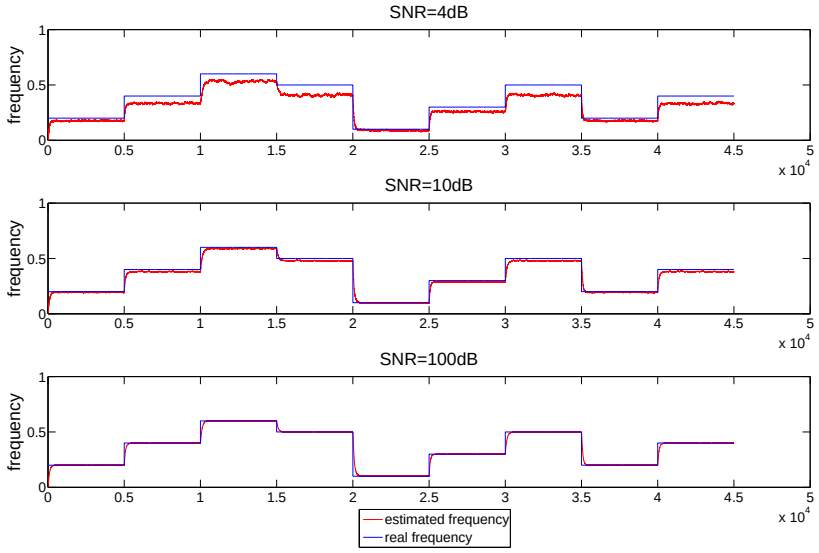

Figure 3.13: Tracking of a stepwise function of ω at different SNR with μ=0.005 and L (length of the segments)=5000.

In Figure 3.13 the influence of different noise levels is not clear, this is because of the combination of long segments and short stepsize, so the same calculation is done reducing the segment length and increasing the step-size. The result is plotted in Figure 3.14.

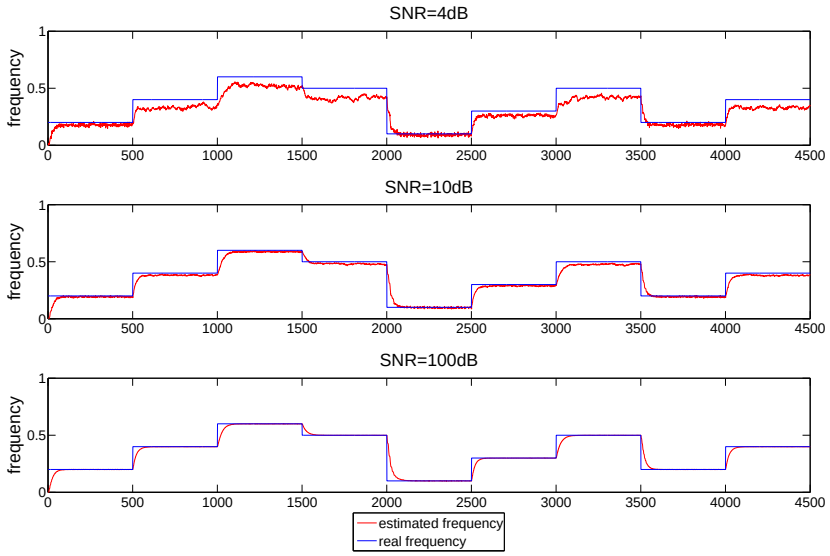

Figure 3.14: Tracking of a stepwise function of ω at different SNR with μ=0.02 and L (length of the segments)=500.

To conclude the investigation about the noise level, the mean square error is also computed, but in a steady state sense, that means that for each segment only the last samples are considered, such that the transition from a frequency to the next does not affect the estimate.

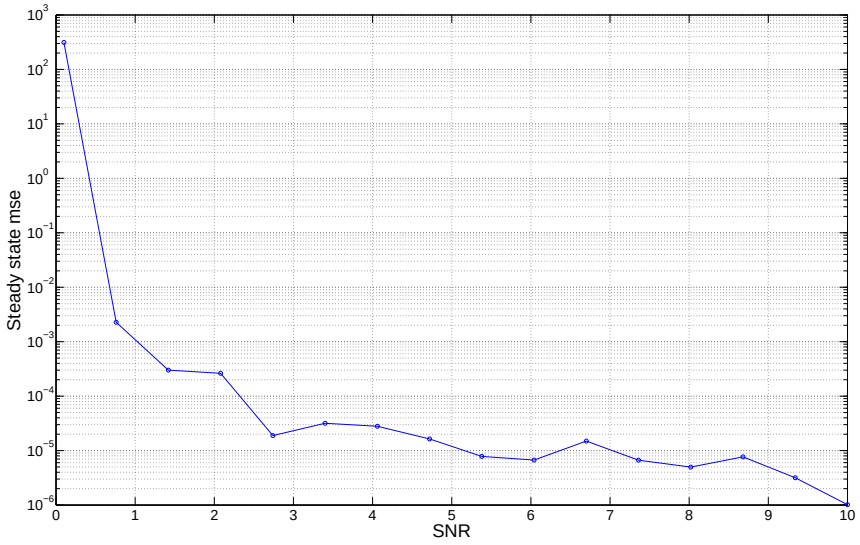

Figure 3.15: the steady state mean square error for different SNRs.

A logarithmic scale for the mean square error is used, in order to better represent the variation for 15 different values of SNR, between 0.1 and 10 dB. As Figure 3.15 shows, the mean square error decreases when the signal power is higher than the noise one.

So far it seems that the stepsize plays a key role for the accuracy of the performance, in fact, as mentioned before, the step size has to guarantee a good speed of convergence, but at the same time the variance as low as possible. It has to be properly sized according to the number of samples that the signal has.

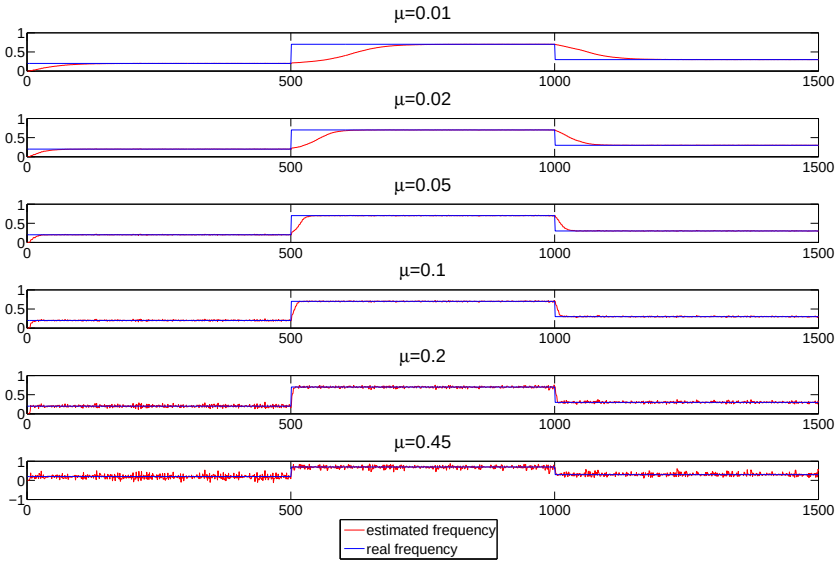

Figure 3.16: Tracking of ω with 6 different step-size μ

Figure 3.16 consists of six simulations with the same signal, but with six different values of the step size. Increasing the stepsize, the frequency changes are tracked faster, almost no delay is introduced, but the estimate is more noisy and the variance is larger. This is the reason why a good trade off is required. According to the LMS convergence theory, there is an upper bound for the step size, that is defined as one half of the signal power. Here, it holds the assumption that the simulated signal has unit power, hence the upper bound for μ is 0.5. To demonstrate the instability of the algorithm and the wrong estimate that it results when upper bound exceeding, the tracking of ω is plotted in Figure 3.17:

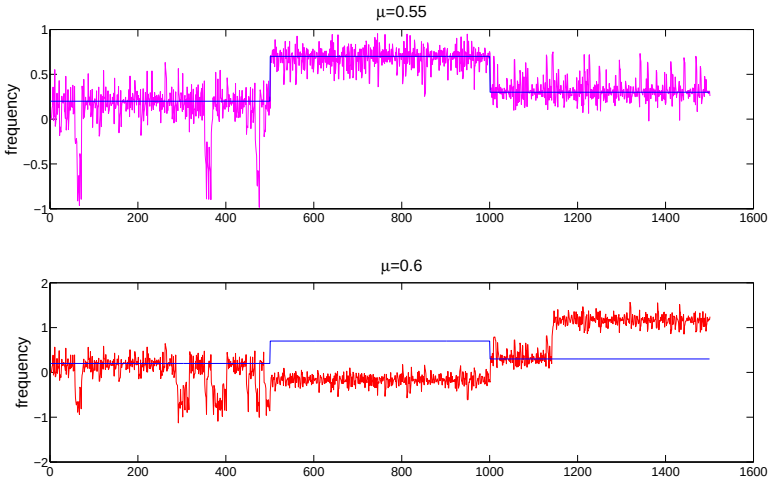

Figure 3.17: Tracking of ω with step size that not belong to the allowed range

All the values are overestimated and trackiing of the simulated signal is lost. The μ influence for the DFE algorithm is finally tested computing the steady state mean square error, that is plotted in logarithmic scale. It can be observed that even though both estimates are unstable, the estimated ω presents a larger variance and is able to track the frequency less time, when a larger μ is used. In other words, the instability increases with the step-size.

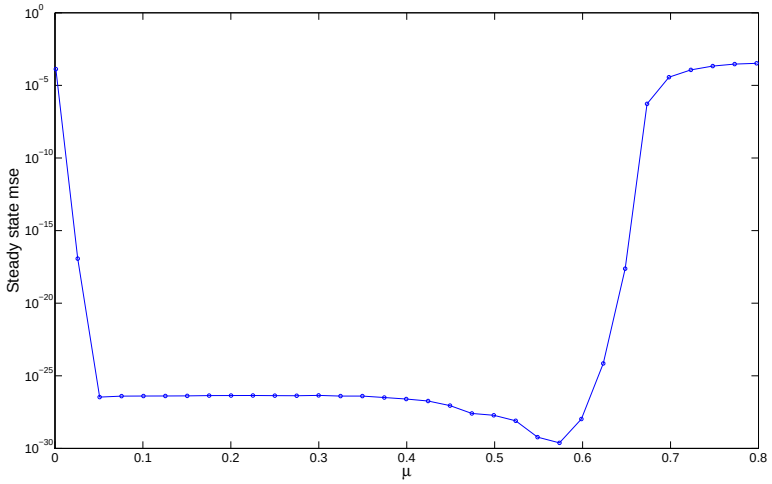

Figure 3.18: The steady state mean square error for $\mu \in (0.001,0.8)$

Looking at Figure 3.18 , it is observable an almost constant behaviour of the error for the safety range of the μ, then sidewise there are two branches where the error increases. On the right side, the upper bound is exceeded; on the left side, this is due to the number of samples that are not enough to achieve convergence.

An interesting feature of the DFE algorithm is that its performance is different according to the frequency, as it is shown in the Figure 3.19

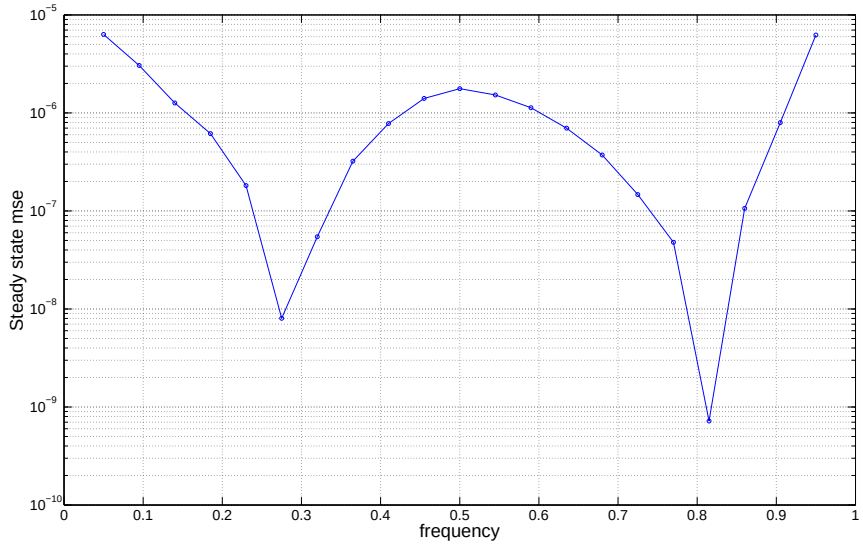

Figure 3.19: The steady state mean square error for different values of ω.

The variance of the frequency estimate is higher on the boundaries of the ω interval. This is because the variance has the following espression:

$$var(\hat{\omega}) \approx \frac{\mu\sigma_q^2}{2SNR\sin(\omega)}\left(\frac{\cos(4\omega)}{2+\cos(2\omega)}+1\right) \tag{3.21}$$

and mathematically goes to infinity when ω=0 and ω=π. This behaviour is observed also in some tracking experiment, for example when there is a large step changes in frequency. The estimate frequency is higher than the simulated one or rather negative, that is unacceptable for a frequency. Figure 3.20 shows exactly this.

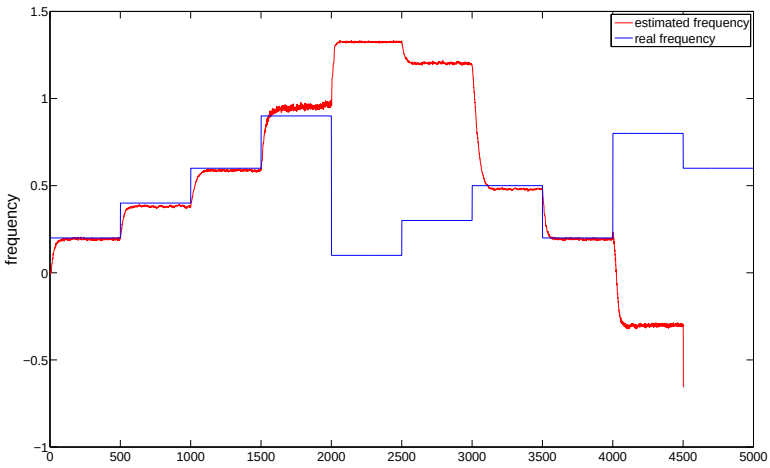

Figure 3.20: Tracking of the frequency in case of large step changes.

Incorrect estimates can be observed both on the falling edge and on the rising edge, when ω passes from 0.9 to 0.1 and from 0.25 to 0.8. This instability is not performed when smaller step in frequency changes are considered, both really small and really high frequency can be estimated, even at those frequency the estimates are quite noisy, with more overshoot and ringing than the frequency in the middle of the range. This is shown in Figure 3.21 where all the steps in the range of frequencies are estimated by the DFE.

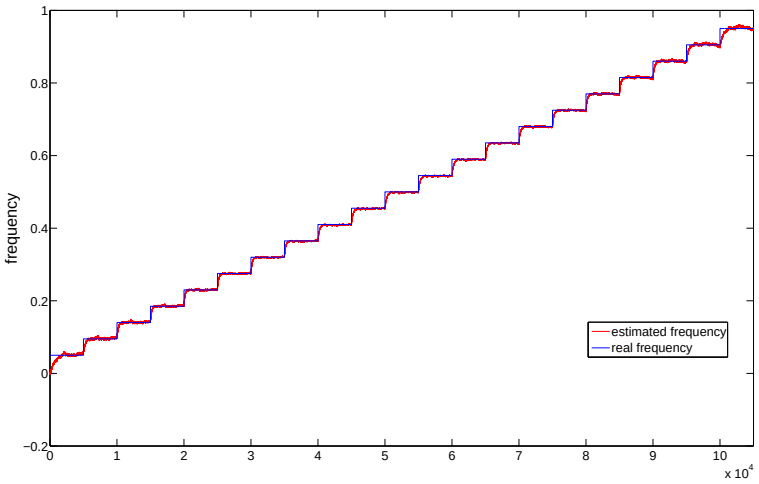

Figure 3.21: Tracking of the frequency in case of short step changes.

Similar to the results of the ANF, this paragraph is concluded by the time-frequency analysis. So, using the Short Time Fourier Transform, the spectrogram is plotted for signals both without noise and with three different noise levels in Figure 3.22.

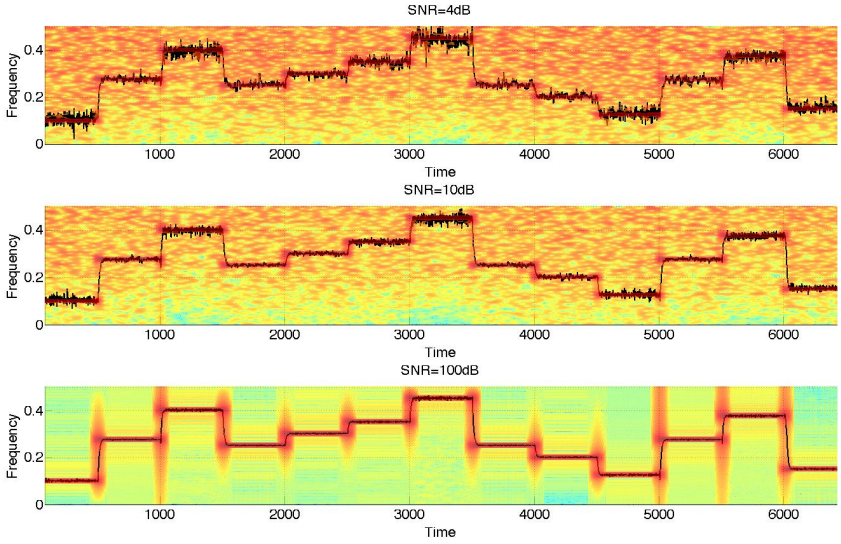

Figure 3.22: Spectrogram, with μ=0.05, with SNR=4dB, 10dB, 100dB.

3.4 Performance comparison

Now the behaviour of the two algorithms is compared. For the comparison the algorithms have to be equivalent in their parameters, therefore the following relation between μ and δ is considered:

$$\mu = 1 - \delta \tag{3.22}$$

These parameters are fixed for all investigations and set to δ=0.95. The simulated signals are equal to the signal used to test the DFE algorithm and in particular the frequency trend is stepwise, whose length and amplitude are denoted L and H respectively, see Figure 3.23. The comparison is done at different levels:

- tracking

- estimate's delay
- influence of the noise

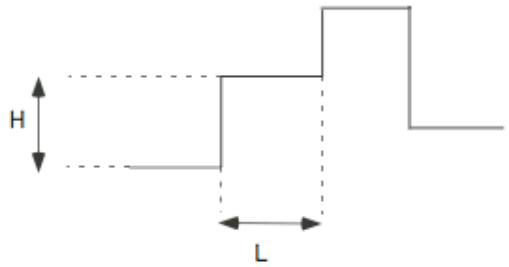

Figure 3.23: H and L studied in the step-wise signal

The tracking capability is analyzed in the absence of noise and takes different values of L into account. It can be noticed that, first of all, the DFE algorithm does not introduce any important delay, as expected by the well known property of LMS. Secondly the ANF algorithm has a certain delay in the estimate, that is constant and independent of L. Furthermore, the estimate is characterized by overshoot and small ringing phenomena, before achieving the convergence value, see Figure 3.24

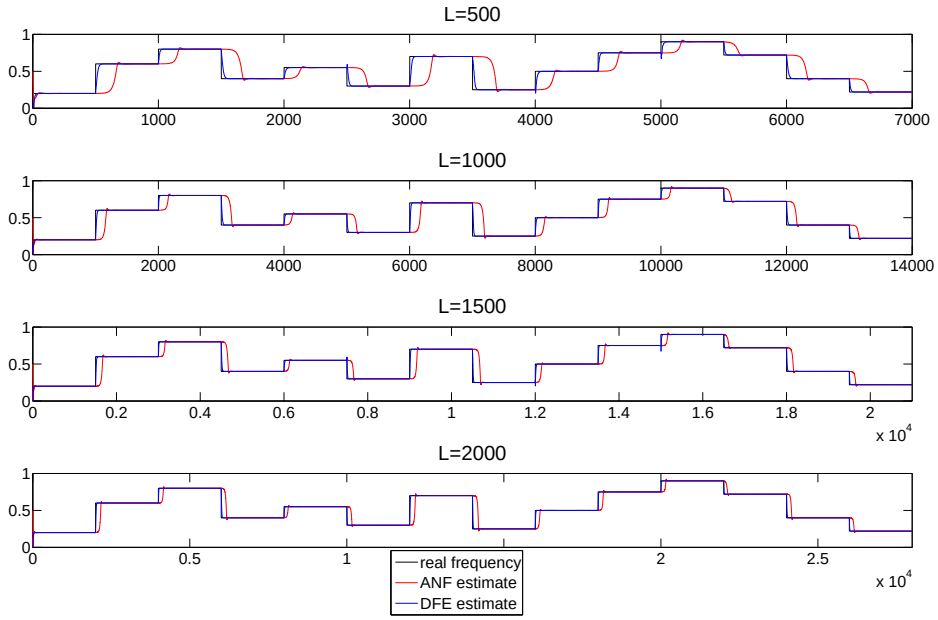

Figure 3.24: Delay in the tracking for L=500,1000,1500,2000.

On the other hand, a dependence in the delay is observed when different values of H are used. This dependence is observable in Figure 3.25. Even though sharp frequency changes are not expected in AF signals, the delay in the tracking will be measured in a large range of stair amplitudes which corresponds to large frequency variations ($\Delta\omega$) .

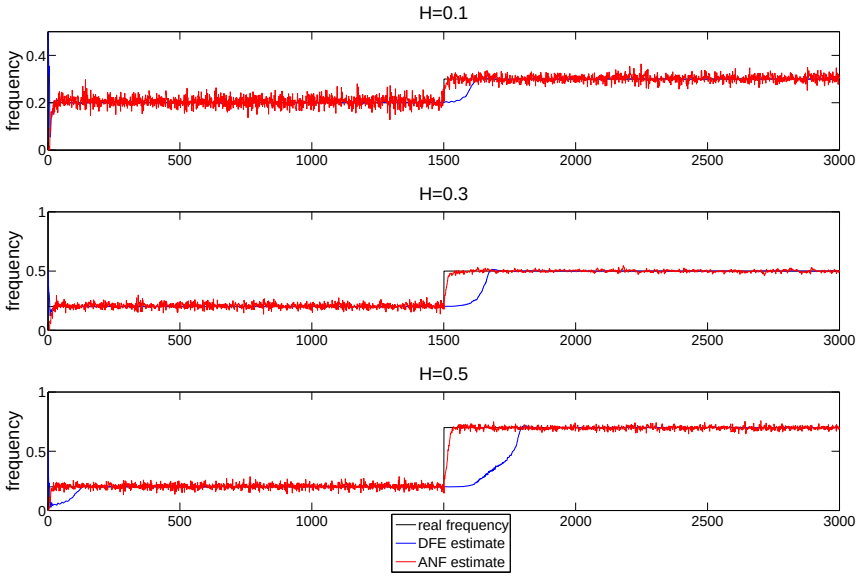

Figure 3.25: Tracking capability for different H

The delay is defined as the time instant when the estimate achieves 90% of the convergence value. In order to investigate the amount of the delay introduced with different stairs size, it is computed for both the algorithms and presented in Figure 3.26.

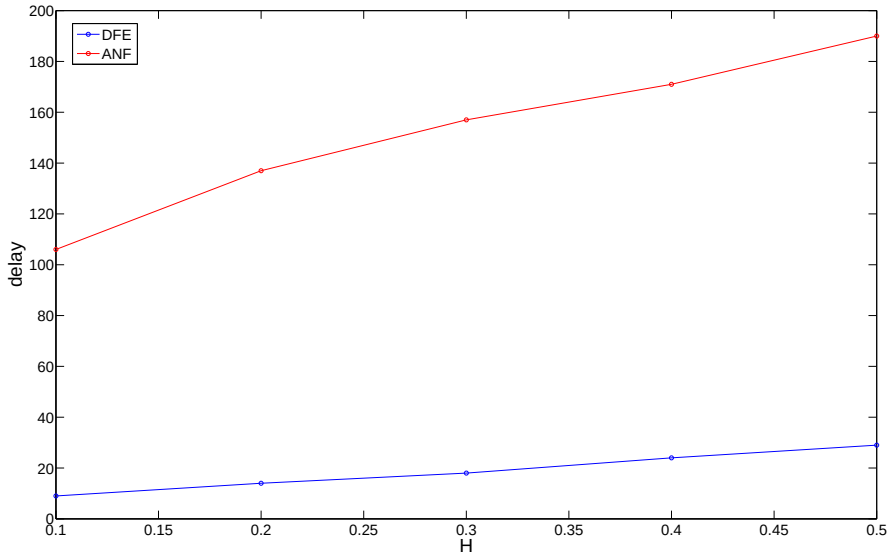

Figure 3.26: Delay in the tracking for diferent H

So far, keeping in mind that no noise is added, a part from Figure 3.25, one can conclude that the perfomance of the DFE is better than the ANF's one, from different points of views, such as speed of convergence and delay. In fact the DFE delay is almost constant, or at least it does not increase that much, as the ANF delay does, and it is anyway smaller. Additionally the DFE does not present any overshoots, in accordance to the features of LMS algorithms. The investigation goes forward with the addition of different level of gaussian noise; the results are plotted in Figure 3.27.

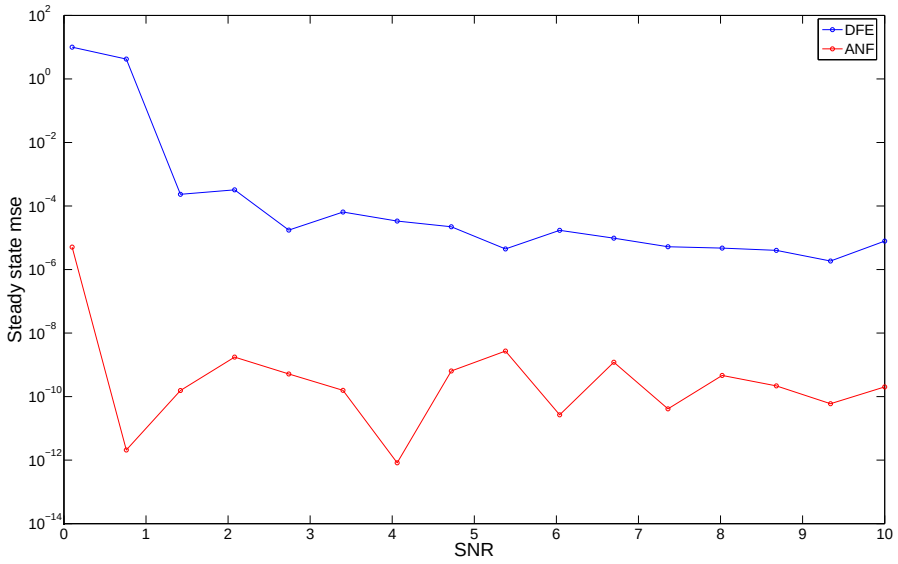

Figure 3.27: Steady state mse for different SNR

With worse noisy conditions the ANF acts with smaller steady state mean square error. The tracking capability is also checked in presence of noise at different level and the performances are presented in Figure 3.28.

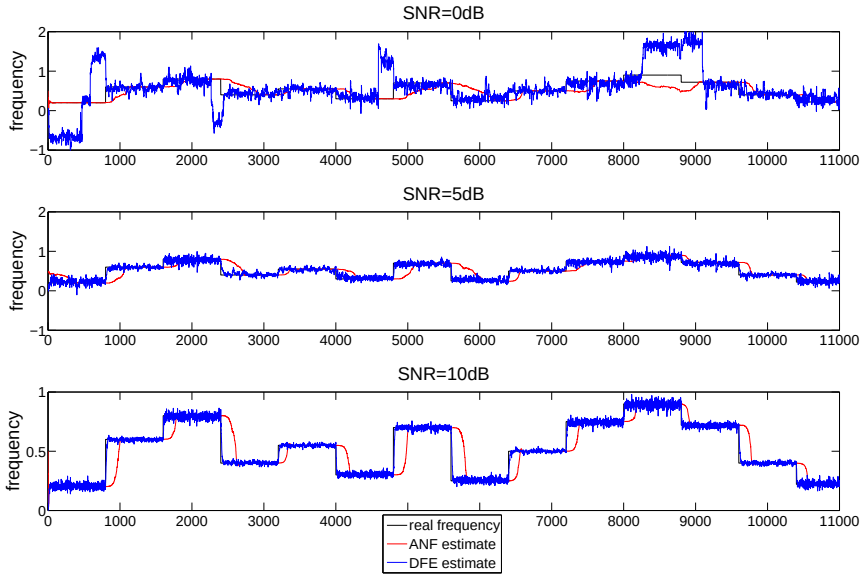

Figure 3.28: tracking performance with 3 different SNR 0,5,10dB.

These different conditions show the better time properties of the DFE. This method is faster at each noise level and it seems not to introduce any significant delay, so it is a good tracker. Its main negative aspect is that, maybe because of this property, it returns an estimate charachterized by a quite large variance, that can be explained as a noise's track. On the other hand, the ANF needs more samples to achieve the steady value, but its estimate has a smaller variance. Finally it has to be mentioned that the DFE has some stability problems when tracking noisy sinusoids if the SNR is below 0dB. It has a similar behaviour if high or low frequencies are picked.

3.5 Conclusions

In this chapter two algorithms for frequency tracking during atrial fibrillation have been introduced and their features studied both separately and compared with the same simulated input signal and equivalent parameters, δ and μ.

The Adaptive Notch Filter shows a good frequency tracking with some overshoot and ringing in the estimate. The method returns an unbiased estimate. It is demonstrated that β parameter rules the bandwidth of the bandpass filter as δ controls the dependence on the previous samples in the adaptive algorithm.

On the other hand, the DFE is based on the LMS algorithm. For the chosen value of μ, the method is able to track all frequencies without any overshoot, even though in case of sharp frequency variations instability is performed. Since it was ruled by the same properties as all the LMS systems, a compromise has to be reached in order to have a fast tracker, with low size variance affecting the estimate.

Applying the same simulated signal and taking in account an equivalence between δ and μ, it has been demonstrated that the DFE presents an smaller delay. This delay is independent of the SNR and it behaves almost as a constant when a wise-step function with different frequency stairs is simulated. On the contrary, the delay in the ANF is larger and more dependent on the SNR and the size of this frequency variations. Finally, the ANF shows less mean square error in the steady state for a large range of SNRs. Anyway this can be solved by decreasing μ, being aware of an increase in the DFE delay.

Chapter 4

Detection of Atrial Fibrillation

4.1 Introduction

The detection of AF in a 2-leads ECG recording or a signal from 24h-Holter monitoring is one of the most important aims that the Biomedical Signal Processing has. Having an algorithm that, given a Holter record, is able to determine if a patient is affected by AF, is a key point for screening. The presence of AF, its classification and its cure could be identified easily and quickly. In this Chapter a brief overview on what it has been done so far in literature is present, as well as a method developed in this project. While in literature many methods are based on the ventricular activity, in this project a possible detection will be done starting by the atrial activity.

4.2 AF detection: the ventricular approach

Most of the methods present in literature are based on the RR-intervals. Two are the main reasons for using the RR-intervals [14]:

- QRS spike is predominant over all the ECG signal and it is less affected by the muscular activity;

- the QRS detection returns an accurate computation of the RR-intervals, regardless the leads positions.

In presence of AF, the RR-intervals are characterized by a larger variance, because the irregularity and high frequency of atrial depolarization is reflected on the ventricular response.

This is used for making detection of AF. A study, [14], focused its attention on robust AF detection in the face of significant muscle artifact and potentially changing morphology. The approach was based on the R-R intervals since the QRS spike is the most prominent feature of an ambulatory ECG and the least confounded by muscle noise. To compute R-R intervals, the morphology-independent QRS detector wqrs was applied, then the RR-intervals were normalized with the following formula:

$$RR_{norm} = \frac{RR}{\overline{RR}} * 100 \tag{4.1}$$

where

$$\overline{RR} = 0.75 * \overline{RR} + 0.25 * RR \tag{4.2}$$

The variance of the RR_{norm} was computed over 10 second sliding windows. AF detection was implemented according to whether the variance over each 10s window was greater than a settable threshold. These initial classications are then smoothed to eliminate spurious errors.

Temporal information was considered by [38], with the Sequential RR distribution, that was computed with consecutive RR histogram distribution in successive temporal windows, plotted prospectically, like in Figure 4.1.

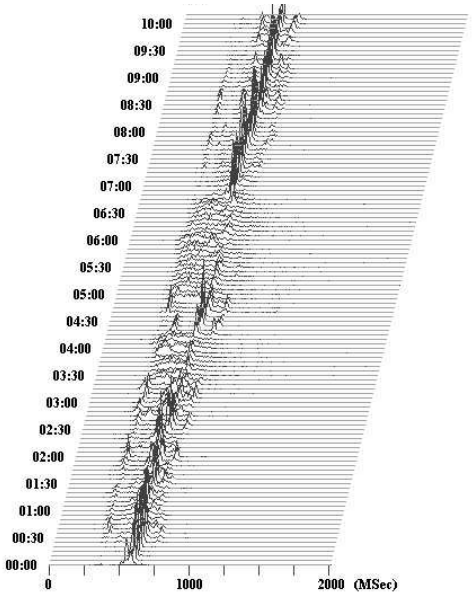

Figure 4.1: The tridimensional display of the RR distribution, obtained with SRRD. Here AF episodes are recognizeble because they are characterized by a broader and lower distribution. Reprinted from [38].

The accuracy of the description depends on the lenght of the window, the shorter window the higher the accuracy, even if larger memory is required. The detection of AF consisted in a graphic interface that two expert cardiologist used to annotate manually the onset and the end time of each episode. This method performed with sensitivity of 97%, referred to episodes, and it has the advantage to provide tridimensional display of RR distributions that facilitate the operator in recognizing immediately and with high accuracy AF episodes and monitoring heart rate variability before and after the episodes.

The RR intervals have been the base for the method suggested by [39], where the goal was the monitoring of episodes with a duration of weeks. The choice of the RR intervals was made among other alternatives, such as the fluttuation of the baseline and the replacement of the P waves with f-waves, but those did not provide, with a prospective of duration of weeks, a signal with necessary stability and quality. In this study two methods have been proposed, one based on the RR prematurity histogram and one based on ΔRR histogram. The RR prematurity

was calculated considering this formula:

$$P(i) = \frac{NN(i) - N_{mean}}{NN_{mean}} * 100$$

where $NN(i)$ is the actual normal to normal interval, NN_{mean} is the average. From the histogram two geometrical parameters are extracted, such as number of non empy bins and main distribution width, helpful to describe uni or bi modal pattern. While the ΔRR is considered as the difference of two consecutive NN intervals, and its histogram in presence of AF is lower, wider and unimodal. The latter is computationally faster and simpler that the prematurity method, furthermore it provided a higher episodes sensitivity.

A very high value of sensitivity was achieved by [40]. This study suggested the detection of AF episodes by using linear and non linear method in order to extract nine parameters from a known AF episodes, input episodes, made by 32 RR intervals each. The reduction of nine parameters to four a was done by the application of linear discriminant analysis, to improve the learning efficiency of the classifier and reduce the time necessary for learning. The classification was performed by the support vector machine, that is able to identify the best separating hyperplane between two classes of training cases placed at the edge of class descriptors.

The detection procedure was automated by [41], using three purely statistic tools, such as the Turning Points Ratio, the Root mean square of successive RR differences and the Shannon Entrophy, to characterize variability, randomness and complexity of RR intervals when AF occurs. The results were evaluated in sensitivity and specificity with different values of Shannon entropy as threshold, plotted in ROC curves; the high sensitiviy was 94.4%.

4.3 The choice of processing the atrial activity

Processing ventricular activity is without doubs successfull; as described in the previous section there is much information that can be extracted by the variabil-

ity of the ventricular responce, despite the robustness of those algoriths gives reliability of results. But there are details that have to be pointed out:

- the ventricular rate during AF is determined firstly by the irregularity of the atrial activity, characterized by f-waves, and secondly by the properties of the AV node, so the ventricular variabilty may be considered as a scaled version of the atrial one, by a factor that takes into account the pathways of conduction of AV node [36];

- the method based on the RR intervals are able to threat episodes of AF with minimum duration of order of minutes [38].

Hence how much is reasonable processing the ventricular activity to detect atrial arrhythmia? What about patients with short duration episodes?
During this project solutions to these questions have been searched, starting by choosing the atrial activity as substrate for processing and analysis. Atrial signals are characterized by noise and instability, but they represent the fibrillatory process that is the cause of AF, not the consequence, as the ventricular activity. Furthermore, while the detection based on the RR-intervals requires a certain number of beats to evaluate a distribution with its features, the atrial activity concentrates a frequency content that is related to sinus rhythm or arrhythmia phenomenona, and by processing it, it is possible to discriminate AF episodes from sinus rhyhtm, without the necessity of having an episode of a certain length. This is because the frequency analysis of the atrial activity allows the detection of episodes of order of seconds and that is the very innovation of the developed method.
The frequency tracking is the first step and two algorithms have been studied in the previous chapter, both of them can estimate the frequency of a signal in a noisy background. They have been tested with ECG signals, including sinus rhythm and AF. The results of these tests have showed that the ANF introduces more delay but it is more stable than DFE. A real signal is characterized by differ-

ent noise levels, artifacts and spikes and the best choice to handle those features is the ANF.

4.4 The contribute of the prefiltering: a possible way to detect

The ANF algorithm described in the previous Chapter works with a signal that it has been preprocessed by a band pass filter that reduces the possible range of frequencies that the ANF has to identify. Considering that the signal of the case is the AF signal, which main frequency is around 7 Hz this range is set from 3 to 12 Hz.

Since the goal of this project is to figure out a method to distinguish, in a cardiac signal, segments where AF occurs from segments with normal sinus rhythm, a simulated signal (described in details in the next Chapter), as the one in the Figure 4.2, composed by AF and sinus rhythm segments is processed by the ANF algorithm in presence of the band pass prefiltering. To the naked eye, the estimated frequency signal does not present features that let any detection as Figure 4.3 shows; variance and standard deviation have been also investigated, by using a sliding window, but the performance was not satisfying enough for detection.

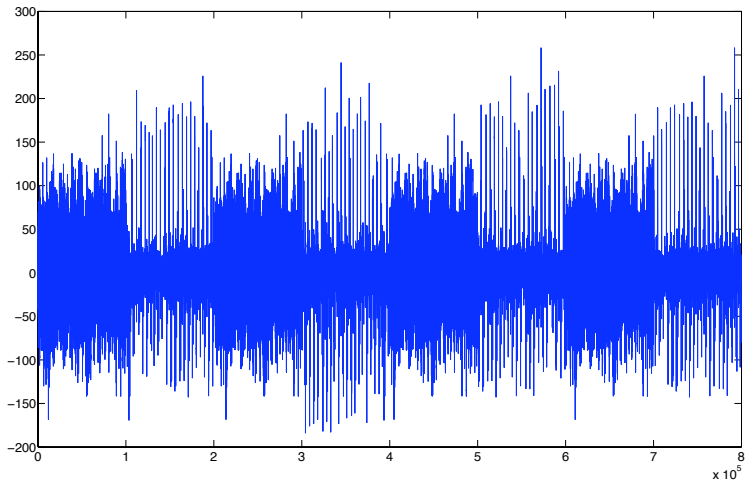

Figure 4.2: Samples of the simulated signal composed by AF segments and SR segments, described in details in Chapter 5.

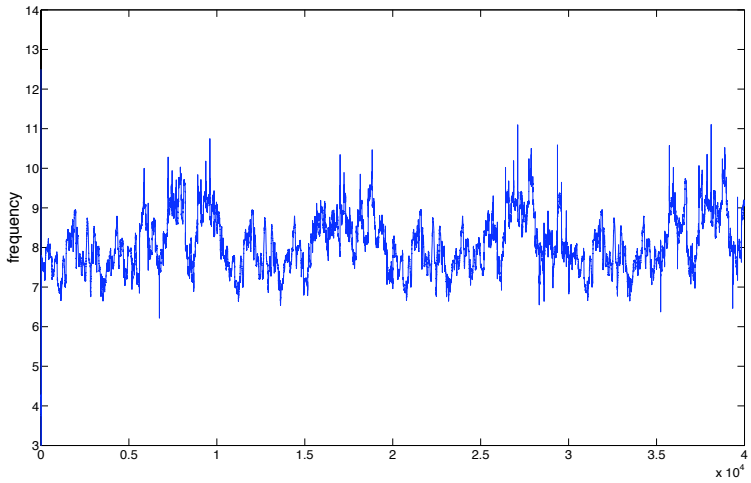

Figure 4.3: The estimated frequency of the signal in Figure 4.2 using the ANF algorithm only with prefiltering.

It has been noticed, during the testing of the algorithm on both atrial fibrillation and sinus rhythm segments, that:

- for AF segments the performance of the algorithm does not change with or without the band pass prefiltering, the estimated frequency is the same

and this is because the dominant frequency of the AF signal is in the range of preselected frequency but, since it is dominant, the algorithm is able to identify it even without prefiltering;

- for sinus rhythm segments the performance of the algorithm changes with or without prefiltering, the estimated frequency is not the same, furthermore there is an overestimate of 4Hz when there is not the band pass prefiltering. This is due to the shape that the spectrum of the residual signal has after the QRST complex removal, which does not fit the frequencies that the prefilter allows. Consecuently, the estimate given by the algorithm may vary depending on the use or not use of this filter.

Given this different performance, the presence or the absence of the band pass prefiltering can be used as a possible way to detect AF segments. The difference performance is shown in the Figure 4.4.

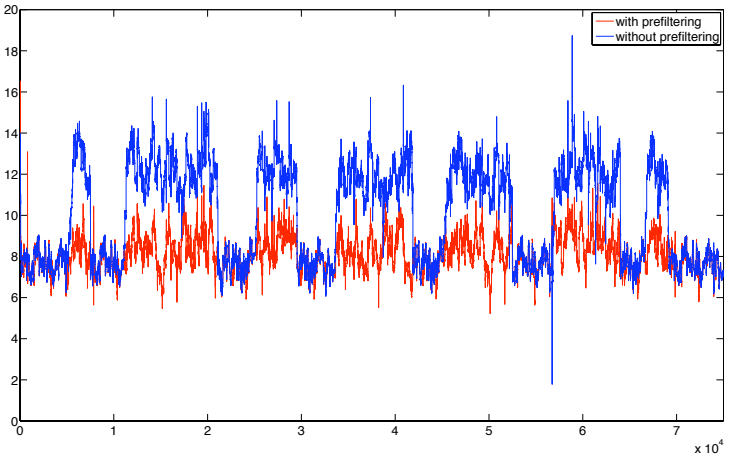

Figure 4.4: The different performances between Sinus Rhythm and Atrial fibrillation segments.

4.5 The developed method

The developed method is represented in the block diagram in Figure 4.5.

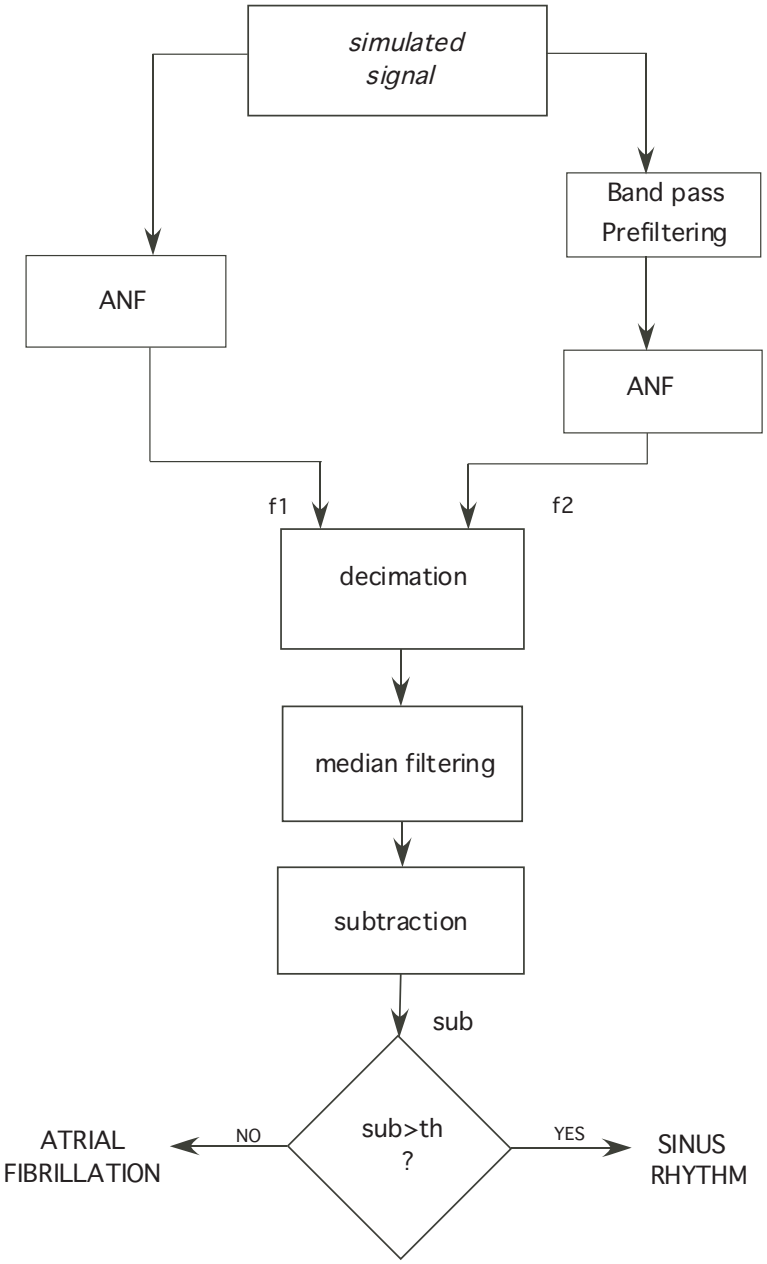

Figure 4.5: The block diagram of the developed method.

Let f_1 be the estimated frequency in presence of the band pass prefiltering and f_2 be the estimated frequency without the application of this prefiltering. The subtraction between those two signals is considered, such that the resulting signal

sub is zero in correspondence to the AF segments, since, as it has mentioned above, the estimated frequencies are the same, and a value different from zero in presence of sinus rhythm. Subtraction is chosen instead of division because it is less sensitive to noise.

$$sub = f_2 - f_1 \tag{4.3}$$

The *sub* signal, represented in Figure 4.6, shows clearly the difference between AF and sinus rhythm, permitting a detection, prior application of some preprocessing. There are in fact two important operations that have been done to the *sub* before performing detection and they are the following:

1. *decimation*. Providing that the original cardiac signal has a sampling frequency equal to 50Hz, the frequency estimate had an initial rate of 50 estimates for second, decimated of a factor of 10 such that the final rate is 5 estimates for second. The decimation is helpful because it reduces the number of point, making the computation faster and the signal less noisy.

2. *median filtering*, in order to remove as many peaks as possible. The median filter is often used in the literature as a method for removing impulsive noise at both audio signals and images. One of its biggest drawbacks, which will be used in the method, is the fact that it makes a lowpass filtering of the signal: the idea is to compare each sample one by one with a certain number of samples surrounding it. If this particular sample differs too much from the rest of the samples in the segment, it will be considered an undesired peak. The number of samples that are taken into account corresponds to the order of the median filter.

The effect of those two operation is shown in the Figure 4.6.

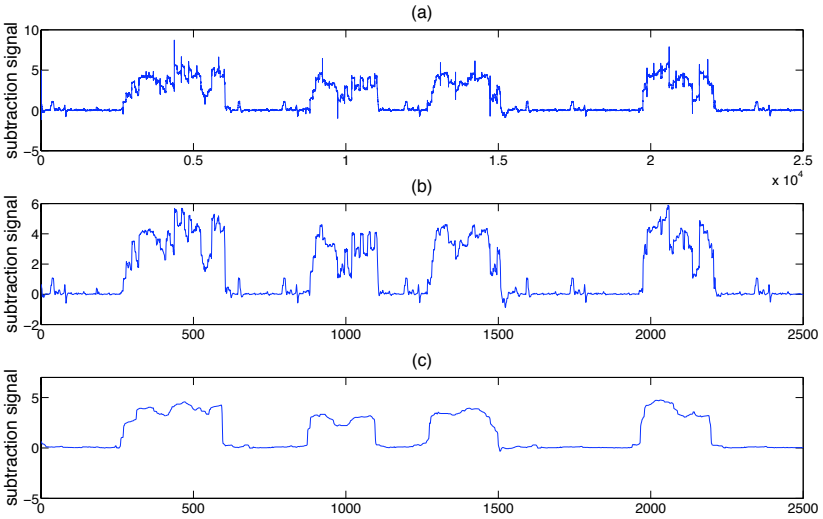

Figure 4.6: The effects of decimation and median filtering: (a) none preprocessing is done to f_1, f_2; (b) decimation is done prior to subtraction, (c) both decimation and medial filtering are applied.

The detection is implemented by the application of a threshold, the samples exceeding the threshold are classified like sinus rhythm samples because the f_1 and f_2 differ from each other and the *sub* is different from zero, while the samples that are below the threshold are classified like AF samples, since the f_1 and f_2 are equal and the *sub* is around zero.

Chapter 5

Results

5.1 Introduction

The developed method has been applied both on simulated and real signals (paroxysmal AF). Its performance has been regarded from different points of view and evaluated in terms of error and delay. This Chapter is divided into two Sections: the former contains the performance of the detector, considering the so called *simulated signals*, that will be described afterwards; the latter contains the performance of the detector considering *real PAF*.

5.2 Perfomance with *simulated signals*

5.2.1 Description of the *simulated signals*

The detection capability of the developed method has been tested building signals that could mimic PAF, paroxysmal atrial fibrillation, that is that kind of AF that ends spontaneusly. The term build is adoperated because the used signals, that will be called *simulated signals*, are a collage of segments of only AF and segments of only sinus rhythm. The signals are built alternating segments of AF and segments of sinus rhythm, and varying the length of each segment at every simulation. These segments come from recordings (ECG and Holter) of AF pa-

tients hospitalized in Lund's Universitetssjukhus, already depurated by the QRS complex, that has been removed applying the method of *spatio-temporal QRST cancellation*, suggested by [42] and described in Chapter 2.
The **AF segments** belong to two different types of signal:

- 24-hour Holter monitoring, that includes two signals, called *98f* and *36f*, both containg only AF. The difference between them is the noise that affected the recording: the noise level of the *98f* is lower than the *36f*.
- 12-lead ECG recording, that consists of 3 leads taken from the bunch of 12 leads originally recorded, each of them 300 seconds long.

The **sinus rhythm segments** are from 12-lead ECG recording. The signal contains two minutes of sinus rhythm. This signal is residual of the QRST detection and cancellation.
The calculations of the results exposed in Section 5.2.2 are based on *simulated PAF*, 500000 samples long, made by 4 segments of AF and 3 segments of SR, where the minimum length of the AF segmets varies from 10 to 50 seconds.
The calculations of the results exposed in Sections 5.2.3 and 5.2.4 are based on 40 simulations, so sorted:

- 20 simulations with the AF segments from 12-lead ECG recording;
- 20 simulations with the AF segments from 24-hour Holter monitoring, in particular:
  - 10 with *98f*;
  - 10 with *36f*.

Each simulated signal is composed of 15 segments, 8 of AF and 7 of sinus rhythm, and is 1500000 samples long, that correspond to 1500 seconds, given an initial sampling rate of 1000 Hz. The length of each segment varies from simulation to simulation. Furthermore two things have to be underlined: first, the

minimum length of a segment has been fixed to 50 seconds; second, the samples of each segment are taken from different parts of the original signal.
Since the only available sinus rhythm segments are from a 12-lead ECG recording, the best choice for the AF segments is the 12-lead ECG recording. This is because the way to record the heart activity is the same, so the segments show the same features and the simulated signal turns to be closer to a real one. Nevertheless it is also interesting to evaluate the performance of the detector with Holter recording, hence both Holter monitoring and ECG recording have been used.

5.2.2 Detection Error and Parameters setting

The detection error is computed using two binary signals that are made in the following way:

1. the first binary signal comes from the *simulated signal*, made by segments of both AF and sinus rhythm; one is assigned to the samples belonging to AF segments, zero is assigned to the samples of sinus rhythm.

2. the second binary signal comes from the *sub*; after thresholding it, one is assigned to the samples that are under the threshold, hence AF, and zero is assigned to the samples that exceed the threshold, rather sinus rhythm.

Comparing those two binary signals, sample by sample, the error is increased by one every time a sample is not equal to the corresponding one. To compute the error, this amount is then divided by the total length of the signal and multiply by 100, as shown in the following formula:

$$error = \frac{wrong\ samples}{total\ length\ of\ the\ signal} * 100 \tag{5.1}$$

In the wrong samples mentioned in 5.1, both AF samples, that are dismissed, and sinus rhythm samples, that are identified as AF, are included.
The investigation of the error is done taking in account the influence of different

parameters, that characterize both the ANF and the method implementation. The ANF parameters that have been considered for the error study are:

- δ
- β

The δ parameter, that has the same meaning of the γ, is the forgetting factor present in the expression of the polynomial that are used for computing the α coefficient. The error is computed considering γ and δ in the range $(0.88, 0.98)$, as recommended by [33], and it is presented in the Figure 5.1.
The best values for δ are around 0.9, and furthermore the value that returns the lowest error depends on the length of the segments, in fact if the minimum length is reduced, an higher forgetting factor is required. This is because the forgetting factor decides the weight of the previous samples on the the current value of the polynomial for computing the α coefficient, and as γ and δ increase, the error increases as well so when they approach to 1, the estimate is totally unstable. A good trade off between stability and speed of tracking, in fact a larger δ, like 0.96, is suitable when there are short segments, because it provides a faster tracking, since less samples are considered and the computation is faster.

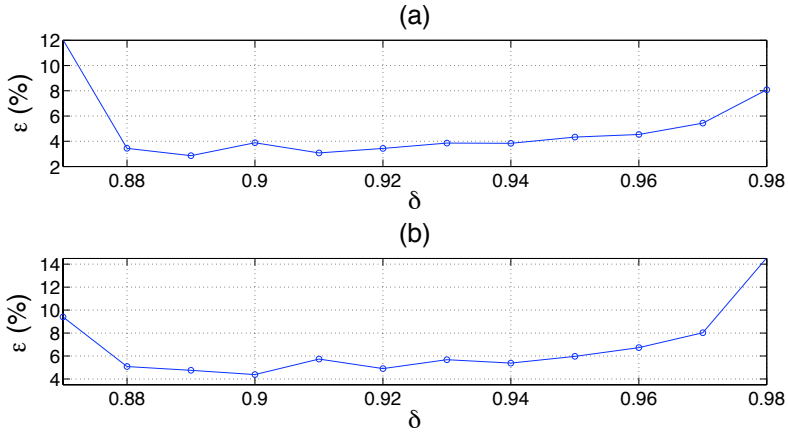

Figure 5.1: The detecting error as function of different values of the forgetting factor, with $threshold$ = 1, β= 0.94, $median\ filter's\ order$ = 90, and with (a) minimum length equal to 50 seconds, (b) minimum length equal to 10 seconds.

The β parameter represents the bandwidth of the ANF: basically, how many frequencies are picked by the filter during the frequency estimation process. It represents in some sense the accuracy of the estimate. The relation between the error and β, with β in a range from 0.05 to 0.98 in order to investigate all the possible bandwidth, is plotted in the Figure 5.2.

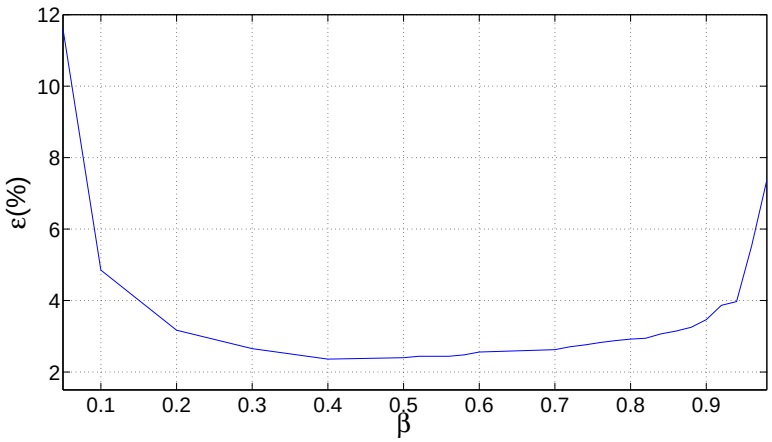

Figure 5.2: The detecting error as function of different β .

The error is quite high both for β really small and for β large. When β is a small value, the bandwidth of the ANF is wide and the considered frequencies are many; in this case the error is high because the estimate is not accurate. When β is a large value, the bandwidth of the ANF is more narrowed, it picks only one component tends to giving a quite wrong estimate and this is the reason of a such large error.

The parameters that characterize the method implementation are:

1. bandwidth of the prefiltering
2. order of the median filter
3. threshold

The detecting error is investigated also considering the bandwidth of the prefiltering. Considering that the central frequency of 8 Hz has to be preserved, the

bandwidth of the prefiltering goes from a range of frequencies 6 to 9 Hz, so equal to 3 Hz, to the range $(2,\ 13$ Hz), corresponding to 11. The smallest error is for the bandwidth equal to 7 Hz, as it it plotted in the figure 5.3.

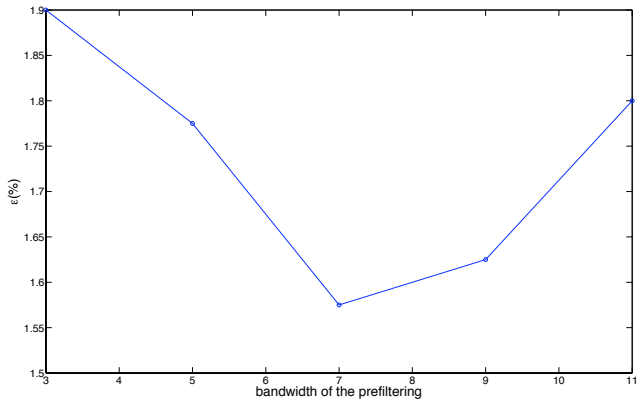

Figure 5.3: The detecting error as function of different bandwidth of the prefiltering, with β=0.94, δ=0.95, $threshold$=1, $median\ filter's\ order$=90.

A study has been done in order to investigate the best order of the output of the median filter. A simulated signal described above is tested with different order of the filter and the error in detection is computed and the best order, the one that returns the lowest error, is found to be 80. This result is plotted in Figure 5.4.

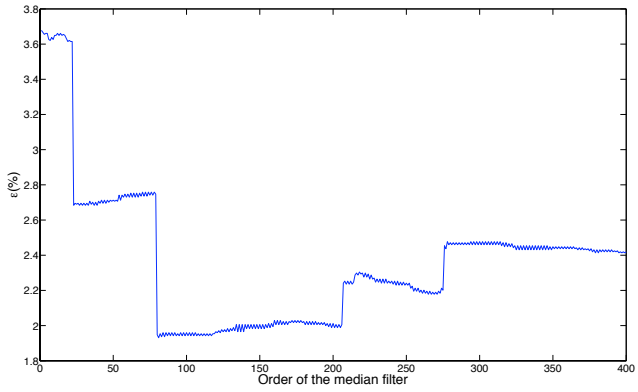

Figure 5.4: The detecting error for different possible order of the median filter, with β=0.94, δ=0.95, $threshold$=1, $bandwidth\ prefiltering$=9Hz.

The threshold depends on the minimum length of the AF that has to be detected. In fact if the minimum length of the AF segment is around 50 seconds than the threshold that returns the lowest error in detecting is equal to 1, while it is equal to 2.5 when shorter segments are used, as it is shown in the Figure 5.5. In those simulations δ was set equal to 0.96.

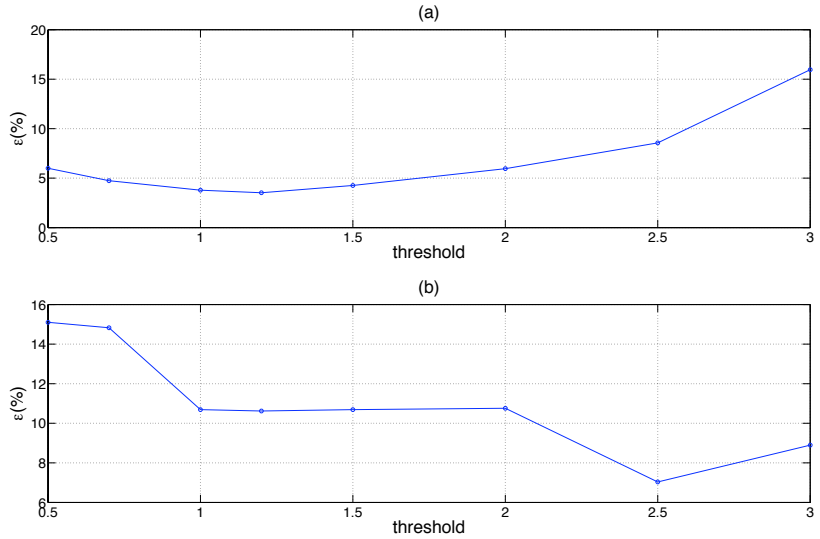

Figure 5.5: The detecting error with 8 different values of the threshold, (a) with minimum length of AF segment equal to 50 seconds, (b) with minimum length of AF segment equal to 10 seconds.

If the minimum length of the AF segment in the simulated signal is increased, then the threshold needs to be raced up as well, in order to keep an acceptable detecting error and do not miss any episode. Figure 5.6 shows the advantage of this racing, in fact a threshold equal to 1 in the (b) case doesn't permit to detect the small AF episode that is present .

This is due to time that takes the algorithm to converge, in fact if the segment is shorter than this time, the considered value is higher than the steady one, because the algorithm has not achieve yet the steady state. Hence the threshold has to be increased otherwise the error may be quite larger.

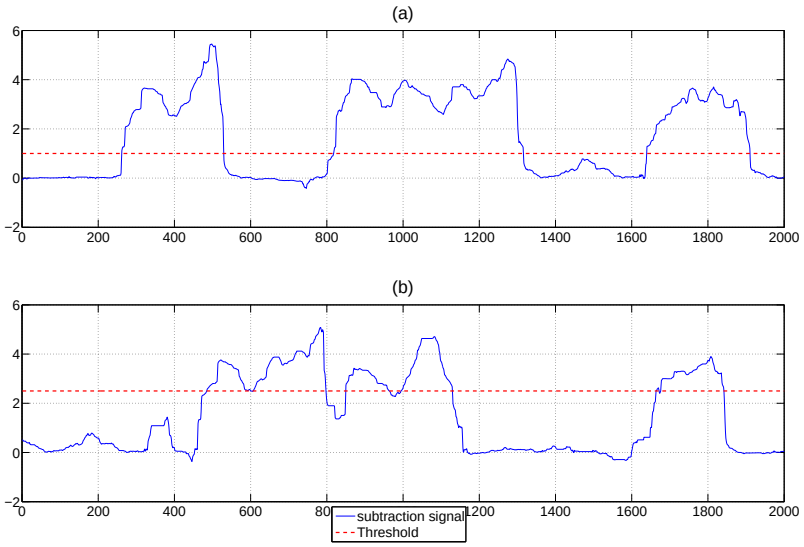

Figure 5.6: The subtraction signal with threshold superimposed, (a) with $threshold$ = 1 and $minimum\ length$ = 50seconds,(b)with $threshold$ = 2.5 and $minimum\ length$ = 10seconds.

5.2.3 Delay in the detection of the AF

The delay of the detection of AF episode is measured using the same idea of the error described in the Section 5.2.2. In the delay study, the two binary signals are compared and for each detected AF episode the onset index and the end index are determined. The delay is estimated as the difference between the index of the detected episode and the index of the simulated episode, both for the onset and the ending.

$$onset\ delay_i = real\ onset_i - detected\ onset_i \tag{5.2}$$

$$ending\ delay_i = real\ end_i - detected\ end_i \tag{5.3}$$

Since for each simulated signal, there are 8 episodes of AF , and 40 different signals are used, the data points that are available for making some statistics are 320 for the onset delay and 320 for the ending delay. The results are presented in two different paragraphs, one for the 12-lead ECG recording and one for 24-hour Holter monitoring and consist of:

- *mean* and *standard deviation*,

- *box plot* of the data, which is a box that has lines at the lower quartile, median, and upper quartile values. The whiskers, that are the lines extending from each end of the box, represent the extent of the rest of the data. Outliers are represented by a cross and their values are outside the extent aforementioned.

Regarding the parameters for the ANF algorithm and the detector, these are the chosen values:

- Bandwidth of the BPF: $\beta = 0.94$;
- Forgetting factor: $\delta = 0.96$;
- Threshold: $th = 1$;
- Median filter size: $N = 90$;
- Prefilter bandwidth: $\Delta f = 9Hz$.

12-lead ECG recording The results are computed making the mean and the standard devia-tion over all the available delay points, coming from the 20 simulations with ECG recording; the values are the following ($mean \pm standard\, deviation$):

- for the onset of the AF episodes: $\tau^o_{ecg} = 2.38 \pm 2.93\ secs$
- for the end of the AF episodes: $\tau^e_{ecg} = 3.95 \pm 2.69\ secs$

In Figure 5.7 the box plot of the data concerning the simulations with ECG recordings, both for the onset and ending, is presented. The plot confirms what mean and standard deviation report: the delay in detecting the end of the episode is larger than the one for the onset, even if the standard deviation is smaller, so the ending points are less spread out.

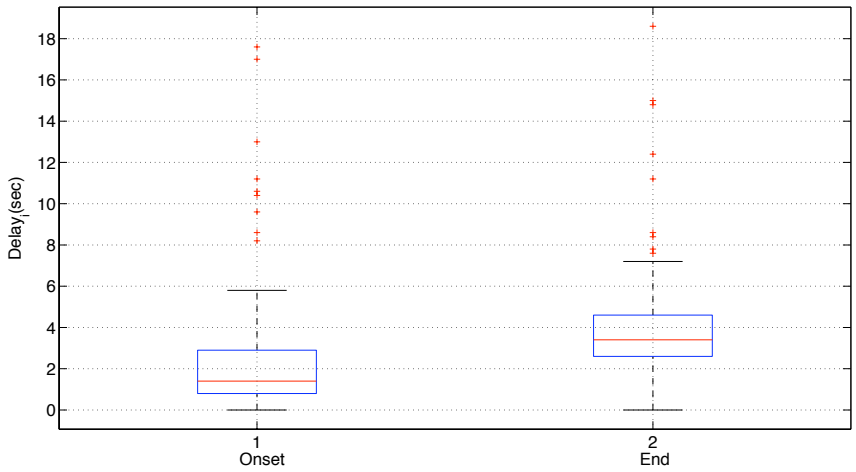

Figure 5.7: Delays in the detection: ECG recordings.

24-hour Holter monitoring The mean and the standard deviation, and the box plot as well, are computed mixing the data coming from the 10 simulations with the signal *98f* and the ones from the 10 simulations with the signal *36f*. The values are the following:

- for the onset of the AF episodes the delay is $\tau^o_{holter} = 3.54 \pm 5.33\ secs$
- for the end of the AF episodes: $\tau^e_{holter} = 4.23 \pm 2.47\ secs$

In Figure 5.8 the boxes corresponding to this delay is plotted.

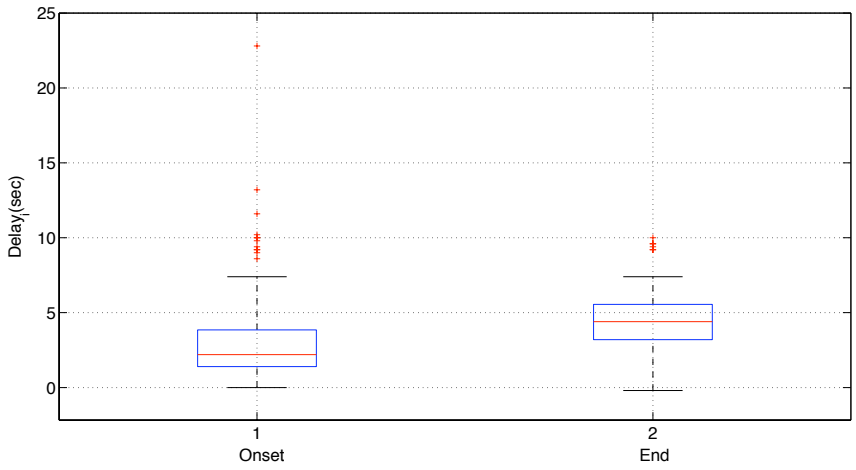

Figure 5.8: Delays in the detection: Holter Monitoring.

The trend of the data from the Holter monitoring is similar to the data from the ECG recording. In fact the delay is larger in detecting the end of the AF episodes than the start, even if the ending points have a smaller standard deviation.This means that the detector is not symmetrical, in other words, the detection of a change from sinus rhythm to AF is faster than a change from AF to sinus rhythm.

As expected the performances are better considering the segments, both sinus rhythm and atrial fibrillation, from ECG recording. In fact the introduced delay is lower using the AF segments coming from the ECG recording.

5.2.4 Detection Error of AF samples

During each simulation, together with the delay points, the detection error, described in the Section 5.2.2, is evaluated. The mean and the standard deviation are computed considering 10 simulations with ECG recorded AF segments and 10 simulations with Holter monitoring AF segments. The values for the different parameters used are the ones chosen for the simulations of Section 5.2.3.

. 12-lead ECG recording: $\epsilon_{ecg} = 3.01 \pm 1.14\%$

. 24-hour Holter monitoring: $\epsilon_{holter} = 3.82 \pm 1.37\%$

The box plot is displayed in Figure 5.9. The plot shows that there is a difference between the signals indeed, with both mean and standard deviation that are larger for the signals that include Holter monitoring AF segments, as it was expected.

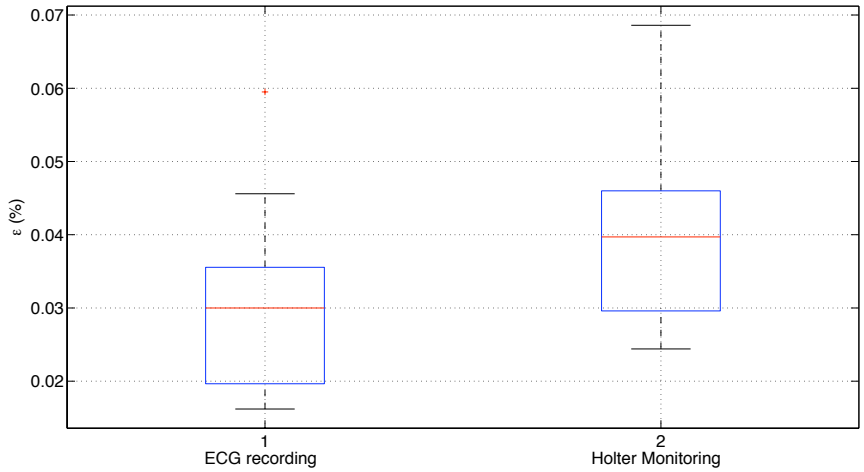

Figure 5.9: Detection error for Holter and ECG signals (definition of the error from Section 5.2.2).

5.2.5 Detection Error of AF episodes

In this section the error is studied from another point of view and hence re-defined as follows:

$$\epsilon_{episodes} = \frac{false\ positives\ +\ false\ negatives}{total\ number\ of\ AF\ episodes} * 100 \tag{5.4}$$

An example of a incorrectly detected episode (false positive) is given in Figure 5.10.

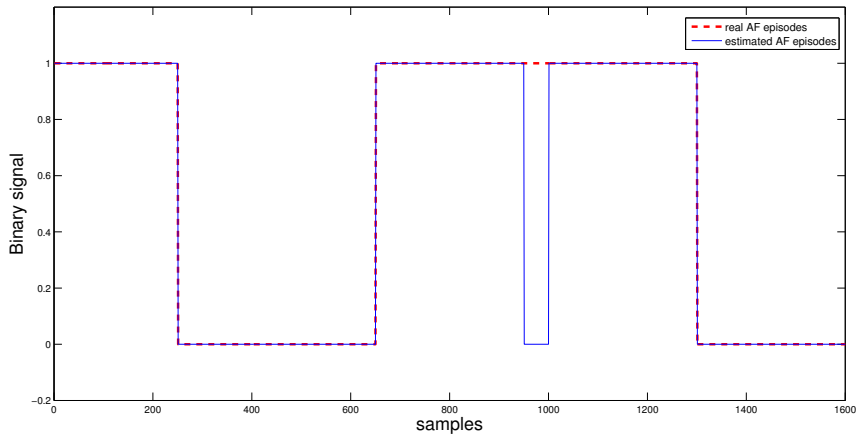

Figure 5.10: Exemple of false positive, that is generated when samples of AF are too spiky and the frequency tracks exceeds the threshold, returning their classification as sinus rhythm and one extra AF episode, not real.

A false positive can be generated when the input signal is too noisy and the frequency track is characterized by spikes that let the signal sub exceeding the threshold.

An episode can be missed (false negative) for 2 reasons:

. the episode is too short, like it is shown in Figure 5.11;

. two episodes are too close to each other, so the algorithm does not recognize them as different and detects only one episode instead of two, like shown in Figure 5.12.

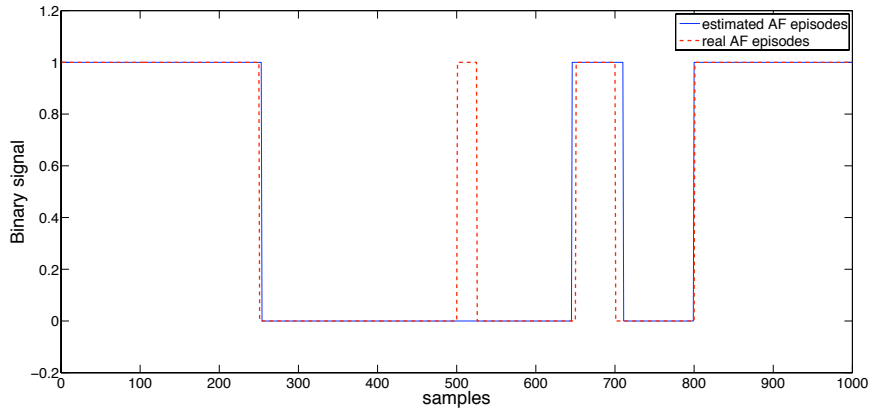

Figure 5.11: Example of a missed AF episode (false negative), because it was too short.

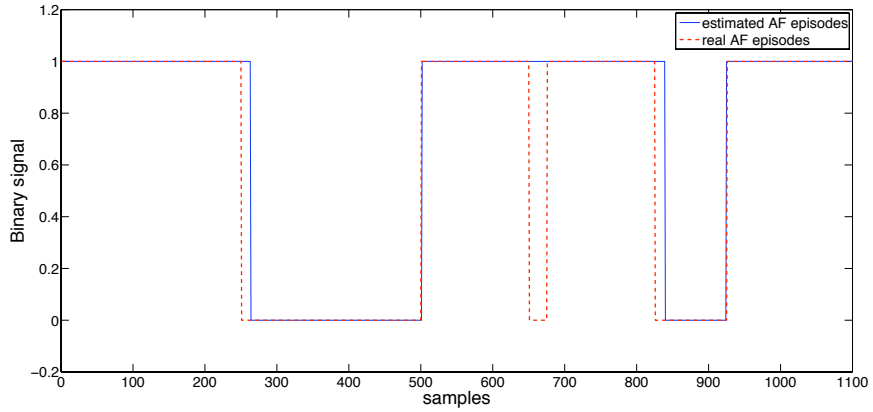

Figure 5.12: Example of a missed AF episode (false negative), being too close to the next one.

If the error described in Section 3.6 is described in terms of samples, here the error is an index of missed or incorrectly detected episode, that will be used to optimize some parameters that characterize the working of the developed detector. Those parameters are basically three:

1. *threshold*, that has been already mentioned in the previous chapter and plays a key role in the performance of the detector;

2. *L: minimum duration*, defined as minimum length of an AF episode to be detected;

3. *D: temporal resolution*, defined as the minimum distance between two consecutive AF episodes, that permits to the detector to distinguish them as separate.

The temporal resolution and the mimum duration are shown in Figure 5.13; again, the higher lever corresponds to the presence of AF and the lower values indicate sinus rhythm.

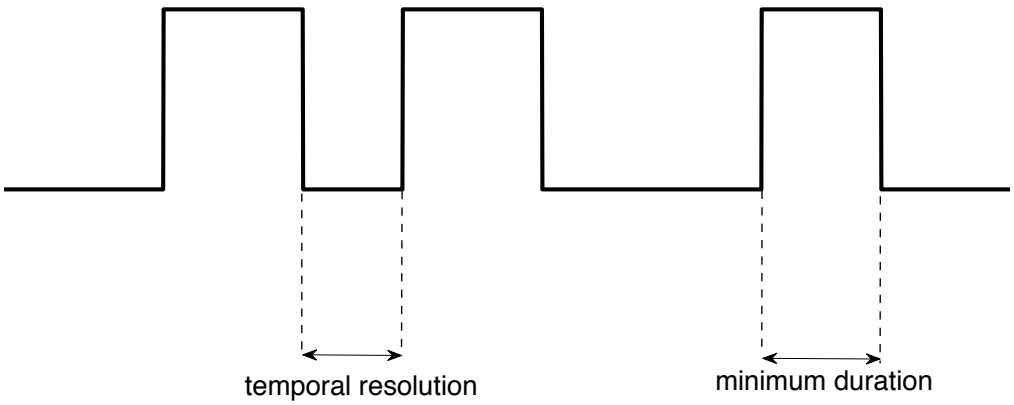

Figure 5.13: Temporal resolution and minimum duration

The threshold has been related with the two resolutions. The error rate, $\epsilon_{episodes}$, is evaluated for different combinations of threshold and the other parametes. The results are presented in table and each cell of the table represents the sum of the either incorrectly detected and missed AF episodes divided by the total number of AF episodes present in the signal, over 10 simulations. In Table 5.1 the results for the minimum duration are reported for four different values of the threshold. It has been said that the threshold needs to be raised up from the initial value of 1 up to the highest value of 2.5, above all if the length of the AF episode is reduced. If for a minimum length of 50 seconds, the threshold equal to 1 was the best choice, reducing the minimum length to 10 seconds and even less, the thresholds with the smaller error are always larger than 1, such as 2 and 2.5. In Table 5.2, the results for the temporal resolution are reported for four

		Threshold			
		1	**1.5**	**2**	**2.5**
minimum duration (sec)	**10**	8.75	6.25	5	5
	8	13.75	12.5	6.25	8.75
	6	31.25	22.5	16.25	11.15

Table 5.1: $\epsilon_{episode}$ for short AF episodes

		Threshold			
		1	**1.5**	**2**	**2.5**
Temporal resolution (sec)	**25**	5	2.5	2.5	7.5
	20	10	6.25	7.5	6.25
	15	2	7	10	8
	10	50	50	50	50

Table 5.2: $\epsilon_{episode}$ for AF episodes close in time

different values of the threshold. Looking at Table 5.2, it is possible to say that the temporal resolution can be decreased to 15 seconds with an acceptable error, but it cannot be equal to 10 seconds because the error in this case is intolerable and half of the episodes are missed ($\epsilon_{episodes} = 0.5$).

5.2.6 The exclusion of spurious peaks

In order to reduce the percentage of false positives, such the one shown in Figure 5.10, a modification is done to the method. Assuming that an AF episode cannot be shorter than $5 - 7$ seconds [43], the duration of every detected episode is computed and then all the episodes that have a duration smaller than 6 seconds

are dismissed. 10 simulations have been done to check if this modification is actually improving the performance of the detector. The parameters for each simulation are set as follow:

. both sinus rhythm and AF segments are from ECG recordings;

. threshold equal to 2;

. minimum length equal to 15 seconds;

. temporal resolution equal to 20 seconds

. minimum duration acceptable for the AF episode equal to 6 seconds;

. the error is computed according the formula 5.1;

. the difference between the real episodes and the detected ones is calculated (*diff*).

The results, in terms of *diff* and *error*, are presented respectively in Table 5.3 and Table 5.4. Looking at the results of those 10 simulations, it is possible to conclude that this modification improves the performance of the detector. The number of erroneously detected episodes and the error decrease including this cancellation of spurious peaks as last step of the developed method. False positives are often called spurious peaks, because they are short events that are detected where the signal *sub* was too spiky and exceed the threshold, even though the application of median filter.

Simulation	*diff* without exclusion	*diff* with exclusion
1	2	0
2	1	0
3	2	1
4	3	0
5	1	0
6	0	0
7	0	0
8	1	1
9	2	0
10	1	0

Table 5.3: Exclusion of spurious episodes evaluated by *diff*.

Simulation	*error* without elimination	*error* with elimination
1	6.92	6.43
2	9.87	9.36
3	10.55	9.82
4	10.63	7.87
5	9.87	9.12
6	11.15	11.15
7	7.44	7.44
8	9.77	9.76
9	8.44	7.67
10	8.94	7.65

Table 5.4: Exclusion of spurious episodes evaluated by *error*.

5.3 Performance with *real PAF*

In this Section the detector has to deal with *real PAF*. Totally 10 patients affected by PAF are considered and in particular:

- 9 are taken from Long Term ECG Database, [44]
- 1 is a patient of Valencia Hospital.

For all of them, the extraction of the atrial activity was performed by LTH, Lunds Tekniska Högskola, with the spatiotemporal QRST cancellation. The residuals show the presence of one or more AF episodes, according to the patient. The starting and ending samples of the AF episodes were known, thanks to annotations made manually by specialists.
The method's parameters are set as follows:

- Bandwidth of the BPF: $\beta = 0.94$;
- Forgetting factor: $\delta = 0.96$;
- Threshold: $th = 1$;
- Median filter size: $N = 90$;
- Prefilter bandwidth: Δf=9Hz;

Besides, the assumption done in 5.2.6 is kept, so in the end all the episodes shorter than 6 seconds are considered false positive and discarded.
Every patient is indicated by a letter, in particular the 9 patients of the Long Term ECG Database are represented by letters from A to I, while the single patien from the Valencia Hospital is identified by X. Besides here comes a short description of the ECG and of the output of the detector for each patient.

- **patient A** the signal contains one AF episode, about 30 minutes long, that is correctly detected, without delay, even on ending detection; a false positive is present.

- **patient B** the signal contains two AF episodes, respectively 22 minutes and 25 seconds longs; the first episode is the beginning of the signal, correctely detected, together with the short episode.

- **patient C** the signal containts three AF episodes, two are correctly individuated, with length of 110 and 16 seconds, while the last one is not, because the processing of those samples turns into unstability. The onset of the first episode is detected in advance, while the ending with delay; the second episode is detected with delay both in onset and delay; between them there is the false positive.

- **patient D** the signal contains one AF episode, 12 minutes long, that is correctly detected, with a bigger delay in the ending than in the onset; there is one false positive.

- **patient E** the signal contains one AF episode, 24 minutes long, that is detected, without any false. This is a particular case, where there is the usual ending delay , but for the onset there is rather an advance.

- **patient F** the signal contains three AF episodes, 1048, 577 and 4088 seconds longs respectively; they are all detected, even if with one false positive. The signal has been cut in two parts, in the former the largest delays are recorded among all the patients, there is one false positive and the estimated sinus rhythm segment has less samples than the real one; in the latter everything is regular.

- **patient G** the signal contains two Af episodes, one 400 seconds long, at the beginning, and the other one 244 minutes long, so for a faster computation the signal is cut and the signal ends with AF; in this case the onset of the first episode is not determined, in fact the estimate starts directly with AF and this is due to the few samples of sinus rhythm that precede the initiation of the AF episode.

- **patient H** this signal is charaterized by a an episode of AF, 40 minutes long, that persists until the end of the signal; it is correctly detected without any false.

- **patient I** this signal has the same behaviour , but of the ECG of patient H, but in this case there is one false positive.

- **patient X** the signal contains one AF episode, about 44 seconds long. There is delay both in ending and onset the AF episodes and two false positive that can be removed if the minimum acceptable length for the AF episode is raised to 10 seconds.

All those information, together with delay (in second) in detecting onset and ending of each episode) are collected in the Table 5.5.

Patient	*onset delay*	*ending delay*	*false positive*	*false negative*	*AF episode*
A	0	0	1	0	1
B-1	-	3.04	0	0	1
B-2	2.36	2.42	0	0	1
C-1	1.68	4.41	0	0	1
C-2	2.9	7.42	0	0	1
D	2.68	5.48	1	0	1
E	1.72	4.53	0	0	1
F-1	-	25.96	1	0	1
F-2	25.36	10.58	0	0	1
F-3	3.68	-	0	0	1
G-1	onset not detected	0	1	0	1
G-2	0.56	-	0	0	1
H	-	9.26	0	0	1
I	9.18	-	1	0	1
X	8	6	2	0	1

Table 5.5: After the application of the detector, the onset and ending delay of the detection is measured; eventual false positives and negatives are counted. There are patients with more than one episode, so for each of them it is indicated the letter and the AF episode. The notation (-) means that the considered signal starts or ends with AF, according to the notation characterizing the onset or the ending, respectively.

Given those data, it is possible to clearify that:

- totally there are 15 AF episodes;
- there are 7 false positives and none false negative;
- $\epsilon_{episode}$= 46%;
- sensitivity is 100 %, but this is why there are not false negatives;

- taking in account all the onset and ending values of the delay, collected in Table 5.5, the mean and standard deviation for the onset delay τ^o_{PAF} and for the ending delay τ^e_{PAF} are calculated:

$$\tau^o_{PAF} = 4.7 \pm 7.16 \; secs$$
$$\tau^e_{PAF} = 5.62 \pm 7.07 \; secs$$

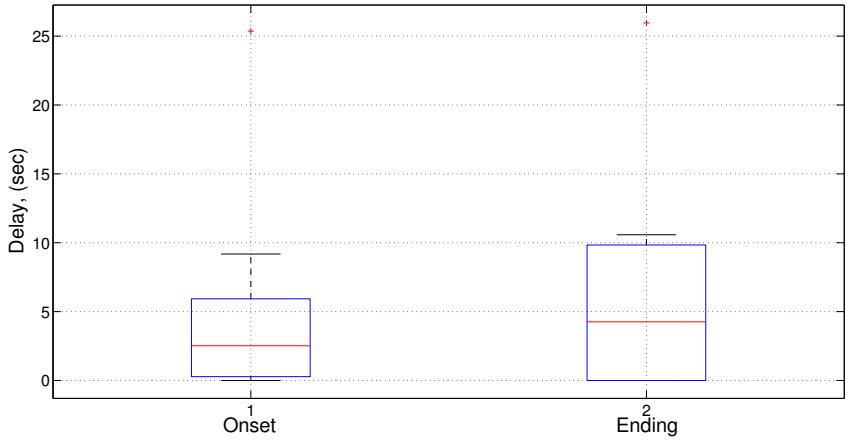

Figure 5.14: Delays in the detection of onset and ending time of AF episodes with PAF.

Figure 5.14 shows the box plot concerning the onset and ending delay in detection. As it possible to note, the ending delay is larger both in mean ans standard deviation than the onset delay, confirming what it was found in the previous section for the *simulated signals*.

Finally Figure 5.15 and Figure 5.16 concentrate the binary representation of the AF real episodes and the estimated ones, one representation for patient, except for patient F, where two immages have been necessary, since the lenght of the signal and the location of the episodes. It is observable the delay and the significative presence of false positives, probably due to the noise that affects the recordings.

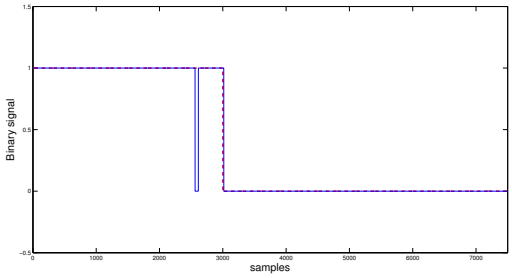

(a) Patient A

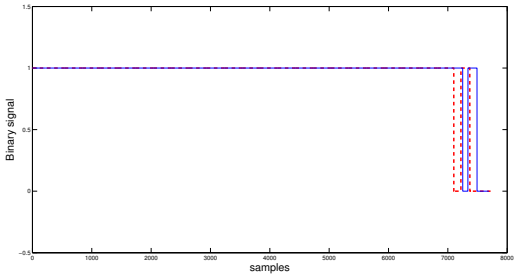

(b) Patient B

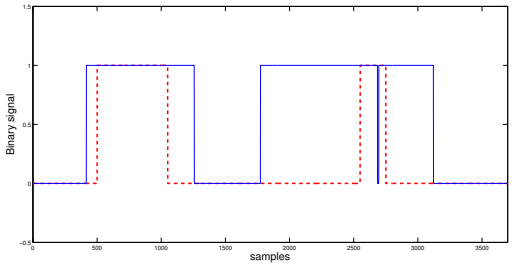

(c) Patient C

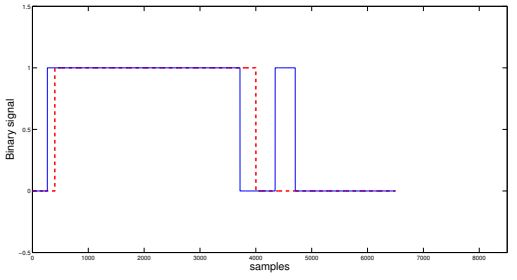

(d) Patient D

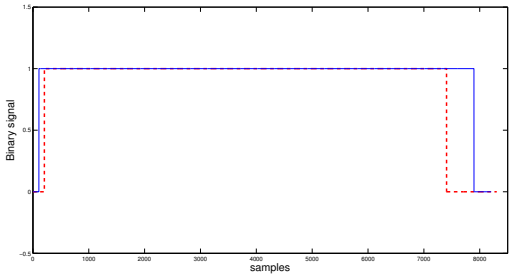

(e) Patient E

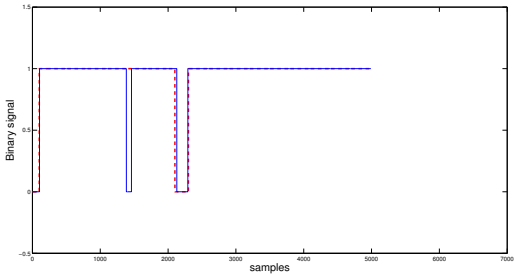

(f) Patient G

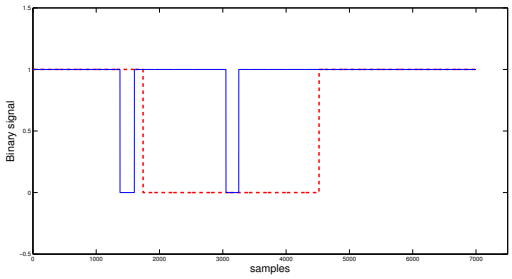

(g) Patient F-1

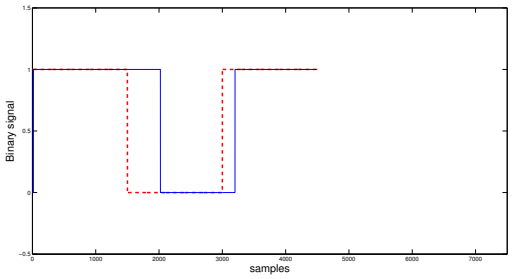

(h) Patient F-2

Figure 5.15: Binary representation of the real AF episodes, corrisponding to 1, (in red dashed line) and their estimates (in blue solid line), for patient A, B, C, D, E, G and F. False positive are present in patient A (a), D (d), G (f), F-1(g).

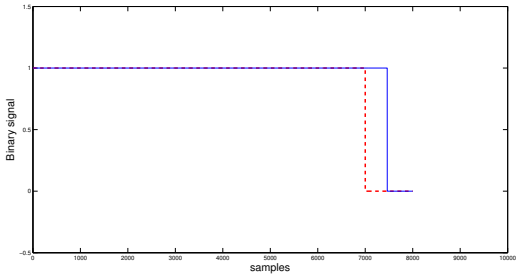

(a) Patient H

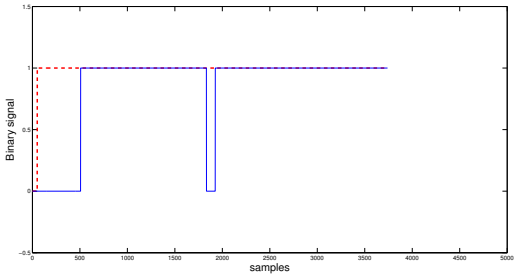

(b) Patient I

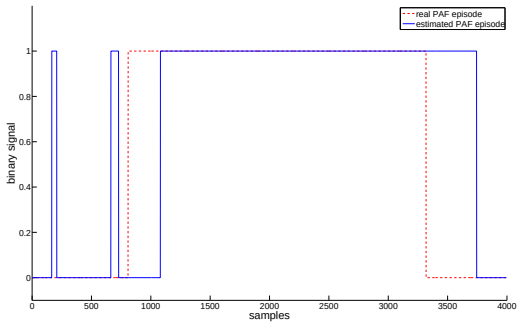

(c) Patient X

Figure 5.16: Binary representation of the real AF episodes, corrisponding to 1, (in red dashed line) and their estimates (in blue solid line), for patient H, I, D, X. False positive are present in patient I (b), X (c).

The baggage of results aquired in this Chapter will be used in the next one for Discussions.

Chapter 6

Discussions and Conclusions

AF is one of the most common arrhythmia that regards the atria. From electric-physiological point of view, it is characterized by the replacement of P waves by f-waves, or fibrillatory waves, consisting in an oscillating baseline of low amplitude in range of frequency between 3 and 12 Hz. Symptoms are chest pain, palpitations, irregular heart rate, even if there are cases of asymptomatic AF [2]. It has been demostrated that AF can be a risk factor for stroke and death, specially for elder subjects; so, above all in asymptomatic patients, it is extremely important the detection. One of the main consequences of this atrial arrhythmia is the irregular heart rate and the variability of the ventricular responce, described by the distribution of the RR-intervals, that is different from the health subjects. This feature has been used, even if in different ways, for making detection by many studies in literature [38], [39], [41]. The results are succesfull, in terms of sensitivity and specifity, but there is one main limit: the uncapability to detect episodes shorter than one minute.
As it was declared, the goal of this thesis was double:

1. providing an algorithm for frequency tracking of the atrial signal;

2. developing a method that, based on the obtained frequency track, could be able to detect AF, above all short episodes.

For the first goal, two algorithms, ANF and DFE, have been implemented with MATLAB, tested and compared in Chapter 3. The ANF results to be the most suitable for ECG applications, for stability to different noise conditions and tracking capability of frequency changes. ANF has been applied to signals implemented in MATLAB, like stairwise functions, where each stair was a sinusoid of different frequency, but also to real ECG records, showing stability and returning a frequency value that was plausible both for sinus rhythm and AF, without being particular expensive from the computational point of view.

For the second goal, the developed method consists in a differential detection, beacuse of the different estimate that returns ANF with or without prefiltering, in case of sinus rhythm, while in case of AF there is no difference. This detector was applied to *simulated PAF*, described in Chapter 5, and to *real PAF*. On one hand, simulations based on *simulated PAF* have permitted to size the capability of the detector, in terms of temporal resolution and minimum duration of the detectable episodes: if an error, $\epsilon_{episode}$, of at most 5% is accepted, the detector has been estimated to detect episodes of minimum duration of 10 seconds and with temporal resolution of 25 seconds. On the other hand, those parameters, estimated in simulations, have been checked with *real PAF*, a set of 10 patients, one from Valentia Hospital and the remaining nine from [44]. There were 15 AF episodes totally, that have been all detected, together with 7 false postives.

This dataset is made mainly by AF episodes some minutes longs; given the purpose of detection of very short episodes, more ECG traces with very short episodes could be desireble, but there were some difficulty to find them.

It is time from making the assessment of pros and cons. Positive features are the following:

- good stability and good tracking of the frequency changing of the ANF algorithm;
- in the assumption of the AF episodes not shorter than 6 seconds, the method is able to detect the episodes without dismissing any of them;

- the estimate in terms of number of AF episodes is quite reliable, taking the introduction of the delay into account;
- the method is able to detect episodes on order of seconds, as it was wished.

The main limitations of this method are found to be:

- the generation of spurious peak (false positive episodes) that are not excluded, above all when the input signal is very noisy;
- the introduction of a delay, that has to be compensated, in order to make the method more reliable and accurate in the detection;
- the computational cost is higher than most of the detection methods, present in literature, because a QRS removal has to be done prior to the application of the method, that provides it self the running of the ANF algorithm twice.

Finally, we can conclude that, for what concerns frequency tracking, the ANF algorithm has been used for purpose of detection, but another point of interest can be to study more deeply the frequency tracking capability of this algorithm, improving the accuracy of the estimate; whereas for what concerns the detection, the method centres the objective of the detection of short episodes and its estimate is based on the atrial activity, that is coherent considering that the AF is an atrial disease. Certainly it needs more than ten cases to be validated and it has an intrinsic weakness respect to the others methods present in literature, given by the fact that in general the atrial activity is weaker than the ventricular activity and it is more difficult to isolate, while the QRS is really easy to be detected, because of its higher amplitude, so there are less problem of artifacts and noise's introduction.

Bibliography

[1] L. Mainardi, L. Sörnmo and S. Cerutti ”Understanding Atrial Fibrillation: The Signal Processing Contribution”, *Morgan & Claypool publishers*.

[2] R.L. Page,W.E. Wilkinson, W.K. Clair, E.A. McCarthy, and E.L. Pritchett, ”Asymptomatic arrhythmias in patients with symptomatic paroxysmal atrial fibrillation and paroxysmal supraventricular tachycardia”, *Circulation*, vol.89, pp.224-227, 1994.

[3] M.Thurman and J.Janney, ”The diagnostic importance of fibrillatory wave size”, *Circulation*, vol.25, pp. 991-994, 1962.

[4] Fuster V, Rydn LE, Cannom DS, ”ACC/AHA/ESC 2006 Guidelines for the Management of Patients with Atrial Fibrillation: a report of the American College of Cardiology, *American Heart Association*, 2006 Aug 15;114(7):e257-354.

[5] Y.Miyasaka, M.E. Barnes, B.J. Gersh, S. S. Cha, K.R.Bailey, W.P. Abhayaratana, J.B.Seward and T.S. Tsang, ”Secular trends in incidence of atrial fibrillation in Olmsted Country, Minnesota, 1980 to 2000, and implications on the projections for future prevalence”, *Circulation*, vol.114, pp. 119-125, 2006.

[6] T.S. Tsang and B.J. Gersh,”Atrial Fibrillation: An Old disease, a new epidemic”, *American Journal of Medicine*, vol.113, pp 432-435, 2002.

[7] P.A. Wolf, R.D. Abbott, and W.B. Kannel, ”Atrial fibrillation as an independent risk factor for stroke: The Framingham Study”, *Stroke, American Heart Association*, vol. 22, pp.983-988, 1991.

[8] J.Heeringa, D.A. van der Kuip, A. Hofman, J.A. Kors, G. van Herpen, B.H. Stricker, T.Stijnen, G.Y. Lip and J.C. Witteman, ”Prevalence, incidence and lefttime risk of atrial fibrillation: The Rotterdam study”, *European Heart Journal*, vol.27, pp.949-953, 2006.

[9] C.D. Furberg, B.M. Psaty, T.A. Manolio, J.M. Gardin, V.E. Smiith and P.M. Rautaharju, ”Prevalence of Atrial Fibrillation in elderly subjects(The Cardiovascular Health Study)”, *American Journal Cardiology*, vol. 74, pp.236-241, 1994.

[10] E.J. Benjamin, D. Levy, S.M. Vaziri, R.B. D’Agostino, A.J. Belanger ad P.A. Wolf, ”Independent risk factors for atrial fibrillation in a population-based cohort”. The Framingham Heart Study”, *JAMA*, vol. 271, pp. 840-844, 1994.

[11] S.M Vaziri, M. G. Larson, E.J. Benjamin and D.Levy, ”Echocardiographic predictors of non rheumatic atrial fibrillation. The Framingham Heart Study”, *Circulation*, vol.89, pp. 724-730, 1994.

[12] R.Nieuwlaat, A. Capucci, A.J. Camm, S.B. Olsson, D. Andresen, D.W.Davies, S.Cobbe, G.Breithardt, J.Y. Le Heuzey, M.H. Prins, S.Levy and H.J. Cijins, ”Atrial Fibrillation menagment: a prospective survey in ESC member countries: The Euro Heart Survey on Atrial Fibrillation”, *European Heart Journal*, vol.26, pp. 2422-2434,2005.

[13] Hsuan-Ming Tsao and Shih-Ann Chen, ”CT and MR images in Atrial Fibrillation”, *Humana Press*, Atrial Fibrillation, pp 341-347, 2008

[14] B Logan, J Healey, ”Robust Detection of Atrial Fibrillation for a Long Term Telemonitoring System”, *Computers in Cardiology*, 2005; 32 :619-622.

[15] F.Pinciroli, R. Rossi, P. Valenza, ”Self Monitoring of Paroxysmal Atrial Fibrillation Episodes in Ambulatory Patients” *Computers in Cardiology*, 1993; 503-506.

[16] F Beckers, W Ann, B Verheyden, C van der Dussen de Kestergat, E Van Herk, L Janssens, R Willems, H Heidbchel, AE Aubert, ”Determination of Atrial Fibrillation Frequency Using QRST-Cancellation with QRS-Scaling in Standard Electrocardiogram Leads”. *Computers in Cardiology*, 2005; 32 :339-342.

[17] M. M. Gallagher and A.J. Camm, ”Classification of Atrial Fibrillation”, *American Journal of Cardiology*, vol.82, pp. 18N-28N, 1998.

[18] S. Chen, M. Hsieh, C. Tai, C. Tsai, V. S. Prakash, W. Yu, T. Hsu, Y. Ding and M. Chang, ”Initiation of Atrial Fibrillation by Ectopic Betas Originating From the Pulmonary Veins: Electrophysiological Responses, and Effects of Radiofrequency Ablation”, *American Heart Association, Inc* Circulation. 1999;100:1879-1886.

[19] H. Nakashima, K. Kumagai, H. Tojo, T. Yasuda, H. Noguchi, N. Matsumoto and K. Saku, ”Simaultaneous Catheter Mapping of the Pulmonary Veins in Focal Atrial Fibrillation: Significance of Rapid Focal Activation, Effectiveness for Catheter Ablation”, *Japanese Heart Journal*, vol.43, No.4, July 2002.

[20] I. Steiner, P. Hájková, J. Kvasnička and I. Kholová, ”Myocardial sleeves of pulmonary veins and atrial fibrillation: a postmortem histopathological study of 100 subjects”, *Virchows Arch (2006)*, 449: 88-95.

[21] Chin-Feng Tsai, Ching-Tai Tai, Ming-Hsiung Hsieh, Wei-Shiang Lin,” Initiation of Atrial Fibrillation by Ectopic Beats Originating From the Superior Vena Cava : Electrophysiological Characteristics and Results of Radiofrequency ablation ”,*Circulation*, 2000; 102; 67-74.

[22] C. Pappone, G. Oreto, F. Lamberti, G. Vicedomini, M.L.Loricchio, S. A. Ben-Haim, M. Rillo, M.P. Calabr, A. Conversano,R. Cappato and S. Chierchia, Shlomo , " Catheter Ablation of Paroxysmal Atrial Fibrillation Using a 3D Mapping System", *Circulation*, 1999; 100; 1203-1208.

[23] C. Pappone, S. Rosanio, G. Oreto, M. Tocchi, F. Gugliotta, G. Vicedomini, A. Salvati, C. Dicandia, P. Santinelli, S. Gulletta and S. Chierchia, "Circumferential Radiofrequency Ablation of Pulmonary Vein Ostia : A New Anatomic Approach for Curing Atrial Fibrillation ", *Circulation*, 2000; 102; 2619-2628 .

[24] M. Hassaguerre, D. C. Shah, P. Jas, M. Hocini, T. Yamane, I. Deisenhofer, M. Chauvin, S. Garrigue, J. Clmenty, " Electrophysiological End Point for Catheter Ablation of Atrial Fibrillation Initiated From Multiple Pulmonary Venous Foci ", *Circulation*, 2000;101;1409-1417.

[25] M. Hassaguerre, D. C. Shah, P. Jas, M. Hocini, T. Yamane, I. Deisenhofer, M. Chauvin, S. Garrigue, J. Clmenty, "Electrophysiological Breakthroughs From the Left Atrium to the Pulmonary Veins ", *Circulation*, 2000; 102; 24632465 .

[26] L. Guilherme Grossi Porto and Luiz F. Junqueira, "Comparison of Time-Domain Short-Term Heart Interval Variability Analysis Using a Wrist-Worn Heart Rate Monitor and the Conventional Electrocardiogram", *Blackwell publishing*, Pacing and Clinical Electrophysiology, vol.32, pp 43-51, 2009.

[27] Q Xi, A V Sahakian, J Ng, S Swiryn, "Stationarity of Surface ECG Atrial Fibrillatory Wave Characteristics in the Time and Frequency Domains in Clinically Stable Patients", Computers in Cardiology, vol. 30, pp.133-136, 2003

[28] P. G. Chan, M. Logue and P.Kligfield, ”Effect of Right Bundle Branch Block on Electrocardiographic Amplitudes, Including Combined Voltage Criteria Used for the Detection of Left Ventricular Hypertrophy”, *Journal compilation, 2009, Wiley Periodicals, Inc.*, Annals of Noninvasive Electrocardiology, vol. 11, issue 3, pp 230-236.

[29] M. K. Das, Anil V. Yadav and Douglas P. Zipes, ”Atrial Fibrillation: Future Directions”, Chapter 31, pp 429-443, 2008.

[30] A. Bollmann, D. Husser, L. Mainardi, F. Lombardi, P. Langley, A. Murray, J. Rieta, J. Millet, S. Bertil Olsson, M. Stridh, and L. Sörnmo, ”Analysis of surface electrocardiograms in atrial fibrillation: techniques, research, and clinical applications”, *Europace*, vol. 8, pp.911-926, 2006.

[31] S.Pehrson, M. Holm, C. Meurling, M.Ingemansson, B. Smideberg, Leif Sörnmo and S. Olsson, ”Non-invasive assessment of magnitude and dispersion of atrial cycle length during chronic atrial fibrillation in man”, *European Heart Journal*, vol.19, pp.1836-1844, 1998.

[32] A. Bollman, K. Sonne, H.Esperer, I. Toepffer, and H. Klein, ”Circadian variations in atrial fibrillatory frequency in persistent human atrial fibrillation”, *Pacing Clinical Electrophysiology.*, vol.23, pp. 1867-1871, 2000.

[33] Ho-En Liao ”Two Discrete Oscillator Based Adaptive Notch Filters (OSC ANFs) for Noisy Sinusoids”. *IEEE Transactions on signal processing*, vol.53, no.2, February 2005.

[34] H.C. So and P.C Ching ”Adaptive algorithm for direct frequency estimation” , *IEE Proc.-Radar Sonar Navigation*, Vol. 151, No. 6, December 2004.

[35] S.Rokas, S. Gaitanidou, S. Chatzidou, C. Pamboucas, D. Achitipis and S. Stamatelopoulos, ”Atrioventricular Node Modification in Patients with

cronic atrial fibrillation: Role of the morphology of RR-interval variation", *Circulation*, vol.103, pp. 2942-2948, 2001.

[36] A. Climent, M.Guillema, D.Husserb, F. Castellsa, J.Milleta and A.Bollmann, "Relation between Atrial Rate and Preferential RR intervals during Atrial Fibrillation", *International Journal of Bioelectromagnetism*, vol. 11, pp. 17-21, 2009.

[37] A. Climent, M.Guillema, D.Husserb, F. Castellsa, J.Milleta and A.Bollmann, "PoincareŚurface Profile. Novel non invasive Method to detect preferential ventricular responce during Atrial Fibrillation", *Computers in Cardiology*, vol 34, pp. 585-588, 2007.

[38] E. Petrucci, V. Balian, G. Filippini, L.T. Mainardi, "The use of sequential RR distributions to detect Atrial Fibrillation episodes in very long term ECG monitoring", *Computers in Cardiology*, vol 33, pp. 945-948, 2006.

[39] E. Petrucci, V. Balian, G. Filippini, L.T. Mainardi, "Atrial fibrillation Detection algorithms for very long term ECG monitoring", *Computers in Cardiology*, vol 32, pp. 623-626, 2005.

[40] M. Mohebbi, H. Ghassemian, "Detection of Atrial Fibrillation Episodes using SVM", IEEE EMBS Conference Vancouver, British Columbia, Canada, August 20-24, 2008.

[41] S. Dash, K. H. Chon, S Lu, E.A. Reader, "Automatic real time detection of Atrial Fibrillation", *Annals of Biomedical Engineering*, 2009.

[42] M. Stridh and L. Sörnmo, "Spatiotemporal QRST cancellation techniques for analysis of atrial fibrillation", IEEE 1*Trans. Biomed. Eng.*, vol.38, pp.105-111, 2001.

[43] R. Wolk, P. Kulakowski, S. Karczmarewicz, G. Karpinski, E. Makowska, A. Czepiel and L. Ceremuzynski "The incidence of aymptomatic paroxys-

mal atrial fibrillation in patients treated with propanolol or propafenone" *International Journal of Cardiology*, Volume 54, Issue 3, June 1996, Pages 207-211.

[44] Goldberger AL, Amaral LAN, Glass L, Hausdorff JM, Ivanov PC, Mark RG, Mietus JE, Moody GB, Peng CK, Stanley HE. PhysioBank, PhysioToolkit, and PhysioNet: Components of a new research resource for complex physiologic signals. Circ 2000;101:e215e220.